โภชนพันธุศาสตร์เพื่อเพิ่มการเจริญเต็มวัยด้านการสืบพันธุ์ของกุ้งกุลาดำ

Penaeus monodon

นางสาวจินตนา อินนุพัฒน์

วิทยานิพนธ์นี้เป็นส่วนหนึ่งของการศึกษาตามหลักสูตรปริญญาวิทยาศาสตรมหาบัณฑิต
สาขาวิชาเทคโนโลยีชีวภาพ
คณะวิทยาศาสตร์ จุฬาลงกรณ์มหาวิทยาลัย
ปีการศึกษา 2554
ลิขสิทธิ์ของจุฬาลงกรณ์มหาวิทยาลัย

NUTRIGENOMICS FOR INCREASING REPRODUCTIVE MATURATION OF
THE BLACK TIGER SHRIMP *Penaeus monodon*

Miss Jintana Innuphat

A Thesis Submitted in Partial Fulfillment of the Requirements
for the Degree of Master of Science Program in Biotechnology
Faculty of Science
Chulalongkorn University
Academic Year 2011

Thesis Title   NUTRIGENOMICS FOR INCREASING
                      REPRODUCTIVE MATURATION OF THE BLACK
                      TIGER SHRIMP *Penaeus monodon*

By   Miss Jintana Innuphat
Field of Study   Biotechnology
Thesis Advisor   Professor Piamsak Menasveta, Ph.D.
Thesis Co-advisor   Sirawut Klinbunga, Ph.D.

Accepted by the Faculty of Science, Chulalongkorn University in Partial Fulfillment of the Requirements for the Master's Degree

………………………………… Dean of the Faculty of Science

(Professor Supot Hannongbua, Dr.rer.nat.)

THESIS COMMITTEE

………………………………… Chairman

(Associate Professor Thaithaworn Lirdwitayaprasit, Ph.D.)

………………………………… Thesis Advisor

(Professor Piamsak Menasveta, Ph.D.)

………………………………… Thesis Co-advisor

(Sirawut Klinbunga, Ph.D.)

………………………………… Examiner

(Associate Professor Chanphen Chanchao, Ph.D.)

………………………………… External Examiner

(Sittiruk Roytrakul, Ph.D.)

จินตนา อินนุพัฒน์ : โภชนพันธุศาสตร์เพื่อเพิ่มการเจริญเต็มวัยด้านสืบพันธุ์ของกุ้งกุลาดำ *Penaues monodon*. (NUTRIGENOMICS FOR INCREASING REPRODUCTIVE MATURATION OF THE BLACK TIGER SHRIMP *Penaeus monodon*) อ. ที่ปรึกษาวิทยานิพนธ์หลัก : ศ.ดร. เปี่ยมศักดิ์ เมนะเศวต, อ. ที่ปรึกษาวิทยานิพนธ์ร่วม : ดร. ศิราวุธ กลิ่นบุหงา, 129 หน้า.

การแยกและวิเคราะห์การแสดงออกของจีนที่เกี่ยวข้องกับการเจริญพันธุ์มีความสำคัญต่อความเข้าใจกลไกระดับโมเลกุลของการพัฒนารังไข่ในกุ้งกุลาดำ จึงหาลำดับนิวคลีโอไทด์ของจีน *nuclear hormone receptor 96* (*PmNHR96*) และ *son of sevenless* (*PmSOS*) ด้วยเทคนิค RACE-PCR พบว่ามี open reading frames (ORFs) บางส่วนยาว 869 และ 1183 คู่เบส เมื่อทำการตรวจสอบการแสดงออกของจีนต่างๆ ในเนื้อเยื่อของกุ้งกุลาดำโตเต็มวัยด้วยวิธี RT-PCR พบว่าจีน *asparagenyl tRNA systhertase* (*PmAtNS*), *aspartate amino tranferase* (*PmAST*) และ *PmSOS* มีการแสดงออกในรังไข่สูงกว่าในอัณฑะของกุ้งกุลาดำเต็มวัย

ตรวจสอบการแสดงออกของจีนต่างๆ ในรังไข่ของแม่พันธุ์กุ้งกุลาดำจากธรรมชาติ ด้วยวิธี quantitative real-time PCR พบว่า *PmAtNS* และ *Pm-magonashi* มีการแสดงออกที่ไม่แตกต่างกันในรังไข่ระยะต่างๆ ในกุ้งเต็มวัยปกติ ในขณะที่ *PmAST* และ *PmNHR96* มีการแสดงออกที่สูงขึ้นในรังไข่ระยะที่ IV โดยการตัดตาส่งผลให้การแสดงออกของ *PmAST* ในรังไข่ระยะที่ II สูงกว่าในรังไข่ระยะเดียวกันในกุ้งเต็มวัยปกติ ($P < 0.05$) ในขณะที่การแสดงออกของจีน *Pm-mago nashi* ในรังไข่ระยะที่ I-IV และ *PmNHR96* ในรังไข่ระยะที่ I-III ในกุ้งกุลาดำที่ตัดก้านตาสูงกว่าในกุ้งปกติอย่างมีนัยสำคัญทางสถิติ ($P < 0.05$) ผลการศึกษาบ่งชี้ได้ว่าจีน *PmAST*, *Pm-mago nashi* และ *PmNHR96* มีหน้าที่เกี่ยวข้องกับการเจริญพันธุ์ของกุ้งกุลาดำ

ทำการตรวจสอบการแสดงออกของยีนต่างๆ ในรังไข่กุ้งกุลาดำภาวะเลี้ยงที่มีอายุ 5 9 14 และ 19 เดือน พบว่าจีน *PmAtNS* มีการแสดงออกที่ต่ำลงที่อายุ 14 เดือน ($P < 0.05$) *PmAST* มีระดับการแสดงออกที่สูงขึ้นที่อายุ 19 เดือน ($P < 0.05$) *PmNHR96* มีระดับการแสดงออกที่สูงขึ้นที่อายุ14 เดือน ($P < 0.05$) ในขณะที่ *Pm-mago nashi* มีการแสดงออกที่ไม่แตกต่างกันในกุ้งเลี้ยงที่มีอายุแตกต่างกัน ($P > 0.05$)

ศึกษาผลของการฉีด 17β-estradiol ที่ความเข้มข้น 0.01μg/g น้ำหนักตัวต่อการแสดงออกของจีนต่างๆ ในรังไข่ของกุ้งกุลาดำเลี้ยงอายุ 14 เดือน ทำการตรวจสอบการแสดงออกของจีนต่างๆ ด้วยวิธี quantitative real-time PCR พบว่าจีน *PmAtNS* มีระดับการแสดงออกที่ลดลงหลังการฉีด 17β-estradiol เป็นเวลา 7 วัน ($P < 0.05$) โดย 17β-estradiol ไม่ส่งผลต่อการแสดงออกของ *PmAST* และ *Pm-mago nashi* ($P > 0.05$) ในขณะที่จีน *PmNHR96* มีแนวโน้มการแสดงออกที่สูงหลังการฉีด17β-estradiol ($P > 0.05$) ส่วนผลของการตัดตานั้นพบว่า ส่งผลต่อการแสดงออกของจีน *PmAST*, *Pm-mago nashi* และ *PmNHR96* ที่สูงขึ้นหลังตัดตาเป็นเวลา 28 7 และ 14 วัน ตามลำดับ แต่ไม่ส่งผลต่อการแสดงออกของจีน *PmAtNS*.

ทำการทดสอบอาหารที่เพิ่มส่วนผสมของ 17β-estradiol ที่ความเข้มข้น 1mg/kg และ 10mg/kg ให้แก่กุ้งเลี้ยงอายุ 14 เดือน เป็นเวลา 35 วัน ผลการทดลองพบว่า อาหารที่มี 1mg/kg 17β-estradiol ส่งผลให้จีน *PmAST* ในรังไข่มีการแสดงออกที่สูงกว่าในกุ้งที่ให้อาหารปกติที่ 35 วันของการทดลอง ($P < 0.05$) และพบว่าอาหารที่มี 10 mg/kg 17β-estradiol ส่งผลให้ *PmAtNS* และ *PmAST* มีการแสดงออกที่ต่ำกว่าในกุ้งที่ให้อาหารปกติที่ 7 วันของการทดลอง ($P < 0.05$) นอกจากนี้พบว่าอาหารที่ผสม 10 mg/kg 17β-estradiol ส่งผลให้ *Pm-magonashi* มีการแสดงออกที่เพิ่มขึ้นที่ 7 วันของการทดลอง โดยอาหารที่ผสม 1 mg/kg และ 10 mg/kg 17β-estradiol ส่งผลให้การแสดงออกของ *Pm-magonashi* ต่ำลงที่ 14 วัน ของการทดลอง ทั้งนี้อาหารที่มี 1 mg/kg 17β-estradiol และ 10 mg/kg 17β-estradiol ไม่ส่งผลต่อการแสดงออกของจีน *PmNHR96* ในรังไข่ตลอดช่วงเวลาในการทดลอง ($P > 0.05$) ผลของการตัดตาพบว่ามีผลต่อการแสดงออกของจีน *PmAtNS*, *PmAST* และ *PmNHR96* ที่สูงในวันที่ 28 35 และ14 ตามลำดับ

สาขาวิชา _____เทคโนโลยีชีวภาพ_____ ลายมือชื่อนิสิต...

ปีการศึกษา _____2554_____ ลายมือชื่อ อ.ที่ปรึกษาวิทยานิพนธ์หลัก...............

ลายมือชื่อ อ.ที่ปรึกษาวิทยานิพนธ์ร่วม..................

JINTANA INNUPHAT : NUTRIGENOMICS FOR INCREASING REPRODUCTIVE MATURATION OF THE BLACK TIGER SHRIMP *Penaeus monodon* ADVISOR : PROF. PIAMSAK MANASVETA, Ph.D.,CO-ADVISOR : SIRAWUT KLINBUNGA, Ph.D., 129 pp.

Isolation and expression analysis of reproduction-related genes is important for understanding molecular mechanisms of ovarian development in the giant tiger shrimp (*Penaeus monodon*). In this thesis, the partial cDNA sequences of nuclear hormone receptor (*PmNHR96*) and son of sevenless (*PmSOS*) were isolated. Their partial open reading frames (ORFs) were 879 and 1183bp, respectively. RT-PCR analysis revealed that *asparagenyl tRNA systhetase (PmAtNS), aspartate amino transferase (PmAST)* and *PmSOS* were more preferentially expressed in ovaries than testes of *P. monodon*.

Quantitative real-time PCR indicated that the expression level of *PmAtNS* and *Pm-mago nashi* was not significantly different during ovarian development in both wild intact and eyestalk-ablated broodstock. The expression level of both *PmAST* and *PmNHR96* was significantly increased in stage IV ovaries in intact *P. monodon* broodstock ($P < 0.05$). Eyestalk ablation resulted in significant greater expression levels of *PmAST* in stage II ovaries ($P < 0.05$), *Pm-mago nashi* in stages I-IV and *PmNHR96* in stages I-III ovaries compared to those in intact broodstock ($P < 0.05$). Results suggested that these genes should play the important role during ovarian development of *P. monodon*.

In domesticated shrimp, the expression level of *PmAtNS* was significantly decreased in 14-month-old shrimp ($P < 0.05$). In contrast, the expression level of *PmNHR96* was significantly increased at 14 month-old shrimp ($P < 0.05$) and *PmAST* was significantly increased at 19-month-old shrimp ($P < 0.05$). Nevertheless, *Pm-mago nashi* was comparably expressed in different ages of domesticated shrimp.

Exogenous injection of 17β-estradiol resulted in significantly reduction of ovarian *PmAtNS* at 7 days post injection but did not affect the expression level of *PmAST* and *Pm-mago nashi*. Nevertheless, the expression level of ovarian *PmNHR96* seemed to be slightly increased at 7 days after injection ($P > 0.05$). Eyestalk ablation resulted in significant greater expression levels than that of the negative control for *PmAST* at 28 days post injection, for *Pm-mago nashi* at 7 days post injection and for *PmNHR96* at 14 days post injection ($P < 0.05$) but did not affect the expression level of *PmAtNS*.

The feeding trials for diet supplemented with 1 and 10 mg/kg 17β-estradiol was carried out for the duration of 35 days. The expression level of *PmAtNS* after feeding with the diet supplemented with 10 mg/kg of 17β-estradiol for 7 days was significantly lower than that of the control ($P < 0.05$). Similar results were also found for *PmAST*. Nevertheless, the treatment with 1 mg/kg of 17β-estradiol resulted in an increase expression level of *PmAST* after feeding for 35 days ($P < 0.05$). For *Pm-mago nashi*, its expression level was induced after feeding with the diet supplemented with 10 mg/kg of 17β-estradiol for 7 days. In contrast, feeding of diets supplemented with both 1 and 10 mg/kg of 17β-estradiol resulted in a lower expression level of *Pm-mago nashi* than that of the control at 14 days post treatment ($P < 0.05$). The expression levels of *PmNHR96* were not significantly changed for both 1 and 10 mg/kg of 17β-estradiol ($P < 0.05$). Eyestalk ablation resulted in significant greater expression levels than negative control for *PmAtSN, PmAST* and *PmNHR96* at 28, 35 and 14 days after treatment, respectively.

Field of Study :   Biotechnology   Student's Signature

Academic Year :   2011   Advisor's Signature

Co-advisor's Signature

ACKNOWLEDGMENTS

I would like to express my deepest sense of gratitude to my advisor Professor Dr. Piamsak Menasveta and my co-advisor, Dr. Sirawut Klinbunga for their encouragement, valuable suggestion and supports throughout my study.

My gratitude is also extended to Associate Professor Dr. Thaithaworn Lerdwithayaprasith, Associate Professor Dr. Chanphen Chanchao and Dr. Sittiruk Roytrakul for serving as thesis committee, for their recommendations and also useful suggestion.

I would particularly like to thank the Center of Excellence for Marine Biotechnology, National Center for Genetic Engineering and Biotechnology (BIOTEC), Faculty of Science, Chulalongkorn University and National Science and Technology Development Agency (NSTDA) for providing facilities.

I would like to extend my special thank to Ms. Natechanok Thamniemdee, Ms. Kanchana Sittikhankaew, Ms. Sasithorn Petkon, Ms. Witchulada Talakhun and everyone in our laboratory for best friendship and friendly assistance.

Finally, I would like to express my deepest gratitude to my parents and members of my family for their love, understanding and encouragement extended throughout my study.

CONTENS

LIST OF TABLES

LIST OF TABLES

LIST OF FIGURES

LIST OF FIGURES

LIST OF FIGURES

LIST OF FIGURES

LIST OF FIGURES

LIST OF ABBREVIATIONS

bp	base pair
°C	degree celcius
DEPC	diethylpyrocarbonate
DTT	dithiothreitol
dATP	deoxyadenosine triphosphate
dCTP	deoxycytosine triphosphate
dGTP	deoxyguanosine triphosphate
dTTP	deoxythymidine triphosphate
DNA	deoxyribonucleic acid
HCl	hydrochloric acid
IPTG	isopropyl-thiogalactoside
Kb	kilobase
kDa	kilo dalton
M	molar
$MgCl_2$	magnesium chloride
mg	milligram
ml	millilitre
mM	millimolar

ng	nanogram
OD	optical density
PCR	polymerase chain reaction
pI	isoelectric point
RNA	ribonucleic acid
RNase A	ribonuclease A
rpm	revolution per minute
RT	reverse transcription
SDS	sodium dodecyl sulfate
SDS-PAGE	SDS polyacrylamide gel electrophoresis
Tris	tris (hydroxyl methyl) aminomethane
μg	microgram
μl	microlitre
μM	micromolar
UV	ultraviolet

CHAPTER I

INTRODUCTION

1.1 Background information

The black tiger shrimp (*Peneaus monodon*) is one of the most economically important cultured species. Since 1994, Thailand has been regarded as the world leading shrimp (mainly *P. monodon*) producer of approximately 200,000 metric tons (Limsuwan, 2004). However, the aquacultural production has decreased since the last few years, as a result, domesticated Pacific white shrimp (*Litopenaeus vannamei*) has recently been introduced to Thailand as a new cultured species (Khamnamtong *et al*., 2005).

Farming of *P. monodon* in Thailand relies almost entirely on wild-caught broodstock for supply of juveniles because of poor reproductive maturation of cultured *P. monodon* females (Withyachumnarnkul *et al*., 1998; Preechaphol *et al*., 2007). The high demand on wild female broodstock leads to overexploitation of the natural *P. monodon* in Thai waters (Klinbunga *et al*., 1999; Khamnamtong *et al*., 2005). In addition, breeding of pond-reared *P. monodon* is extremely difficult and rarely produced enough quality of larvae required by the industry. The low degree of reproductive maturation of captive *P. monodon* has also limited the ability to genetically improve this important species by domestication and selective breeding programs (Withyachumnarnkul *et al.*, 1998; Kenway *et al.*, 2006; Preechaphol *et al.*, 2007).

Therefore, closed-life cycle culture (the use of genetically improved pond-reared instead of wild broodstock) is required for the sustainable aquaculture. The domestication and selective breeding programs of penaeid shrimp would provide a more reliable supply of seed stock and the improvement of their production efficiency (Makinouchi and Hirata, 1995; Clifford and Preston, 2006; Coman *et al*., 2006).

Molecular mechanisms involving gonadal development of *P. monodon* have long been of interest by aquaculture industries (Benzie, 1998; Preechaphol *et al*.,

2007). An initial step toward understanding molecular mechanisms of ovarian (and oocyte) maturation in *P. monodon* is the identification and characterization of reproduction-related genes that are differentially expressed during ovarian development of this economically important species.

Unilateral eyestalk ablation is used commercially to induce ovarian maturation of penaeid shrimp (Okumura, 2004; Okumura *et al*., 2006), but the technique leads to an eventual loss in egg quality and death of the spawners (Benzie, 1998). Therefore, predictable maturation and spawning of captive penaeid shrimp without the use of eyestalk ablation is a long-term goal for the shrimp industry (Quackenbush, 2001).

Estrogen-like compounds in invertebrates were first described in the ovaries of an echinoderm (Donahue and Jennings, 1937). In *P. monodon*, the titers of conjugated pregnenolone and unconjugated and conjugated dehydroepiandrosterone (DHEA) were found to be maximal at early and late vitellogenesis. Unconjugated progesterone was found in ovaries at the late vitellogenic and mature stages of ovarian development whereas conjugated testosterone was only detected in the mature ovaries (Fairs and Quinlan, 1990).

Results from several studies indicated that sex steroids (progesterone and 17β-estradiol) enhance the reproductive maturation of penaeid shrimp (Fingerman et al., 1993; Yano and Hoshino, 2006). Understanding mechanisms and functions of genes and proteins in different stages of ovarian development would provide a new tool applicable for understanding of their important biological and molecular processes and finally, for improving reproductive maturation *P. monodon* in captivity to resolve the major constraint of this economically important species

1.2 Objective of this thesis

1. Identification of the cDNA sequences of genes in the signal transduction pathways of oocyte development in *P. monodon*.

2. Determination of the expression levels of transcripts functionally involved with reproductive development and maturation of *P. monodon*.

3. Examination of effects of 17β-estradiol on ovarian development of domesticated *P. monodon*.

1.3 Literature review

The black tiger shrimp, *P. monodon* has dominated production of farmed shrimp along with the Pacific white shrimp (*Litopenaeus vannamei*) and is one of the most economically important penaeid species in South East Asia. Farming of *P. monodon* has achieved a considerable economic and social importance, constituting a significant source of income and employment in this region.

In Thailand, *P. monodon* had been intensively cultured for more than two decades and formerly, had contributed approximately 60% of the total cultivated shrimp production. The reasons for this are supported by several factors including the appropriate farming areas without serious disturbing from typhoons or cyclone, small variable of seawater during seasons, and ideal soils for pond construction. Culture of *P. monodon* had increased the national revenue, therefore *P. monodon* was, until recently, the most economically important cultured species in Thailand.

Farming of *P. monodon* in Thailand relies almost entirely on wild-caught broodstock for supply of juveniles because reproductive maturation of cultured *P. monodon* female is extremely low. As a result, breeding of pond-reared *P. monodon* is extremely difficult and rarely produced enough quality of larvae required by the industry. The high demand on wild female broodstock leads to overexploitation of the natural populations of *P. monodon* in Thai waters (Klinbunga *et al*., 1999).

Despite the success of the farmed production, the shrimp industry has encountered problems outbreaks of diseases and environmental degradation. Besides these, the lack of high quality wild and/or domesticated broodstock of *P. monodon* has possibly caused an occurrence of a large portion of stunted shrimp at the harvest time. The farmed production of *P. monodon* has significantly decreased since the last several years. As a result, domesticated Pacific white shrimp, *Litopenaeus vannamei*, has recently been introduced to Thailand as a new cultured species and initially contributed approximately 360,000 MT of the cultured production in 2004 and dramatically increased to 640,000 MT in 2010 (Table 1.1) (Source : http ://www.thaiahpa.com/Feed5.pdf).

Currently, *L. vannamei* accounts for approximately 98% of the total shrimp production in Thailand (Figure 1.1). However, the price of *L. vannamei* is quite low and broodstock used relies almost entirely on genetically improved stocks brought from different sources. In addition, the labor costs in Thailand are higher than other countries (e.g. Vietnam and China) preventing the advantage of competition for the world market. In contrast, the market of premium-sized *P. monodon* is still opened for Thailand because *L. vannamei* is not suitable for that market. Accordingly, *P. monodon* culture is currently promoted for increasing its farming production.

Table 1.1 Total shrimp production (metric tons) from the aquaculture sector during 2005 – 20010 in Southeast Asia

Country	2005	2006	2007	2008	2009	2010
Thailand	380,000	500,000	530,000	495,000	563,000	640,000
China	380,000	400,000	480,000	523,000	560,000	600,000
Vietnam	115,000	150,000	170,000	200,000	200,000	224,000
Indonesia	230,000	260,000	210,000	230,000	180,000	140,000
India	100,000	103,000	110,000	870,000	100,000	120,000
Malaysia	32,000	42,000	62,000	68,000	92,000	105,000
Philippines	35,000	36,000	38,000	29,000	35,000	410,000
Total	**1,272,000**	**1,491,000**	**1,600,000**	**2,415,250**	**1,730,000**	**2,199,000**

(Source: http://www.thaiahpa.com/Feed5.pdf)
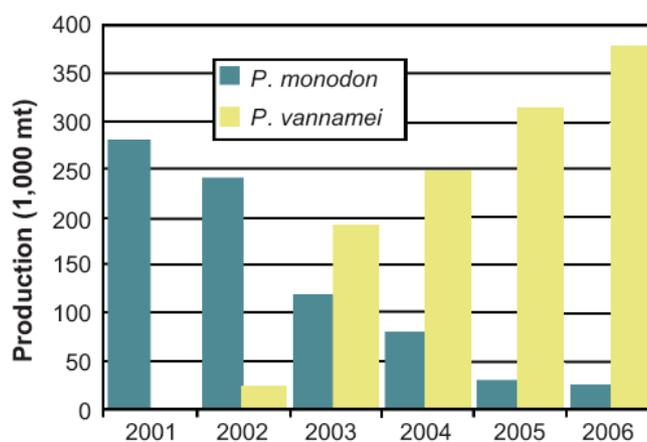
Figure 1.1 A diagram of production of *P. monodon* and *L. vanami* during 2001-2006 in Thailand

1.4 General introduction

1.4.1 Taxonomy of *P. monodon*

The black tiger shrimp is taxonomically classified as a member of Phylum Arthropoda; Subphylum Crustacea; Class Malacostraca; Subclass Eumalacostraca; Order Decapoda; Suborder Natantia; Infraorder Penaeidea; Superfamily Penaeoidea; Family Penaeidae, Rafinesque, 1985; Genus Penaeus, Fabricius, 1798 and Subgenus *Penaeus*. The scientific name of shrimp is *Penaeus monodon* (Fabricius, 1798) where the English common name is giant tiger shrimp or black tiger prawn (Bailey-Brook and Moss, 1992).

1.4.2 Morphology

The exterior of penaeid shrimp is distinguished by a cephalothorax with a characteristic hard rostrum, and by a segmented abdomen (Figure 1.2). Most organs, such as gills, digestive system and heart, are located in the cephalothorax, while the muscles concentrate in the abdomen. Appendages of the cephalothorax vary in appearance and function. In the head region, antennules and antennae perform sensory functions. The mandibles and the two pairs of maxillae form the jaw-like structures that are involved in food uptake (Solis, 1988). In the thorax region, the maxillipeds are the first three pairs of appendages, modified for food handling, and the remaining five pairs are the walking legs (pereiopods). Five pairs of swimming legs (pleopods) are found on the abdomen (Bell and Lightner, 1988; Baily-Brock and Moss, 1992).

The external morphology of *P. monodon* and sex characteristics of male (petasma) and female (thelycum) are illustrated in Figure 1.1.

1.4.3 Distribution and life cycle

The black tiger shrimp is widely distributed throughout the greater part of the IndoPacific region, ranging northward to Japan and Taiwan, eastward to Tahiti, southward to Australia and westward to Africa. The penaeid life cycle includes several distinct stages that are found in a variety of habitats (Figure 1.3). Juveniles prefer brackish shore areas and mangrove estuaries in their natural environment. Most of the adults migrate to deeper offshore areas at higher salinities, where mating and
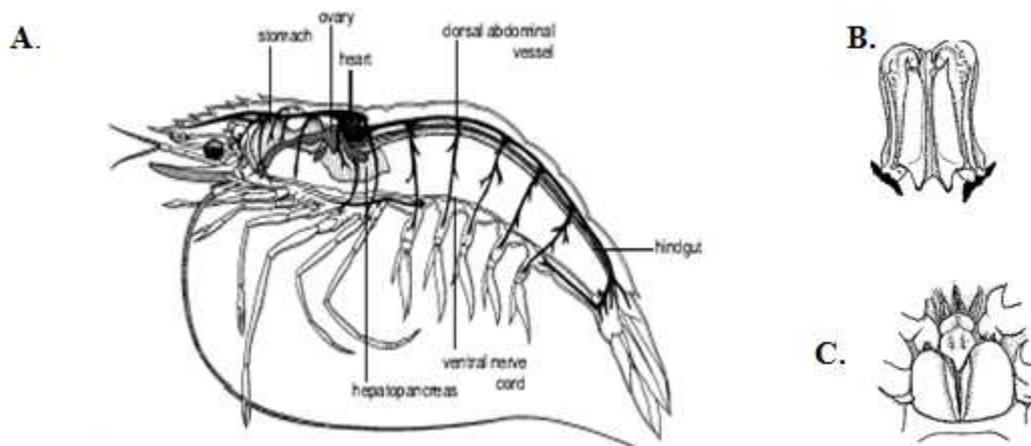
Figure 1.2 External morphology of *P. monodon* (A). Sexes of juveniles and broodstok of penaeid shrimp can be externally differentiated by petasma of male (B) and thelycum of female (C).

reproduction takes place. Females produce between 50,000-1,000,000 eggs per spawning (Rosenberry, 1997). The eggs hatch into the first larval stage, which is the nauplius. The nauplii feed on their reserves for a few days and develop into the protozoeae. The protozoeae feed on algae and metamorphose into myses. The myses feed on algae and zooplankton and have many of the characteristics of adult shrimp and develop into megalopas, the stage commonly called postlarvae (PLs). Larval stages inhabit plankton-rich surface waters offshore, with a coastal migration as they develop (Karin van de Braak / http://edepot.wur.nl/121288).

1.4.4 Ovarian developmental stages of *P. monodon*

Five ovarian maturation stages are recognized for *P. monodon* (Primavara, 1998). The maturation stage can visualized and divide as follows;

-**Stage I (Immature)** Ovaries are thin and lucent. The dorsal of exoskeleton not are visible through. The tissue on the dissection they appear colorless strands, devoid of visible eggs.
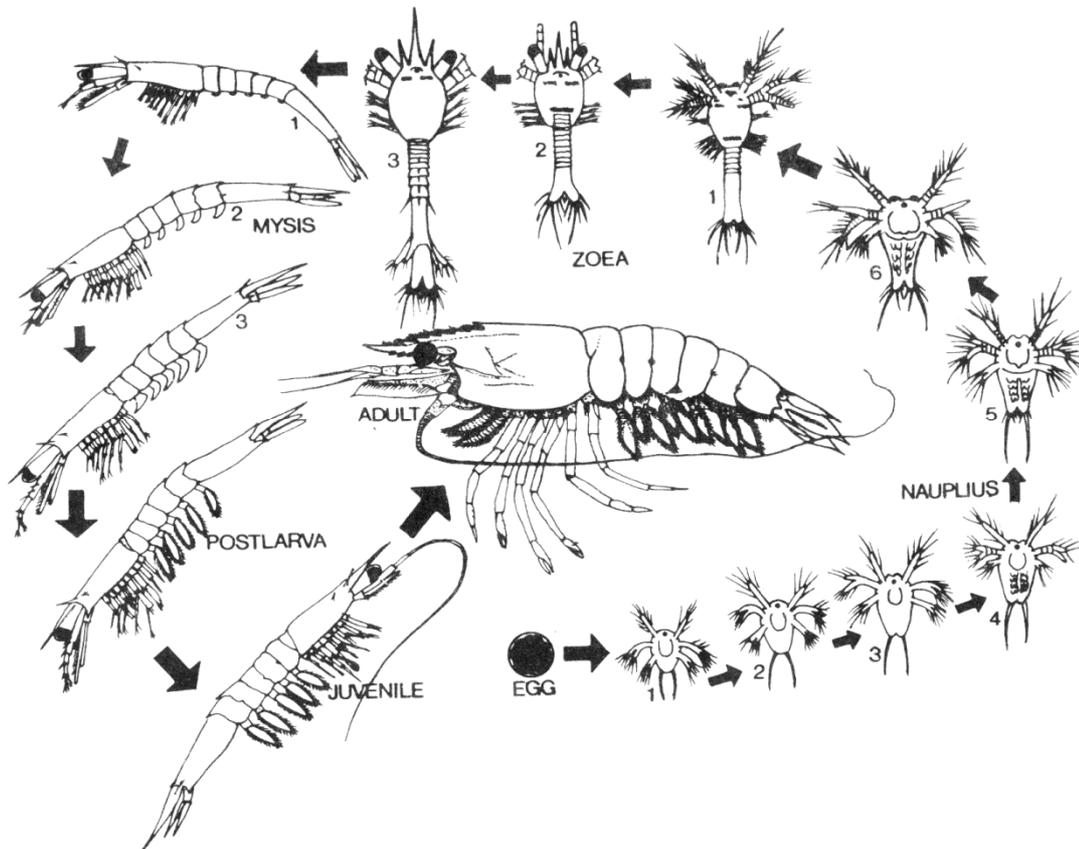
Figure 1.3 Life cycle of *P. monodon* (Rolando R. Platon 1978)

-**Stage II (Early maturing)** Ovaries stare to increase the skeleton size can observed as thin ovaries, linear band, particularly in the anterior and middle lobes. The ovaries of dissected was color from cloudy white to light-brown.

-**Stage III (Late maturing)** Exoskeleton can visible through of ovaries, as a thick, solid, linear band. The abdominal region to posterior thoracic. The tissue on the dissection showed olive-green colorless of ovaries. That can be seen granular and firm in texture with clumps of eggs.

-**Stage IV (Mature or ripe)** Ovaries are showed diamond-shaped expansion at abdominal region of ovaries and linear band is thicker. The dissected are appear dark green and distended. They are available space in the body captivity.

-**Stage V (spent)** Ovaries completely spent are limp, thin and appear similar stage I (Immature).
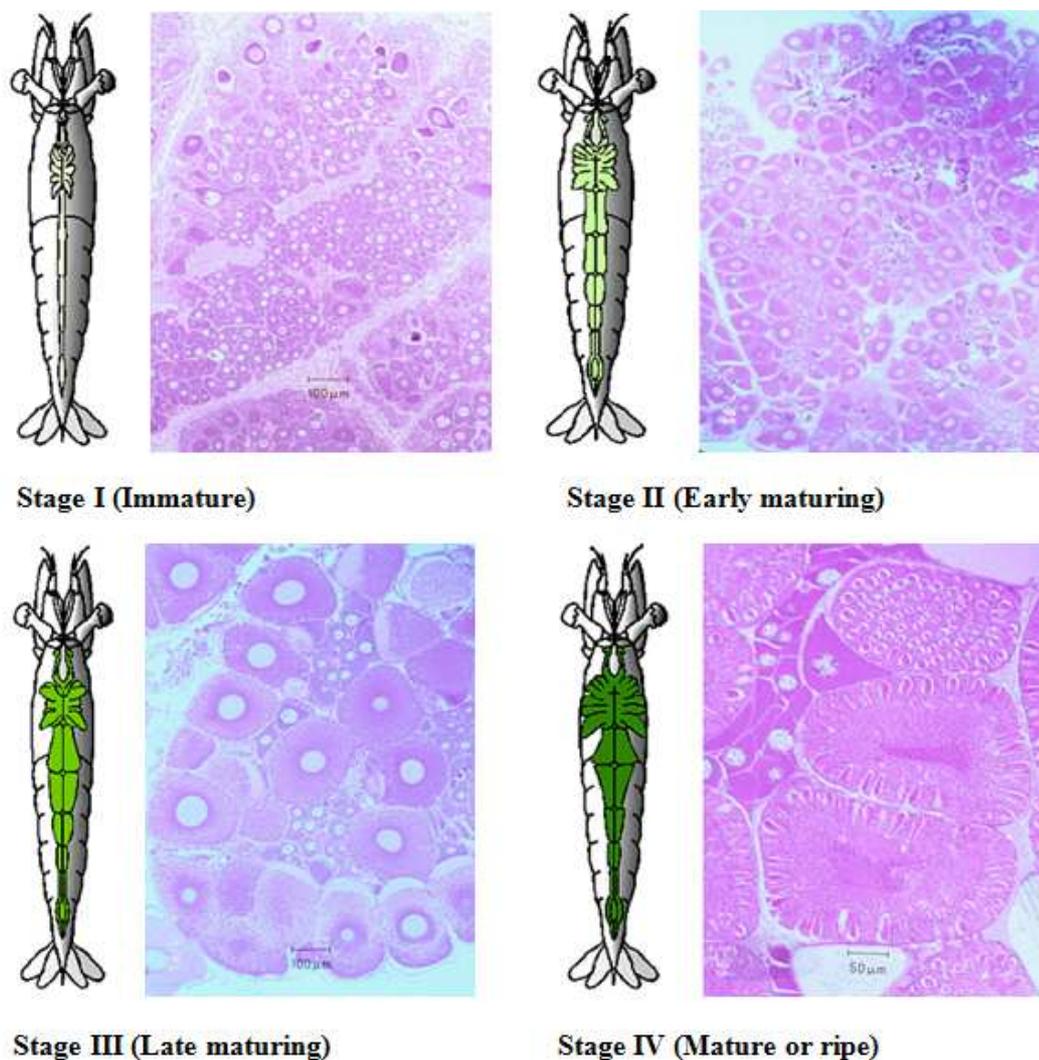
Figure 1.4 Ovarian developmental stages of *P. monodon* visualized externally and conventional histology indicated different stages of oocytes in a particular stage of ovaries.

1.4.5. Changes of ovarian morphology during oogenesis

The reproductive cycle of *P. monodon* includes a series of events starting from activation of primordial germ cells to the differentiation of highly yolk-equipped ova. Staging of reproductive development based on the morphological characters of ovaries is not appropriate. Correct staging of reproductive maturity requires more detailed characteristics like size of the germ cells, nature and arrangement of oogonial cells in ovaries, which is possible through microscopical investigations (Diwan *et al*., 2009). Light microscopic examinations of ovaries of *P. monodon* at different staged

of their maturity revealed the chain of nuclear and cytoplasmic changes that occur inside the developing ovaries. Oogonial cells developed from the primordial germ cells get transforms into the mature ova with sufficient yolk for the development of the embryo. A series of dramatic as well as complicated changes take place in the developing oocyte during its developmental phase. Based on the changes that occur inside the cytoplasm and nucleus of the growing oocytes, process of oogenesis may by classified into six different phases, such as immature, previtellogenic, early vitellogenic, late vitellogenic, mature or gravid and spent oocytes (Diwan *et al*., 2009).

1.4.6 Development of oocytes in different stages of ovaries of *P. monodon*

From conventional histology, the ovarian tissue of *P. monodon* contains a thin ovarian wall, encompass the ovaries. It consists of 3 layers; a thin outer most pavement epithelium, an inner layer of germinal epithelium and a relatively thick layer of connective tissue in between. Blood capillaries are also present in the ovarian wall. A germinal zone (GZ) is found on the lateral periphery in the form of a thin band and this is the "zone of proliferation" from which the displacement of oogonial cells takes place (Figure 1.5). Invasion of this zone into the ovarian lobes is observed from the ventral portion of the ovary. The young oocytes moved farther from the germinal zone upon maturation so the developing oocytes and ova are found towards the center of each ovarian lobe.

Immature stage

An active zone of proliferation with clusters of developing oogonial cells is the characteristic feature of immature ovaries (Figure 1.5). The primary and secondary oogonial cells are arranged in a graded manner in the ovaries so that the growing secondary oogonial cells are shifted to the interior. The nuclei of the primary oogonial cells are not conspicuous. These primary oogonial undergo mitotic division and gives rise to the secondary oogonia. The secondary oogonial cells possess a conspicuous nucleus.
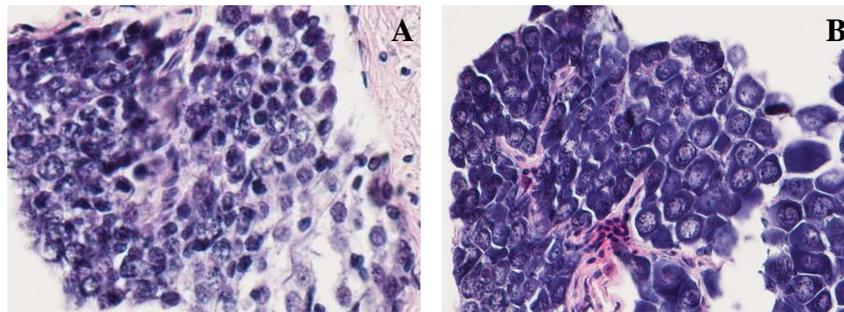
Figure 1.5 Light microscopy showing an immature ovaries. A: germinal zone with developing oogonial cells and B: the oogonial cells. Hymatoxylin and Eosin (HE) staining (40 x) (Preechaphol, 2008).

The oogonial cells appear round ultrastructurally and their large nucleus occupies approximately 80% of the cell volume (Figure 1.5). The oolemma is smooth and without any particular morphological specializations at this stage. The diffused electron-dense chromatin materials as well as small granule like round nucleoli are not present in the nucleolemma of these oogonial cells. Electron-loose cytoplasm in these oogonial cells contains only some small granules and filamentous materials (Figure 1.5). Other cell organelles are not at all visible at this stage of development.

Previtellogenic stage (stage I ovaries)

The most striking feature of previtellogenic ovaries is the presence of highly basophilic primary oocytes with much more increased cytoplasmic volume than that of the oogonial cells. These primary oocytes develop from the secondary oogonial cells through meiotic division. The nuclei contain 10 to 18 centrally located, deeply stained granules like nucleoli and prominent chromatin materials in their nucleoplasm. These oocytes are devoid of individual follicle cell layers. The early previtellogenic oocytes are characterized by the displacement of nucleoli towards the periphery of the nucleoplasm (Figure 1.6).

At the late of this stage, oocytes begin their folliculogenesis around the outer surface of each oocyte. The follicle cells in this stage are rectangular or cubical and a highly vacuolated conspicuous nucleus is also present.
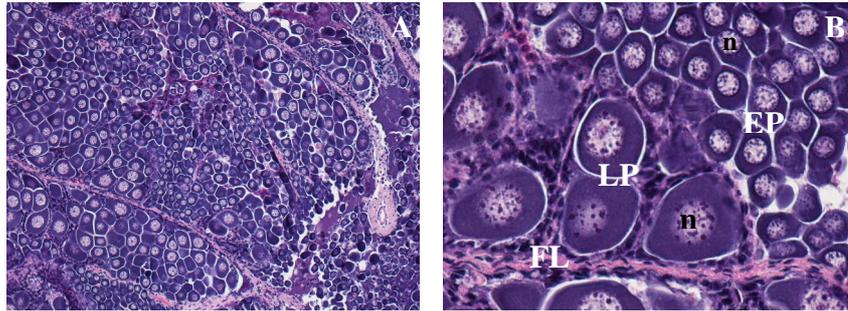
Figure 1.6 Light microscopy showing a previtellogenic ovaries. Hymatoxylin and Eosin (HE) staining (10 x; A and 40 x; B). EP = early previtellogenic oocyte, LP = late previtellogenic oocyte, n = nucleus, FL = follicular layers (Preechaphol, 2008).

Early vitellognic stage (stage II ovaries)

Early vitellogenic ovaries are sudden two fold increase in the size of the oocytes. The nature of the cytoplasm changes suddenly from homogenous to vesicular and little bit granular. From the granular nature of the cytoplasm and its sudden increase in the cytoplasmic volume it is seen that during this stage onwards the oocytes started its active accumulation of yolk. The granular nature is due to the accumulation of oil globules in the cytoplasm, which is the characteristic feature of the primary vitellogenic oocytes. Consequently the nucleolar materials made a halo around the nucleus due to their circular arrangements in the peripheral karyoplasms (Figure 1.7).

During this stage, the formation of follicle cells around each individual oocyte occurs. Because of the sudden increase in the cytoplasmic volume the follicle cells stretched considerably and consequently their thickness decreased (Figure 1.7).
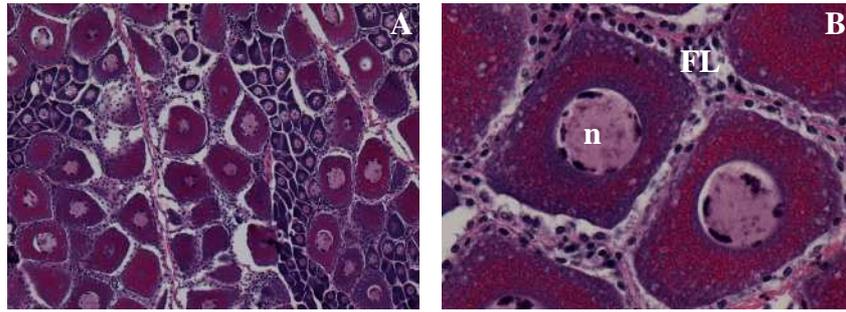
Figure 1.7 Light microscopy showing an early vitellogenic ovaries. Hymatoxylin and Eosin (HE) staining (10 x; A and 40 x; B). n = nucleus, FL = follicular layers (Preechaphol, 2008).

Late vitellogenic stage (stage III ovaries)

Late vitellogenic oocytes are characterized by the appearance of radially arranged well developed of the oocytes. The ooplasm of which is full of eosinophilic yolk granules. The hypertrophied nucleus as well as nucleolus of follicle cells becomes conspicuous during this stage. Due to the increase in the volume of the oocytes, the follicle cells encompassing them stretch further and appear as a narrow band of flattened cells around each oocyte (Figure 1.8).
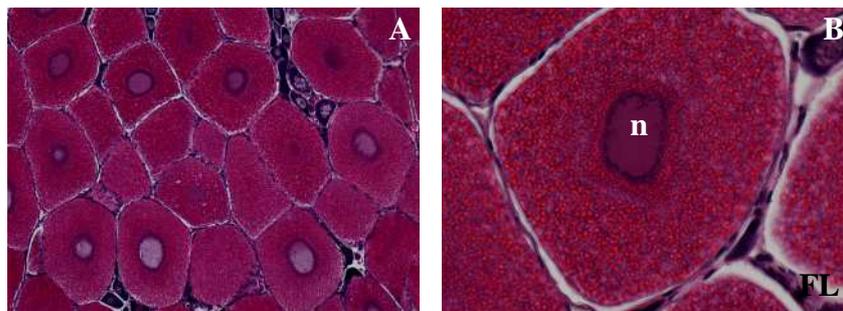
Figure 1.8 Light microscopy showing an late vitellogenic ovaries. Hymatoxylin and Eosin (HE) staining (10 x; A and 40 x; B). n = nucleus, FL = follicular layers (Preechaphol, 2008).

Mature stage (stage IV ovaries)

Mature oocytes develop club shaped structures of the cortical rods in the peripheral ooplasm. The vitellin envelope is visible just at the top of the cortical

crypts (Figure 1.9). At early of this stage, the oocytes appear with a very thin rim of follicle cells around it. The follicle cells disappear from around the oocytes when reach to the late of this stage. Final maturation is finish when germinal vesicle breakdown (GVBD) (Figure 1.9). After GVBD, the spawning immediately proceeds.
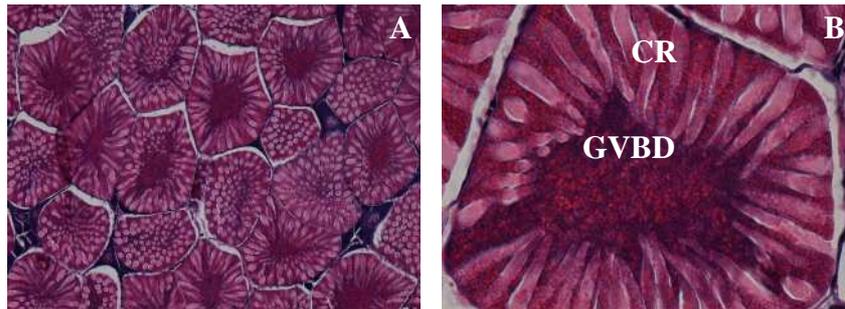
Figure 1.9 Light microscopy showing mature ovaries. Hymatoxylin and Eosin (HE) staining (10 x; A and 40 x; B). CR = cortical granules, GVBD = germinal vesical breakdown (Preechaphol, 2008).

Spent stage (Stage V Ovaries)

Oocytes of the spent ovary are mostly primary oocytes similar to those of pre-vitellogenic oocytes in the immature ovary. Resorbing oocytes are also observed in between the empty thicker follicle cells caused by the retraction of the follicle cells from the oocytes. The zone of proliferation is active with irregular primary oogonial cells and developing oocytes at certain portions of the spent ovary. Some regressing atretic oocytes were commonly observed in the spent ovary.

1.4.7 Hormonal control in shrimp

Biological and physiological processes (growth, reproduction, body color, and metabolism etc.) are hormonal controlled (Figure 1.10). Knowledge from shrimp endocrinology is necessary to develop the hormonal manipulation techniques in these species.

In the female shrimp, gonad maturation is the result of rapid synthesis and accumulation of vitellogenin by the oocytes during vitellogenesis (Figure 1.11) (Sin yan kun *et al*., 2004). The current practice to stimulate ovarian development by eyestalk ablation is stressful to the animal, and it could lead to mortality. In order to

avoid eyestalk ablation, different techniques to stimulate ovarian development such as maturation diet and hormone stimulation have been attempted. The use of these techniques to variable success reveals our lack of general understanding of oocyte development in crustacean. Therefore, the knowledge on hormonal factors influencing the ovarian and oocyte development in crustacean is necessary to develop the hormonal manipulation techniques in shrimp.
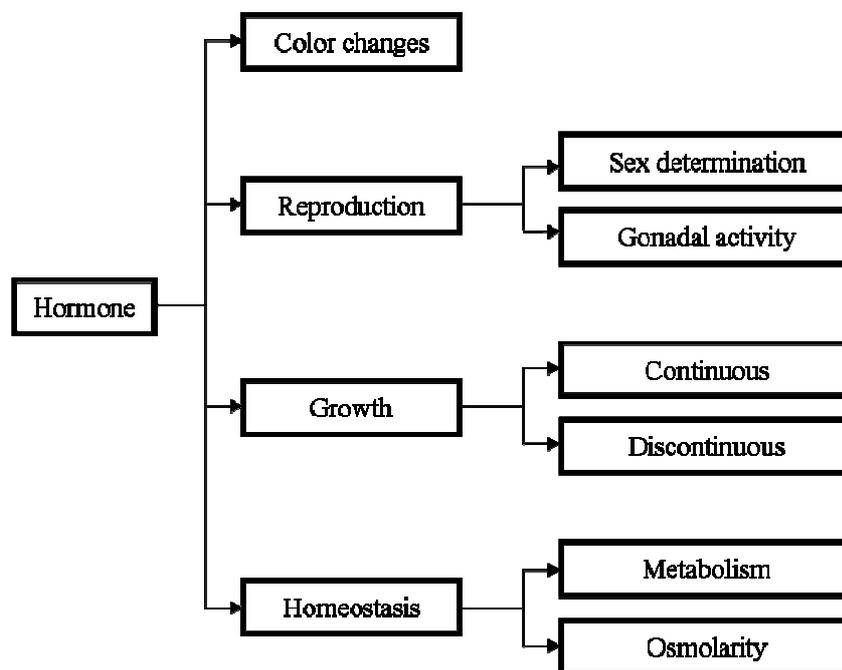
Figure 1.10 Diagram illustrating the hormonal controls of physiological processes in penaeid shrimp.

Hormonal regulation is one of the several factors that control the female reproduction. The female reproductive hormone was produced from various tissues (Figure 1.7) including eyestalks, mandibular organ and Y-organ.

1.4.7.1 Eyestalk hormones

It is well-known that eyestalk ablation induces ovarian development and oviposition. This effect has been attributed to the presence of a vitellogenesis-inhibiting factor present in the MTXO-SG neurosecretory system (Figures 1.8 and 1.9). A group of neuropeptides that directly affect reproductive performances in

crustacean have been identified. Many of these molecules belongs share a high degree of similarity with crustacean hyperglycemic hormone (CHH).

Gonad inhibiting hormone (GIH) is secreted from the X-organ in the eyestalk, and inhibits the synthesis of vitellogenin in the ovary. The peptides also have an impact on the males, and hence it is called gonad inhibiting hormone instead of vitellogenesis inhibiting hormone (Huberman, 2000).

1.4.7.2 Ecdysteroids

Ecdysteroids primarily serves as molting hormones in crustaceans, a similar function as in other arthropods. Their roles in reproduction have been suspected. As reproductive development in crustacean often occurred at the same period of continuing somatic growth (molting), one cannot overlook the importance of the molting cycle when considering various aspects of crustacean reproduction. The roles of ecdysteroids in reproduction are difficult to generalize as each group of species has different reproductive strategies in relation to the timing between molting and reproductive development. For examples, active vitellogenesis and spawning in peneaid shrimp occurs during the prolonged premolt period before ecdysis, while *Macrobrachium* spp. alternates between reproductive molt and non-reproductive molt (Subramoniam, 2000).

Ecdysteroids are synthesized by the Y-organs in crustacean, secreted into the hemolymph, and distributed to target tissues for conversion into active forms; 20-hydroxyecdysone (20E; also called crustecdysone, ecdysterone; Goodwin, 1978) (Subramoniam 2000). There is also evidence that ecdysteroids was also synthesized in ovaries and testes of crustaceans (Brown et al. 2009; Styrishave *et al*. 2008). Its production is negatively regulated by the molt-inhibiting hormone (MIH), secreted from the X-organ, and positively regulated by methyl farnesoate (MF). Important forms of ecdysteroids are 20-hydroxyecdysone (20E or 20HE) and ponasterone A (PoA).
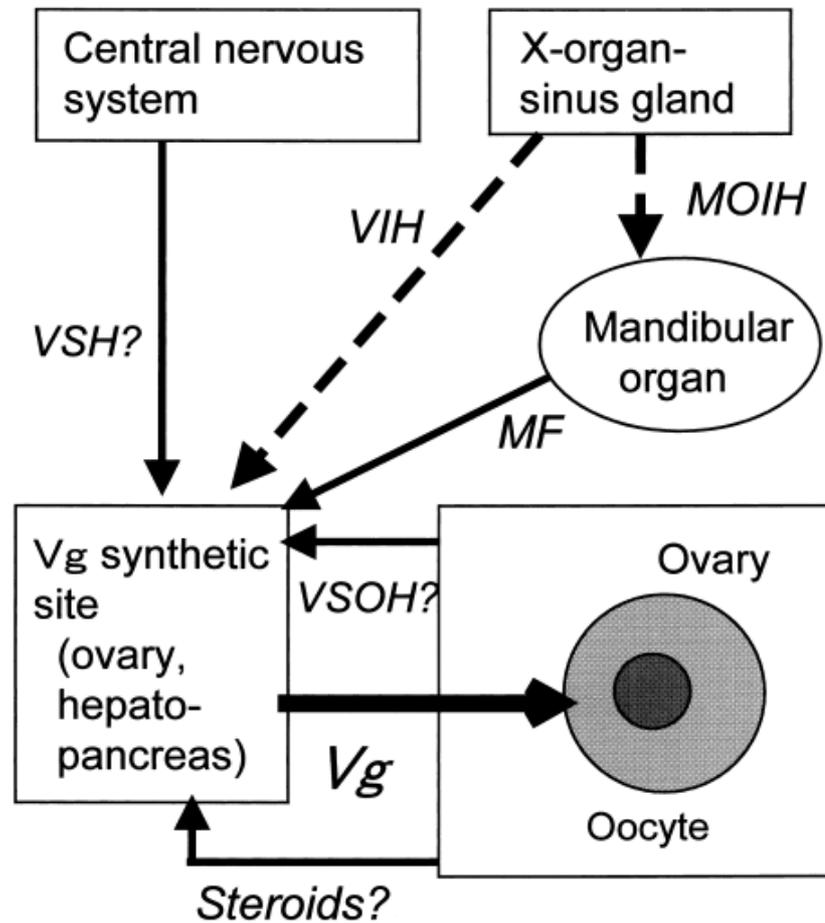
Figure 1.11 Diagram of the endocrine control of vitellogenisis in shrimp (Takuji O. *et al*. 2004)

1.4.7.3 Prostaglandins and other eicosanoids

It has been proposed that prostaglandins play a role in ovarian maturation in crustacean. Prostaglandins are derived from fatty acids such as arachidonic acid or eicosapentaenoic acid. Prostaglandins as a group have many physiological functions in many animals. In invertebrates, prostaglandins were found in sponges, cnidarians, nematodes, platyhelminthes, mollusks, annelids, crustaceans, acari, urochordates, and insects (Rowley *et al*. 2005; Stanley, 2006). Their known functions in invertebrates are diverse including immunity, homeostasis, feeding, larval settlement, and reproduction (Rowley *et al*. 2005).

The reproduction-related functions of prostaglandin in other animals appeared to occur at several stages of oocyte maturation (Rowley *et al*. 2005; Stanley, 2006). So far the concentration profile of prostaglandins in crustaceans during ovarian development suggested its importance at the end of oocyte maturation. This hypothesis still needs to be confirmed with more research. Since precursor of prostaglandins is fatty acids, dietary manipulation could have some effects on prostaglandins in crustaceans.

1.4.7.4 Vertebrate-type steroid hormones

Steroid hormones play important roles in vertebrate reproductive biology. The classical pathways of steroid hormones, including estrogens, androgens, and progestogens, are mediated by specific receptors that are localized in the nucleus of target cells. Steroid hormone receptors are members of a superfamily of ligand-modulated transcription factors that include nuclear progestogen receptor (PR), androgen receptor (AR), glucocorticoid receptor (GR), mineralocorticoid receptor (MR), vitamin D receptor, and the retinoic acid receptor (1). Understanding the roles of steroid hormones on vitellogenesis may lead to the development of ways to induce ovarian maturation in decapod crustaceans (Yano and Hoshino, 2006).

Vertebrate-type steroids have been found in many groups of invertebrate including crustacean (Lafont and Mathieu 2007). Steroids such as progesterone (PG), 17α-hydroxyprogesterone (17-OHP), testosterone, and 17β-estradiol (E2) are present in many crustacean species including kuruma prawn *M. japonicus* (Cardoso *et al*. 1997), giant freshwater prawn *M. rosenbergii* (Martins *et al*. 2007), black tiger shrimp *P. monodon* (Quinitio *et al*. 1994), mud crab *Scylla serrata* (Warrier *et al*. 2001).

Quinitio *et al* (1994) analyzed the profile of steroid hormones in relation to vitellogenin activity in female *P. monodon.* Progesterone and 17β-estradiol were detected in the hemolymph only in shrimp with mature ovaries, while the level was low or undetectable in the hemolymph in those with immature ovaries (Quinitio *et al*. 1994) . The concentration of progesterone showed a positive correlation with vitellogenesis (Quinitio *et al*. 1994).

STEROID HORMONE PATHWAY

Cholestesterol → Pregnenolone

Pregnenolone → Progesterone

Progesterone → Corticosterone & Aldosterone

Cholestesterol → 17-OH-Pregnenolone

Pregnenolone → 17-OH-Pregnenolone

17-OH-Pregnenolone → 17a-OH-Progesterone

Progesterone → 17a-OH-Progesterone

17a-OH-Progesterone → Cortisol

17-OH-Pregnenolone → DHEA

17a-OH-Progesterone → Androstenedione

DHEA ↔ Androstenedione

Androstenedione → Eestrone

Eestrone → Estriol

DHEA ↕ Androstenediol

Androstenedione ↕ Testosterone

Eestrone ↕ Estradiol

Testosterone → Estriol

Figure 1.12 Steroid hormone biosynthetic pathway
(http://www.ntptalk.com/articles/bio-identical-hormone-replacement.php)

Okumura and Sakiyama (2004) compared the hemolymph concentrations of several vertebrate-type steroids in kuruma prawn during both natural and induced (by eyestalk ablation) ovarian development. They observed no correlation and concluded that vertebrate-type steroids were not involved in ovarian development of kuruma prawn (Okumura and Sakiyama, 2004).

Yano and Hoshino (2006) reported that 17β-estradiol induced vitellogenesis and oocyte development in previtellogenic ovary of kuruma prawn *in vitro*. They proposed that 17β-estradiol is an ovarian vitellogenesis-stimulating hormone (OVSH) in immature decapods crustaceans.

Gunamalai et al (2006) monitored the concentration of 17β-estradiol and progesterone in the hemolymph, ovary and hepatopancreas of mole crab *Emeriata asiatica* and freshwater prawn *M. rosenbergii.* Both 17β-estradiol and progesterone peaked in all tissues during the intermolt period of the reproductive molt cycle in freshwater prawn, and the basal level of 17β-estradiol was detectable in the ovary and hepatopancreas during the non-reproductive molt cycle.

Martins et al (2007) performed similar experiment to monitor the hemolymph concentration of 17α-hydroxyprogesterone, testosterone, and 17β-estradiol in female freshwater prawn *M. rosenbergii* and correlated the results with each stage of ovarian development. They reported high concentration of 17α-hydroxyprogesterone throughout the reproductive cycle and the concentration peaked during pre-vitellogenic (*M. rosenbergii* ovarian stage 2) and late vitellogenic/mature (*M. rosenbergii* ovarian stage 5) (Martins et al. 2007). The concentration of the glucuronide-conjugated 17β-estradiol also peaked during the previtellogenis stage, while there was no significant variation in testosterone concentration.

Dietary source of vertebrate type steroids might play a role in ovarian development of penaeid shrimp. Meunpol *et al* (2007) extracted PG and 17α-OHP from polychaetes *Perinereis* sp., a commonly used component in maturation diets for shrimp broodstock. They also reported that PG and 17α-OHP, both from the polychaetes extracts and synthetic, are capable of stimulating development of *P. monodon* oocytes from pre-vitellogenic stage to maturation (cortical rods) (Meunpol *et al*. 2007). It is possible the vertebrate steroids from polychaetes could stimulate the ovarian development in broodstock shrimp or supplement steroids produce by the shrimp.

Estrogen and androgen receptors were detected in the brain and thoracic ganglion of mud crab *Scylla paramamosain* using immunocytochemistry method (Ye *et al*. 2008). The presence of these receptors in the central nervous system suggested the possibility that estrogen and androgen may act as negative feedback in the endocrine system of crustacean (Ye *et al*. 2008).

The effects of 17β-estradiol on induction of vitellogenin synthesis and oocyte development were investigated *in vitro* by incubation of previtellogenic ovary of immature kuruma prawn (*Marsupenaeus japonicus*) with Medium 199 supplemented with 17β-estradiol for 3 days. Vitellogenin concentrations in ovary incubated in media containing 3.6 nM, 36.7 nM, 367 nm and 3671 nM 17β-estradiol were significantly ($P < 0.01$) greater than that of pure ethanol vehicle. The rate of globule stage oocyte in previtellogenic ovaries incubated with various concentrations of 17β-estradiol compared to the control was different. However, there was no difference on this parameter among ovaries incubated with 3.6, 36.7, 367 and 3671 nM of 17β-estradiol (Yano and Hoshino, 2006).

Recently, the full-length cDNA of *progestin membrane receptor component 1* (*Pgmrc1*) of *P. monodon* was successfully identified and characterized. *Pgmrc1* was 2015 bp in length containing an ORF of 573 bp corresponding to a polypeptide of 190 amino acids. Northern blot analysis revealed a single form of Pgmrc1 in ovaries of *P. monodon.* Quantitative real-time PCR indicated that the expression level of *Pgmrc1* mRNA in ovaries of both intact and eyestalk-ablated broodstock was greater than that of juveniles ($P < 0.05$). *Pgmrc1* was up-regulated in mature (stage IV) ovaries of intact broodstock ($P < 0.05$). Unilateral eyestalk ablation resulted in an earlier up-regulation of Pgmrc1 since the vitellogenic (II) ovarian stage. Moreover, the expression level of Pgmrc1 in vitellogenic, early cortical rod and mature (II–IV) ovaries of eyestalk-ablated broodstock was greater than that of the same ovarian stages in intact broodstock ($P < 0.05$). *Pgmrc1* mRNA was clearly localized in the cytoplasm of follicular cells, previtellogenic and early vitellogenic oocytes. Immunohistochemistry revealed the positive signals of the Pgmrc1 protein in the follicular layers and cell membrane of follicular cells and various stages of oocytes.

In addition, a *progesterone receptor-related protein p23* (*Pmp23*) gene homologue was isolated from EST analysis of the cDNA library established from vitellogenic ovaries of *P. monodon*. The full length cDNA of *Pmp23* was further characterized by RACE-PCR and it was 1943 bp, comprising an ORF of 495 bp corresponding to 164 amino acid residues and the 5′ and 3′ UTRs of 7 and 1441 bp, respectively. The predicted molecular mass and *p*I of the deduced Pm-p23 protein was

19.07 kDa and 4.39, respectively. Quantitative real-time PCR analysis revealed that the expression levels of *Pmp23* in ovaries of both intact and eyestalk-ablated broodstock were significantly greater than that of juveniles (4-month-old shrimp) ($P < 0.05$). *Pmp23* was up-regulated since stage II ovaries of intact and stage III ovaries of eyestalk-ablated *P. monodon* broodstock ($P < 0.05$). The mRNA level of *Pmp23* after spawning was not significantly different from stages II–IV ovaries of intact broodstock ($P > 0.05$). In situ hybridization indicated that the *Pmp23* mRNA was localized in ooplasm of previtellogenic oocytes. Recombinant Pmp23 protein was successfully expressed in vitro and its polyclonal antibody was successfully produced. Western blot analysis indicated that the level of ovarian Pmp23 protein peaked at the vitellogenic stage and decreased as oogenesis progressed.

No report of progesterone, estrogen and androgen receptors in other crustacean species at present. The presence of both receptors in the central nervous system of crustacean indicates that vertebrate type steroids might play a role in crustacean endocrine system. Assessing the role of vertebrate steroids in crustaceans could have many applications. The effect of dietary vertebrate steroids on ovarian maturation suggested potential uses of these steroids to stimulate reproductive development.

1.4.8 Control of cortical rods formation and germinal vesicle breakdown

As the eggs of penaeid shrimp reached maturation, cortical rods start forming around the oocytes. Its function during the egg activation process includes establishment of protective jelly layer (Clark *et al*. 1990), and contribution to the induction of the sperm acrosome reaction (Kruevaisayawan *et al*. 2007).

Medina *et al* (1996) reported the inability of pond-reared shrimp *Penaeus kerathurus* to synthesie cortical rods leading to the lack of fully mature oocyes (stage IV). It was suspected that hormones play a more significant role since the sizes of oocytes are not different between then wild and pond-raised shrimp. Eyestalk ablated shrimp was not used in Medina et al experiment.

Palacios *et al* (2003) reported no significant differences in eyestalk-ablated wild or pond-reared *L. vannamei* oocyte's ability of form cortical rods while Peixoto

et al (2008) reported significantly higher frequency of oocytes with cortical rods in domesticated shrimp than that of the wild shrimp.

There are several potentials biomarkers for cortical rods formation. Thrombospondin (TSP) major protein component of cortical rods were cloned and characterized in kuruma prawn *M. japonicus* (Yamano *et al*. 2004) and Chinese shrimp *F. chinensis* (Sun *et al*. 2006) High expression of cathepsin C gene in the ovaries of kuruma prawn coincides with the onset of cortical rod formation suggesting that the gene might play a role during CR synthesis and final oocyte maturation (Qiu *et al*. 2005). The level of cortical rod protein (CRP) and MjTSP expression in the ovary of kuruma prawn did not change after eyestalk ablation, but the protein levels in the ovary did increase (Okumura *et al*. 2006). The results suggested that the regulatory mechanism of the CRP and MjTSP control is occurred during translation.

Yi et al (2005) reported high CRP expression during the previtellogenic and early vitellogenic stage. They suggested that CRP and VG synthesis are regulated by closely-related mechanisms. Cortical rod protein has been cloned and characterized in a species whose oocytes does not form a cortical rod structure such as giant freshwater prawn *Macrobrachium rosenbergii* (Kim *et al*. 2007).

One important step toward oocyte maturation that has yet to be extensively studied in crustacean is that of germ-vesicle breakdown (GVBD), the breakdown of the nuclear membrane surrounding the chromosome prior to meiosis resumption of the oocyte.

In vertebrate, GVBD and oocyte maturation are triggered by gonadotropins, luteinizing hormone (LH) and follicle stimulating hormone (FSH). In fish and amphibians, a steroid hormone intermediate, maturation inducing hormone, is also involved in oocyte maturation (Jalabert 2005; Patio *et al*. 2001). Examples of maturation inducing hormone in fish include 17,20β-dihydroxy-4pregnen-3one (Jalabert 2005) and 17β 2-hydroxy-estradiol (Mishra and Joy 2006).

Yano (1995) hypothesized that final maturation in penaeid shrimp can be induced by prostaglandin whose concentration is related to fatty acid precursors (such as arachidonic acid and eicosapentaenoic acid) in the diet of shrimp. Other

stimulating factor can include mating (for some species), UV-irradiated water, temperature shock or filtration of seawater.

Serotonin (5-HT) in oocyte maturation, particularly GVBD, has been observed in several animal phyla. In mollusks, evidence of serotonin's involvement in oocyte maturation and spawning was observed in zebra mussel *Dreissena polymorpha* (Ram et al. 1996), oyster *Crassostrea gigas* (Kyozuka *et al*. 1997), Manila clam *Ruditapes philippinarum* (Fong *et al*. 1997), and scallop *Argopecten purpuratus* (Martínez et al. 2005). Two separate pathways involving either serotonin or calcium ion was shown to induce oocyte maturation in big ribbon worms *Cerebratulus* sp. (Stricker and Smythe 2000). The involvement of protein kinases and protein phosphatases in the process were also reported in big ribbon worms (Stricker and Smythe 2006a; Stricker and Smythe 2006b). The role of serotonin in oocyte maturation in mammals was also suggested (Dubé and Amireault 2007).

Wongprasert et al (2006) reported the effect on serotonin induction of ovarian maturation and spawning in *P. monodon.* They noted that spawning occurred while the ovaries were in Stage III and the quality of spawns (numbers of eggs, hatching rate, and numbers of nauplii) was better in serotonin-induced group. The stage of ovarian maturation was determined by visual observation in their study, but the correlation to oocyte development was not made. Nevertheless, the study provides the promising evidence for serotonin beneficial role on crustacean reproduction.

1.4.9 Nutrigenomics and expression of genes involved with reproduction of *P. monodon*

Nutrigenomics is the studies of effects of diet supplement on molecular expression of gene, protein or important metabolites. Accordingly, it provides a basis for understanding the biological activity of diet supplement in the examined animal species. Nutrigenomics has also been described for the influence of genetic variation on nutrition by correlated with gene and/or protein expression. Therefore, nutrigenomics promotes an increased understanding of how nutrition influences metabolic pathways and homeostatic control.

In this thesis, effects of exogenous administration feed supplementation of 17ß-estradiol on expression of several genes (*asparaginyl tRNA synthetase*, *aspartate aminotransferase*, *Mago nashi* and *nuclear hormone receptor 96*) previously identified by EST analysis were examined.

-*P. monodon asparaginyl tRNA synthetase*

The tRNA synthetases such as aminoacyl tRNA synthetases play a major role in the translational process during protein synthesis. A homologue of *asparaginyl tRNA synthetase* (*PmAtNS*, *E*-value = 7e-75) was identified by EST analysis. The full-length cDNA of this gene was 1857 bp with an ORF of 1680 bp corresponding to a polypeptide of 560 amino acids.

PmAtNS significantly matched *asparaginyl-tRNA synthetase* of *Aedes aegypti* (*E*-value = 0.0). The calculated *p*I and MW of *PmAtNS* were 6.00 and 64.06 kDa, respectively. An anti -codon binding domain (positions 139 – 219, *E*-value = 9.10e-15) and tRNA synthetases class II domain (positions 236 – 556, *E*-value = 3.70e-76) were found in the deduced PmAtNS protein (Sittikhankeaw, 2006)

-*P. monodon aspartate aminotransferase*

Aspartate aminotransferase catalyzes the reversible transamination between dicarboxylic amino and a keto acids essentially needs in nitrogen and carbon metabolism in the cells. Aspartate aminotransferase activities are usually used as general indicators of the functioning of vertebrate liver. The crustacean hepatopancreas is assumed homologous to the mammalian liver and pancreas (Gibsonand Barker, 1979) and is responsible for major metabolic events, including enzyme secretion, absorption and storage of nutrients, molting, and vitellogenesis (Chanson and Spray, 1992).

Using RACE-PCR, the full-length cDNA of *P. monodon AST* (*PmAST*) was successfully characterized and it was 1944 bp in length with the 5′- and 3′UTRs of 232 and 464 bp (excluding the poly A tail), respectively. The ORF of *PmAST* was 1248 bp corresponding to a polypeptide of 415 amino acids. The closest sequence to *PmAST* was *aspartate aminotransferase* of *Tribolium castaneum* (*E*-value = 5e-176). Its calculated *p*I and MW were 8.55 and 43.29 kDa. An *aminotransferase* domain was

found at positions 20 - 388 (E-value = 8.00e-123) of the deduced PmAST protein. (Sittikhankeaw, 2006)

-*P. monodon mago nashi*

The cDNA of *P. monodon protein mago nashi* was characterized by EST analysis and the full-length cDNA was obtained (Preechaphol et al., 2007). *P. monodon protein mago nashi* was 858 bp in length composing of an ORF of 444 bp corresponding to a polypeptide of 147 amino acids and the 5′ and 3′ UTRs of 27 and 387 bp, respectively. It significantly matched *protein mago nashi* of *Apis mellifera* (E-value = 5 x 10^{-76}). The predicted molecular mass and *p*I of the deduced Pm- protein mago nashi was 17.27 kDa and 5.72, respectively. *P. monodon* protein mago nashi contained Mago nashi domains originally identified in *Drosophila* which is essential for female germplasm assembly (Newmark and Boswell, 1994).

-*P. monodon son of sevenless*

Son of sevenless (SOS) is a dual specificity guanine nucleotide exchange factor (GEF) that regulates both Ras and Rho family GTPases and thus is uniquely poised to integrate signals that affect both gene expression and cytoskeletal reorganization (Yang, 2006). The *SOS* gene functions in signaling pathways initiated by the sevenless and epidermal growth factor receptor tyrosine kinases (Bonfini, 1992).

The partial cDNA sequence of *P. monodon SOS* was previously identified by EST analysis (Clone No. AG-N-N01-1056-W, *E*-value = 2e-61) but the full length cDNA of this gene in penaeid shrimp has not been characterized.

- *P. monodon nuclear hormone receptor 96*

Nuclear hormone receptor proteins is recognized as a class of ligand activated proteins that, when bound to specific sequences of DNA, serve as on-off switches for transcription with in the cell nucleus as well as the continual regulation of reproductive tissues. Nuclear hormone receptors regulate gene expression by interacting with specific DNA sequences upstream of their target genes.

Steroid or nuclear hormone receptors constitute an important superfamily of transcription regulators that are involved in widely diverse physiological functions, including control of embryonic development, cell differentiation and homeostasis. The receptors function as diametric molecules in nuclei to regulate the transcription of target genes in a ligand-responsive manner. Nuclear hormone receptors consist of a highly conserved DNA-binding domain that recognizes specific sequences, connected via a linker region to a C-terminal ligand-binding domain. In addition, certain nuclear hormone receptors have an N-terminal modulatory domain. The ligand-binding domain acts in response to ligand binding, which caused a conformational change in the receptor to induce a response, thereby acting as a molecular switch to turn on transcriptional activity.

The partial cDNA sequence of *P. monodon nuclear hormone receptor 96* was previously identified by EST analysis (Clone No. LP-S01-0404-LF, *E*-value = 2e-37) but the full-length cDNA of this gene in penaeid shrimp has not been characterized.

CHAPTER II
MATERIALS AND METHODS

2.1 Nucleic acid extraction

2.1.1 Genomic DNA extraction

Genomic DNA was extracted from a piece of pleopod of each shrimp using a phenol-chloroform-proteinase K method (Klinbunga et al., 1999). A piece of pleopod tissue was dissected out from a frozen pleopod and placed in a prechilled microcentrifuge tube containing 500 μl of the extraction buffer (100 mM Tris-HCl, 100 mM EDTA, 250 mM NaCl; pH 8.0) and briefly homogenized with a micropestle. SDS (10%) and RNase A (10 mg/ml) solutions were added to a final concentration of 1.0 % (w/v) and 100 μg/ml, respectively. The resulting mixture was then incubated at 37°C for 1 hour. At the end of the incubation period, a proteinase K solution (10 mg.ml) was added to the final concentration of 300 μg/ml and further incubated at 55°C for 3-4 hours. An equal volume of buffer-equilibrated phenol : chloroform : isoamylalcohol (25:24:1) was added and gently mix for 10 minutes. The solution was centrifuged at 10,000 rpm for 10 minutes at room temperature. The upper aqueous phase was transferred to a newly sterile microcentrifuge tube. This extraction process was then repeated once with phenol : chloroform : isoamylalcohol (25: 24: 1) and once with chloroform : isoamylalcohol (24 : 1). The aqueous phase was transferred into a sterile microcentrifuge. One-tenth volume of 3 M sodium acetate, pH 5.2 was added. DNA was precipitated by an addition of two volume of prechilled absolute ethanol and mixed thoroughly. The mixture was incubated at -80°C for 30 minutes. The precipitated DNA was recovered by centrifugation at 12,000 rpm for 10 minutes at room temperature and washed twice with 1 ml of 70% ethanol (5 minutes and 2 – 3 minutes, respectively). After centrifugation, the supernatant was removed. The DNA pellet was air-dried and resuspended in 50 – 80 μl of TE buffer (10 mM Tris-HCl, pH 8.0 and 0.1 mM EDTA). The DNA solution was incubated at 37 ^{o}C for 1 – 2 hours and kept at 4 ^{o}C until further needed.

2.1.2 RNA extraction

Total RNA was extracted from ovaries (or other tissues) of *P. monodon* using TRI Reagent®. A piece of tissue was immediately placed in a mortar containing liquid nitrogen and ground to fine powder. The tissue powder was transferred to a microcentrifuge tube containing 500 μl of TRI Reagent (50-100 mg tissue per 1 ml) and homogenized. Additional 500 μl of TRI Reagent was then added. The homogenate and left for 5 minutes, before adding 0.2 ml of chloroform. The homogenate was vortexed for 15 seconds and left at room temperature for 2-15 minutes and centrifuged at 12,000 rpm for 15 minutes at 4 ^{o}C. The mixture was separated into the lower red, phenol-chloroform phase, the interphase, and the colorless upper aqueous phase. The aqueous phase (inclusively containing RNA) was transferred to a new 1.5 ml microcentrifuge tube. Total RNA was precipitated by an addition of 0.5 ml of isopropanol and mixed thoroughly. The mixture were left at room temperature for 10-15 minute and centrifuged at 12,000 rpm for 10 minutes at 4-25 ^{o}C. The supernatant was removed. The RNA pellet was washed with 1 ml of 75 % ethanol centrifuged at 7,500 rpm for 5 minutes. Total RNA was dissolved in appropriate volume of DEPC-treated H$_2$O for immediately used. Alternatively, the total RNA pellet was kept under absolute ethanol in a -80 ^{o}C freezer for long storage.

2.1.3 Preparation of DNase I-free total RNA

Fifteen micrograms of total RNA were treated with DNase I (0.5 U/1 μg of RNA, Promega) at 37 ℃ for 30 minutes. After the incubation, the sample was gently mixed with a sample volume of phenol : chloroform : isoamylalcohol (25 : 24 : 1) for 10 minutes. The mixture was centrifuged at 12,000 rpm for 10 minutes at 4℃, and the upper aqueous phase was collected. The extraction process was then repeated once with chloroform : isoamylalcohol (24 : 1) and one with chloroform. The final aqueous phase was mixed with one-tenth final sample volume of 3 M sodium acetate (pH 5.2). After that, RNA was precipitated by adding two point five volume of -20 ℃-cold absolute ethanol. The mixture was incubated at -80 ^{o}C for 30 minutes, and the precipitated RNA was recovered by centrifugation at 12,000 rpm for 10 minutes at room temperature. The RNA pellet was then washed twice with 1 ml of -20 ℃ cold

75% ethanol. Alternatively, the RNA pellet was kept in absolute ethanol at -80 °C until required.

2.2 Measuring concentrations of nucleic acids by spectrophotometry and electrophoresis

The concentration of extracted DNA or RNA was estimated by measuring the optical density at 260 nanometre (OD_{260}). An OD_{260} of 1.0 corresponds to a concentration of 50 μg/ml double stranded DNA, 40 μg/ml single stranded RNA and 33 μg/ml oligonucleotide (Sambrook et al., 2001). Therefore, the concentration of DNA/RNA samples (μg/ml) were estimated by multiplying an OD_{260} value with a dilution factor and 50, 40, 33 for DNA, RNA and oligonucleotides, respectively. The purity of DNA samples can be guided by a ratio of OD_{260}/OD_{280}. The ratio much lower than 1.8 indicated contamination of residual proteins or organic solvents whereas the ratio greater than this value indicate contamination of RNA in the DNA solution (Kirby, 1992).

The amount of high molecular weight DNA can be roughly estimated on the basis of the direct relationship between the amount of DNA and the level of fluorescence after ethidium bromide staining after agarose gel electrophoresis. Genomic DNA was run in a 1.0% agarose gel prepared in 1x TBE buffer (89 mM Tris-HCl, 89 mM boric acid and 2.0 mM EDTA, pH 8.3) at 4 V/cm. After electrophoresis, the gel was stained with ethidium bromide (0.5 μg/ml). DNA concentration was estimated from the intensity of the fluorescent band by comparing with that of undigested λDNA.

2.3 Agarose gel electrophoresis

Appropriate amount of agarose was weighed out and mixed with 1x TBE buffer (89 mM Tris-HCl, 8.9 mM boric acid and 2.0 mM EDTA, pH 8.3). The gel slurry was heated until complete solubilization in the microwave. The gel solution was left at room temperature to approximately 55 °C before poured into a gel mould. The comb was inserted. The gel was allowed to solidify at room temperature for approximately 45 minutes. When needed, the gel mould was placed in the gel chamber and sufficient 1x TBE buffer was added to cover the gel for approximately

0.5 cm. The comb was carefully withdrawn. To carry out agarose gel electrophoresis, one-fourth volume of the gel-loading dye (0.25% bromphenol blue and 25% ficoll) was added to each sample, mixed and loaded into the well. A 100-bp DNA ladder or λ-*Hind* III was used as the standard DNA markers. Electrophoresis was carried out at 4 - 5 V/cm until the tracking dye migrated about three-quartered of the gel. After electrophoresis, the gel was stained with ethidium bromide (0.5 µg/ml) for 5 minutes and destained to remove unbound EtBr by submerged in H_2O for 15 minutes. The DNA fragments were visualized under the UV light using a UV transilluminator.

2.4 Isolation and characterization of the partial cDNA sequence of *Nuclear hormone receptor 96 (PmNHR96)* and *son of sevenless (PmSOS)* of *P. monodon* using Rapid Amplification of cDNA Ends-Polymerase Chain Reaction (RACE-PCR)

2.4.1 Preparation of the 5' and 3' RACE template

Total RNA was extracted from ovaries of *P. monodon* using TRI Reagent. The quality of extracted of total RNA was determined by agarose gel electrophoresis. Messenger (m) RNA was purified using a QuickPrep micro mRNA Purification Kit (Amercham Phamacia Biotech) according to the protocol recommended from the manufacturer. RACE cDNA template was prepared by combining 1.5 µg of ovarian mRNA with 1 µl of 5'-CDS primer and 1 µl of 10 µM SMART II oligonucleotide for 5' RACE-PCR and 1 µg of ovarian mRNA with 1 µl of 3' CDS primer A oligonucleotide for 3' RACE-PCR (Table 2.1). The component were mixed and briefly centrifuged. The reaction was incubated at 70 ℃ for 2 minutes and snap-cooled on ice for 2 minutes. The reaction tube was briefly centrifuged. After that, 2 µl of 5x First-Strand buffer, 1 µl of 20 mM DTT, 1 µl of dNTP Mix (10 mM each) and 1 µl of PowerScript Reverse Transcriptase were added. The reaction were mixed by gently pipetting and briefly centrifuged to collect the contents at the bottom of the tube. The reaction was incubated at 42 ℃ for 1.5 hours in an air incubator. The first strand reaction products were diluted with 125 µl of Tricine-EDTA Buffer and heated at 72 ℃ for 7 minutes. The first strand cDNA template was kept at -20 ℃ until needed.

Table 2.1 Primer sequences for the first strand cDNA synthesis and RACE-PCR

Primer	Sequence
SMART II A Oligonucleotide	5′-AAGCAGTGGTATCAACGCAGAGTACGCGGG-3′
3′ RACE CDS Primer A	5′-AAGCAGTGGTATCAACGCAGAGTAC$(T)_{30}$ N_{-1} N-3′ (N=A, C, G orT; N_{-1}= A,G or C)
5′ RACE CDS Primer	5′-$(T)_{25}$ N_{-1} N-3′ (N=A, C, G orT; N_{-1}= A,G or C)
10X Universal PrimerA Mix (UPM)	Long:5′-CTAATACGACTCACTATAGGGCAAGC AGTGGTATCAACGCAG AGT-3′ Short:5′–CTAATACGACTCACTATAGGG C – 3′
Nested Universal Primer A (NUP)	5 –AAGCAGTGGTATCAACGCAGAGT-3′

2.4.2 Primer designed for RACE-PCR

Gene-specific primers (GSPs) were designed from ESTs significantly matched *nuclear hormone receptor 96 (PmNHR96)* (Clone No. LP-S01-0404-LF), *ras GTP exchange factor, son of sevenless (PmSOS)* (Clone No. AG-N-N01-1056-W) (Table 2.2).

2.4.3 RACE-PCR

The same master mix sufficient for 5′ and/or 3′ RACE-PCR and the control reactions was prepared (Tables 2.3 and 2.4). For each 25 μl amplification reaction, 14.0 μl sterile deionized H_2O, 2.5 μl of 10x Advantage$^®$ 2 PCR buffer, 0.5 μl of 10 uM dNTP mix and 0.5 μl of 50x Advantage$^®$ 2 polymerase mix were combined. The reaction was carried out for as described in Table 2.4.

The reaction was carried out for 20 cycles composing of a 94ºC for 30 second, 68ºC for 3 minutes. The primary 5′ and 3′ RACE-PCR products were electrophoretically analyzed. After characterization of primary RACE product, if the discrete expected product is not obtained. The primary PCR product was 50-fold diluted (1μl of the product: 49 μl of TE or deionized water) and amplified with GSP and NUP primer (5′-AAGCAGTGGTATCAACGCAGAGT-3′). The amplification reaction was performed using 5 μl of the dilute PCR product as template using the same condition for the first PCR for 18 cycles. The resulted products are size-fraction

through agarose gels. The expected fragment is elute from the gel, cloned into pGEM-T Easy and further characterized by DNA sequencing.

Table 2.2 Gene-specific primers (GSPs) used for isolation of cDNA sequences of functionally important genes in *P. monodon*

Gene specific primer	Sequence	Tm (°C)
Nuclear hormone receptor 96 (Clone No. LP-S01-0404-LF)		
5´ RACE	R: 5'GACACTTTGCATCTGGTACG-3'	58
3´RACE	F: 5'-ACGTCAATCCGCAAGAAGTCGAACCAC-3'	70
Son of sevenless (Clone AG-N-N01-1056-W)		
5´ RACE	R: 5'CAACCTGTCCTGTGACCGAG-3'	58
5´ RACE	F: 5'CGATGCGCTGACAAGTGCTGGACAAGG-3'	70

Table 2.3 Compositions for amplification of the 5′ end of gene homologues using 5′ RACE-PCR

Component	5′ RACE-PCR	UPM only (Control)	GSP1 only (Control)
5' RACE–Ready cDNA template	1.5 μl	1.5 μl	1.5 μl
UPM (10x)	5.0 μl	5.0 μl	-
GSP1 (10 μM)	1.0 μl	-	1.0 μl
GSP2 (10 μM)	-	-	-
H₂O	-	1.0 μl	5.0 μl
Master Mix	17.5 μl	17.5 μl	17.5 μl
Final volume	25 μl	25 μl	25 μl

Table 2.4 Compositions for amplification of the 3′ end of gene homologues using 3′ RACE-PCR

Component	3′ RACE-PCR	UPM only (Control)	GSP1 only (Control)
5' RACE–Ready cDNA template	1.5 μl	1.5 μl	1.5 μl
UPM (10x)	5.0 μl	5.0 μl	-
GSP1 (10 μM)	1.0 μl	-	1.0 μl
GSP2 (10 μM)	-	-	-
H₂O	-	1.0 μl	5.0 μl
Master Mix	17.5 μl	17.5 μl	17.5 μl
Final volume	25 μl	25 μl	25 μl

Nucleotide sequences of EST and 5′ and 3′ RACE-PCR are assembled and blasted against data previously deposited in the Genbank using BlastX (Altschul et al., 1990; available at http://ncbi.nlm.nih.gov). The protein domain of deduced amino acids of each gene is searched using SMART (http://smart.embl-heidelberg.de/). The p*I* and molecular weight of the deduced protein are estimated using Protparam (http://www.expasy.org/tools/proparam.html).

2.5 Cloning of the PCR-amplified DNA product

2.5.1 Elution DNA fragments from agarose gels

After electrophoresis, the desired DNA fragment was excised from the agarose gel using a sterile scalpel and placed in a pre-weighed microcentrifuge tube. DNA was eluted out from the gel using a HiYield^{TM} Gel Elution Kit (RBC). Five hundred microlitres of the DF buffer was added to the sample and mixed by vortexing. The mixture was incubated at 55°C for 10-15 min until the gel slice was completely dissolved. During the incubation period, the tube was inverted every 2-3 min. A DF column was placed in a collection tube and 800 μl of the sample mixture was applied into the DF column and centrifuged at 6,000 *g* (8,000 rpm) for 30s. The flow-through was discarded. The DF column was placed back in the collection tube. The column was washed by the addition of 500 μl of the ethanol-added Wash Buffer and centrifuged at 8,000 rpm for 30s. After discarding the flow-through, the DF column

was centrifuged for 2 min at the full speed (14,000 rpm) to dry the column matrix. The dried column was placed in a new microcentrifuge tube and 15 μl of the Elution Buffer or water was added to the center of the column matrix. The column was left at room temperature for 2 min before centrifuged for 2 minutes at the full speed to recover the gel-eluted DNA.

2.5.2 Ligation of the PCR product to the pGEM®-T Easy vector

DNA fragments was ligated to the pGEM®-T Easy vector in a 10 μl reaction volume containing 5 μl of 2x Rapid Ligation Buffer (60 mM Tris-HCl, pH 7.8, 20 mM $MgCl_2$, 20 mM DDT, 2 mM ATP and 10% PEG 8000), 3 Weiss unit of T4 DNA ligase, 25 ng of the pGEM®-T Easy vector and approximately 50 ng of the DNA insert. The reaction mixture was incubated overnight at 4 - 8 °C before transformed to *E.coli* JM 109 (or XL1-Blue).

2.5.3 Preparation of competent cells

A single colony of *E. coli* JM109 (or XL1-Blue) was inoculated in 10 ml of LB broth (1% Bacto tryptone, 0.5% Bacto yeast extract and 0.5% NaCl, pH 7.0) with vigorous shaking at 37 °C overnight. The starting culture was then inoculated into 50 ml of LB broth and continued culture at 37 °C with vigorous shaking to OD_{600} of 0.5 to 0.8. The cells was briefly chilled on ice for 10 minutes and recovered by centrifugation at 3,500 rpm for 10 minutes at 4 °C. The pellets were resuspended in 30 ml of ice-cold $MgCl_2$/$CaCl_2$ solution (80 mM $MgCl_2$ and 20 mM $CaCl_2$) and centrifuged as above. The cell pellet was resuspended with 2 ml of ice-cold 0.1 M $CaCl_2$ and the cell suspension was divided into 100 or 200 μl aliquots. These competent cells was used immediately or stored at -80 °C for subsequently used.

2.5.4 Transformation of the ligation product to *E.coli* host cells

The competent cells were thawed on ice for 5 minutes. Two to four microlitres of the ligation mixture were added and gently mixed by pipetting. The mixture was left on ice for 30 minutes. During the incubation period, the ice box was gently moved forward and backward a few times every 5 minutes. The transformation reaction was heat-shocked in a 42 °C water bath (without shaking) for exactly 45 seconds. The reaction tube was immediately placed on ice for 2-3 minutes. The mixture were

removed from the tubes and added to a new tube containing 1 ml of pre-warmed SOC (2% Bacto tryptone, 0.5 % Bacto yeast extract, 10 mM NaCl, 2.5 mM KCl, 10 mM MgCl$_2$, 10 mM MgSO$_4$ and 20 mM glucose). The cell suspension was incubated with shaking at 37 °C for 90 minutes. The mixture were centrifuged for 20 seconds at room temperature, and resuspended in 100 μl of the SOC medium and spread onto a selective LB agar plates (containing 50 μg/ ml of amplicillin and spread with 20 μl of 25 μg/ml of X-gal and 25 μl of 25 μg/ml of IPTG for approximately 1 hr before using) and further incubated at 37 °C overnight. The recombinant clones containing inserted DNA are white whereas those without inserted DNA are blue (Sambrook and Russell, 2001).

2.5.5 Colony PCR and digestion of the amplified inserts by restriction endonucleases

The colony PCR was performed in a 25 μl reaction mixture containing 10 mM Tris-HCl, pH 8.8, 50 mM (NH$_4$)$_2$SO$_4$, 0.1% Triton X-100, 100 mM of each dNTP, 2 mM MgCl$_2$, 0.1 μM each of pUC1 (5′-CCG GCT CGT ATG TTG TGT GGA-3′) and pUC2 (5′-GTG GTG CAA GGC GAT TAA GTT GG-3′), 0.5 unit of *Taq* DNA polymerase (Fermentas). A colony was picked by a pipette tip, placed in the culture tube and served as the template in the reaction. PCR was carried out in a thermocycler consisting of predenaturation at 94 °C for 3 minutes followed by 35 cycles of denaturation at 94 °C for 30 seconds, annealing at 50 °C for 1 min and extension at 72 °C for 1.5 minutes. The final extension was carried out at the same temperature for 7 minutes. The colony PCR products were electrophoresed through a 1.5 % agarose gel and visualized after ethidium bromide staining.

The colony PCR products containing the insert were separately digested with *Alu* I and *Rsa* I (Promega) in a 15 μl reaction volume containing 1x buffer (6 mM Tris-HCl, 6 mM MgCl$_2$, 50 mM NaCl and 1 mM DDT, pH 7.5 for *Alu* I and 10 mM Tris-HCl, 10 mM MgCl$_2$, 50 mM NaCl and 1 mM DDT, pH 7.9 for *Rsa* I), 0.1 mg/ml BSA, 2 units of each enzyme and 4 μl of the colony PCR product. The reaction mixture was incubated at 37 °C overnight. The reaction was analyzed by 1.5 % agarose gel electrophoresis.

2.5.6 Extraction of recombinant plasmid DNA

Plasmid DNA was isolated using a HiYield^{TM} Plasmid Mini Kit (RBC). A discrete white colony was inoculated into a sterile culture tube containing 3 ml of LB broth supplemented with 50 μg/ml of amplicillin and incubated with shaking (200 rpm) at 37 °C overnight. The culture was transferred into a sterile 1.5 ml microcentrifuge tube and centrifuged at 14,000 rpm for 1 min. The supernatant was discarded. The bacterial pellet was resuspended in 200 μl of the PD1 buffer containing RNase A and thoroughly mixed by vortexed. The resuspended cells were lysis by the addition of 200 μl of the PD 2 buffer and mixed gently by inverting the tube for 10 times. The mixture was left for 2 minutes at room temperature. After that, 300 μl of the PD 3 buffer was added to neutralize the alkaline lysis step and mixed immediately by inverting the tube for 10 times. The mixture was then centrifuged at 14,000 rpm for 15 minutes.

A PD column was placed in a collection tube and the clear lysis was applied into the PD column and centrifuged at 6,000 *g* (8,000 rpm) for 30 seconds. The flow-through was discarded. The PD column was placed back in the collection tube. The column was washed by the addition of 400 μl of the W1 buffer and centrifuged at 8,000 rpm for 30 seconds. After discarding the flow-through, 600 μl of the ethanol-added Wash buffer was added and centrifuged as above. The PD column was further centrifuged for 2 minutes at the full speed (14,000 rpm) to dry the column matrix. The dried column was placed in a new micro centrifuge tube and 50 μl of the elution buffer or water was added at the center of the column matrix. The column was left at room temperature for 2 min before centrifuged for 2 min at the full speed to recover the purified plasmid DNA. The concentration of extraction plasmid DNA was spectrophotometrically measured.

2.5.7 DNA sequencing

Cloned DNA fragments from typical PCR, RT-PCR, RACE-PCR analysis were sequenced by automated DNA sequencer using M13 forword and/or M13 reverse primer as the sequencing primer by MACROGEN (Korea).

2.6 RT-PCR and tissue distribution analysis

2.6.1 Primer design

Forward and reverse primers of *asparagenyl tRNA systhertase (PmAtNS), aspartate amino tranferase (PmAST), mago nashi (Pm-mago nashi), nuclear hormone receptor 96 (PmNHR96)* and *son of sevenless (PmSOS)* were designed (Table2.5)

Table 2.5 Gene homologue, primer sequences and expected sizes of the PCR product designed from EST of *P. monodon*

Gene	Primer sequence	size
Aspartate amino transferase (PmAST)	F:5'GACAGCCCAGTTATTGCCGATG-3' R:5'GCTCCACTGAAGTCAAAT CCAC-3'	233
Asparaginyl-tRNA synthetase (PmAtNS)	F:5'GGACACGAACTCCAGGTAGATT-3' R:5'TCATAAGGATTGAACGCAGCCG-3'	172
Nuclear hormone receptor 96 (PmNHR96)	F:5'TAAACACGAACGGTGCTCAT 3' R:5'GACACTTTGCATCTGGTACG 3'	247
Mago nashi (Pm-mago nashi)	F:5'ATGGGCTCCAACGACTTCTACA 3' R:5'CATCACCAATGACAATCTCCAG 3'	286
Son of sevenless (PmSOS)	F: 5'CTCGGTCACAGGACAGGTTG 3' R: 5'GTTGAGCATAACAAGGGCAG 3'	199

2.6.2 First strand cDNA synthesis

One and half micrograms of total RNA from various tissues of *P. monodon* were reverse transcribed to the first strand cDNA using an ImProm-II^{TM} Reverse Transcription System Kit (Promega). Total RNA was combined with 0.5 µg of oligo dT$_{12-18}$ and appropriate amount of DEPC-treated H$_2$O in a final volume of 5 µl. The reaction was incubated at 70ºC for 5 minutes and immediately placed on ice for 5 minutes. The 5x reaction buffer, MgCl$_2$, dNTP mix, RNasin were added to final concentration of 1x, 2.25 mM, 0.5 mM and 20 units, respectively. Finally, 1 µl of ImProm-II^{TM} Reverse transcriptase was added and gently mixed by pipetting. The reaction mixture was incubated at 25 ºC for 15 minutes and 42 ºC for 90 minutes. The reaction was terminated by incubated at 70ºC for 15 minutes to terminate reverse transcriptase activity. Concentration and rough quality of newly synthesized first

strand cDNA was spectrophotometrically examined (OD_{260}/OD_{280}) and electrophoretically analyzed by 1.5 % agarose gel.

2.6.3 RT-PCR

One hundred nanograms of the first strand cDNA of ovaries of female broodstock-sized *P. monodon* were used as the template in a 25 µl RT-PCR reaction composing of 10 mM Tris-HCl, pH 8.8, 50 mM KCl, 0.1% Triton X-100, 100 mM of each dNTP, 2 mM $MgCl_2$, 0.2 µM of each primer and 1 unit of Dynazyme ™ DNA polymerase (FINNZYMES). RT-PCR was carried out with the temperature profile of predenaturation at 94 ºC for 3 minutes followed was denaturation at 94 ºC for 30 seconds 25 cycles, annealing at 53 ºC for 45 second and extension at 72 ºC for 30 seconds. The final extension was carried out at the same temperature for 7 minutes.

Fives microliters of the amplification products are electrophoresed though 1.2-2.0% agarose gel dependent on size of the amplification products. The electrophoresed band was visualized under a UV transilluminator after ethidium bromide staining (sambrook and Russell, 2001).

2.6.4 Tissue distribution analysis of interesting genes using RT-PCR

Total RNA was extracted of each gene in various tissues of female broodstock (antennal gland, eyestalk, gill, hemocytes, heart, hepatopancreas, lymphoid organs, Broodstock ovaries, pleopod, stomach, thoracic ganglia, juvenile and ovaries), ovaries of juveniles and testis of male broodstock of *P. monodon*. The first strand cDNA was synthesized as described previously.

For each target gene, 150 ng of the first strand cDNA from various tissues was used as the template for RT-PCR. *EF-1α$_{500}$* (F: 5'-ATGGTTGTCAACTTTGCCCC-3' and R: 5'-TTGACCTCCTTGATCACACC-3') was included as the positive control. The thermal profiles were predenaturation at 94 ºC for 3 minutes followed by 30 cycles composing of a 94 ºC denaturation step for 30 seconds, annealing at 53ºC for 45 seconds and extension at 72 ºC for 30 seconds. The final extension was carried out at 72 ºC for 7 minutes. The amplicon was electrophoretically analyzed through 1.5% agarose gel and visualized with a UV transsilluminitor after ethidium bromide staining (Sambrook and Russell, 2001).

2.7 Preparation of specimens for expression analysis of interesting genes in ovaries of *P. monodon* by quantitative real-time PCR

2.7.1 Expression levels of reproduction-related genes in wild intact and eyestalk-ablated broodstock and domesticated shrimp of *P. monodon*

For gene expression analysis, female broodstock were wild-caught from the Andaman Sea and acclimated under the farm conditions for 2-3 days. The post-spawning group was immediately collected after shrimp were ovulated (stage V, $N = 6$). Ovaries were dissected out from each broodstock and weighed ($N = 27$, average body weight 217.07 ± 47.10 g). For the eyestalk ablation group, wild broodstock were acclimated for 7 days prior to unilateral eyestalk ablation ($N = 28$, average body weight 209.97 ± 39.45 g). Ovaries of eyestalk-ablated shrimp were collected at 2-7 days after ablation. The gonadosomatic index (GSI, ovarian weight/body weight x 100) of each shrimp was calculated. The ovarian developmental stages of wild shrimp were classified according to the GSI values: <1.5, >2–4, >4–6 and >6% for previtellogenic (stage I, $N = 4$ and 5 for intact and eyestalk-ablated broodstock, respectively), vitellogenic (II, $N = 4$ and 9), early cortical rod (III, $N = 5$ and 9) and mature (IV, $N = 9$ and 5) ovaries, respectively. The ovarian developmental stages of wild shrimp were confirmed by conventional histology (Qiu et al., 2005).

In addition, domesticated juveniles (5- and 9-months old, $N = 6$ for each group with the average body weight of approximately 20 g and 46.68 ± 3.55 g) and domesticated broodstock (14- and 18-month-old, $N = 6$ for each group with the average body weight 64.06 ± 3.20 g and 77.12 ± 3.10 g) of *P. monodon* were collected from the Broodstock Multiplication Center (BMC), Burapha University (Chanthaburi, Thailand) and include in the experiments.

2.7.2 Effects of 17β-estradiol injection on expression of reproduction-related genes in ovaries of domesticated *P. monodon* broodstock

2.7.2.1 Preparation of 17β-estradiol

For preparation of 17β-estradiol stock solution, 17β-estradiol was weighed out (0.0025 g) and 125 µl of absolute ethanol was added to achieve the final concentration of 20 µg/µl. The solution was incubated on ice to facilitate dissolution. The stock

solution was diluted by absolute ethanol to make the final concentration of 2 µg/µl and to 0.2 µg/µl. Finally, the stock solutions were diluted with sterile deionized water to make the working solution (0.01 µg/g body weight of 17β-estradiol in 5% ethanol) immediately before injection.

2.7.2.2 17β-estradiol treatment

To examine effects of 17β-estradiol on expression of reproduction-related genes, domesticated shrimp (approximately 14 month-old with the average body weight of 48.99 ± 4.96 g) were acclimated at the laboratory conditions (28-30ºC and 30 ppt seawater) in 500-liter fish tanks for 1 week. Three groups of shrimp were injected intramuscularly with 17β-estradiol (0.01 µg/g of body weight, $N = 6$ for each group) into the first abdominal segment of each shrimp. The injection was repeated with the original doses at 3 and 6 days post initial injection and specimens are collected at 7, 14 and 28 days post injection. Non-injected shrimp (at 0, 7, 14 and 28 days after the initial injection; $N = 6$ for each group) and those injected with 5% ethanol (at 7, 14 and 28 days after the initial injection; $N = 6$ for each group) were included as the negative and vehicle control, respectively. In addition, shrimp were unilateral eyestalk-ablated and specimens were collected at the same time intervals. Ovaries of each shrimp were sampling and immediately placed in liquid N_2. The samples were stored at -80˚C until needed.

2.7.3 Effects of 17β-estradiol-supplented diets on expression of reproduction-related genes in ovaries of domesticated *P. monodon* broodstock

2.7.3.1 Preparation of diets

Ingredients for preparation of the artificial diets were prepared as described in Table 2.8. A total of 4 kilograms of diets were prepared. The diets were supplemented with 17β-estradiol (1 and 10 mg.kg). The ingredients were mixed together for 20 minutes. The processed diets were streamed at 95 ° C for 5 minutes and dried at 60 °C for 2 hours. The grain size of diets was approximately 2 mM in diameter and 4 mM in length.

Table 2.6 Ingredients of artificial diets used in this study

Component	Amount (kg)/4 kg diet
Fish meal	2.18
Shrimp shell powder	0.16
Soybean meal	0.4
Tuna fish oil	0.216
Chlorophyl pink	0.0008
Multiminerals	0.04
Multivitamin	0.04
Cholesterol	0.04
Lecithin	0.04
Wheat gluten	0.24
Vitamin C	0.0024
Vitamin E	0.0008
Vitamin E	0.24

2.7.3.2 Feeding trials

The feeding experiments were carried out for the duration of 35 days. The domesticated shrimp (approximately 14 month-old) were acclimated at the laboratory conditions (28-30 ºC and 30 ppt seawater) in 1,500-liter fish tanks for 1 week. Two groups of shrimp were fed four times daily (5% body weight) with the diets supplemented with 17β-estradiol (1 and 10 mg/kg, $N = 8$ for each group).Specimens are collected at 7, 14, 28 and 35 days after treament. Non-treated shrimp (at 7, 14, 28 and 35 days after the initial treatment; $N = 8$ for each group) were included as the negative control. Shrimp were unilateral eyestalk-ablated and specimens were collected at the same time intervals. Ovaries of each shrimp were sampling and immediately placed in liquid N_2. The samples were stored at -80˚C until needed.

2.8 Quantitative real-time PCR analysis

2.8.1 Primer design and construction of the standard curves

Expression levels of *PmAtNS, PmAST, Pm-mago nashi* and *PmNHR96* were examined using quantitative real-time PCR analysis. Primers for RT-PCR were further used for quantitative real-time PCR analysis.

Table 2.7 Primer sequences designed from EST of *P. monodon* for quantitative real-time PCR analysis.

Gene	Primer sequence	size
Aspartate amino transferase (PmAST)	F:5'GACAGCCCAGTTATTGCCGATG-3' R:5'GCTCCACTGAAGTCAAAT CCAC-3'	233
Asparaginyl-tRNA synthetase (PmAtNS)	F:5'GGACACGAACTCCAGGTAGATT-3' R:5'TCATAAGGATTGAACGCAGCCG-3'	172
Nuclear hormone receptor 96 (PmNHR96)	F:5'TAAACACGAACGGTGCTCAT 3' R:5'GCGGATTGACGTCTAGAAAGACA 3'	164
Mago nashi (Pm-mago nashi)	F:5'GCTGGAGATTGTCATTGGTG 3' R:5'GTGAAGACCAATCAATGAGAAC 3'	160

For construction of the standard curve of each gene, the DNA segment covering the target PCR product and *EF-1α$_{214}$* (F: 5´-GTCTTCCCCTTCAGGACGT C-3´ and R : 5´-CTTTACAGACACGTTCTTCACGTTG-3´) were amplified from primers for quantitative real-time PCR. The PCR product were cloned Plasmid DNA were extracted and used as the template for estimation of the copy number. A 10 fold-serial dilution was prepared corresponding to 10^3-10^8 molecules/µl. The copy number of standard DNA molecules can be calculated using the following formula :

X g/µl DNA / [plasmid length in bp x 660] x 6.022x10^{23} = Y molecules/µl (Parida *et al*., 2006).

The standard curves (correlation coefficient = 0.995-1.000 or efficiency higher than 95%) were drawn for each run. The standard samples were carried out in a 96 well plate and each standard point was run in duplicate.

2.8.2 Quantitative real-time PCR analysis

The target transcripts and the internal control $EF\text{-}1\alpha_{214}$ (5´-GTCTTCCCCTTCAGGACGTC-3´ and R: 5´-CTTTACAGAC ACGTTCTTCACGTTG-3´) of the synthesized cDNA were amplified in a reaction volume of 10 µl using 2X LightCycler® 480 SYBR Green I Master (Roche, Germany). The specific primer pairs were used at a final concentration of 0.15, 0.2, 0.15, 0.2 and 0.3 µM for *PmAtNS*, *PmAST*, *Pm-mago nashi*, *PmNHR96* and $EF\text{-}1\alpha_{214}$, respectively. The thermal profile for SYBR Green real-time PCR was $95\,^{\circ}C$ for 10 minutes, 1 cycle followed by 40 cycles of $95\,^{\circ}C$ for 15 seconds, $55\,^{\circ}C$ for 30 seconds, $72\,^{\circ}C$ for 30 seconds. The melting curve analysis was carried out at $95\,^{\circ}C$ for 15 seconds, $65\,^{\circ}C$ for 1 minute and at $98\,^{\circ}C$ for continuation and cooling was $40\,^{\circ}C$ for 10 seconds. The real-time PCR assay was carried out in a 96 well plate and each sample was run in duplicate using a LightCycler® 480 Instrument II system (Roche).

A ratio of the absolute copy number of the target gene and that of $EF\text{-}1\alpha_{214}$ was calculated. The relative expression level between different group (ovarian development or treatment) were statistically tested using one way analysis of variance (ANOVA) followed by a Duncan's new multiple rang test. Significant comparisons were considered when the *P*-value was < 0.05.

2.9 *In vitro* expression of the HOLI domain of PmNHR96 using the bacterial expression system

2.9.1 Primers design

A primer pair for amplification of the HOLI domain sequence was designed from the partial cDNA of *PmNHR96*. The forward primer containing a *Bam* HI site, and reverse primer containing a *Xho* I site and six Histidine residues encoded nucleotides (Table 2.9).

Table 2.8 Primers for in vitro protein expression of the HOLI domian of PmNHR96

Gene	Primer sequence
HOLI domain-PmNHR96	F: 5´-CGCGGATCCATGCTATCGGAGGCGAACAAGGGC-3´
	R: 5´-CCGCTCGAGTTAATGATGATGATGATGATGTGG TTCGACTTCTTGCGGATT-3´

2.9.2 Construction of recombinant plasmid in cloning and expression vectors

The HOLI domain sequence was amplified by PCR and digested with the corresponding enzymes. The resulting product was gel-eluted and ligated to pGEM®-T Easy vector and transformed into *E. coli* JM109. Plasmid DNA was extracted from a positive clone and used as the template for amplification using 0.5 µM of each primer, 0.75-1.5 unit *Pfu* DNA polymerase (Promega) and 0.2 mM of each dNTPs. The thermal profiles were predenaturation at 94 °C for 3 minutes followed by 30 cycles of denaturation at 94 °C for 30 seconds, annealing at 60 °C for 30 seconds, extension at 72 °C for 2 minutes and final extension at 72 °C for 7 minutes.

2.9.3 Expression of recombinant proteins

A single colony of recombinant *E. coli* BL21-CodonPlus (DE3)-RIPL or *E. coli* BL21 (DE3)-plysS carrying desired recombinant plasmid (pHOLI-PmNHR96) was inoculated into 3 ml of LB medium, containing 50 µg/ml ampicillin and 50 µg/ml chloramphenicol at 37 °C. Fifty microlittres of the overnight cultured was transferred to 50 ml of LB medium containing 50 µg/ml ampicillin and 50 µg/ml chloramphenicol and further incubated to an OD_{600} of 0.4-0.6. After IPTG induction (1.0 mM final concentration), appropriate volume of the culture corresponding to the OD of 1.0 was time-interval taken (0, 2, 3, 6, 12, 24 hours at 37 °C) and centrifuged at 12,000 rpm for 1 minute. The pellet was resuspended in 1X PBS buffer and examined by 15% SDS-PAGE (Laemmli, 1970).

In addition, 20 ml of the IPTG induced-cultured cells at the most suitable time-interval were taken (6 hours or overnight at 37°C or lower), harvested by centrifugation 5000 rpm for 15 minutes and resuspended in the lysis buffer (0.05 M Tris-HCl ; pH 7.5, 0.5 M Urea, 0.05 M NaCl, 0.05 M EDTA ; pH 8.0 and I mg/ml lysozyme). The cell wall was broken by sonication using Digital Sonifier® sonicator Model 250 (BRANSON). The bacterial suspension was sonicated 2-3 times at 15-30% amplitude, pulsed on for 10 seconds and pulsed off for 10 seconds in a period of 2-5 minutes. Soluble and insoluble portions were separated by centrifuged at 14,000 rpm for 30 minutes. The protein concentration of both portions was measured

using a dye-binding assay (Bradford, 1972). Expression of the recombinant protein was electrophoretically analyzed by 1.5% SDS-PAGE.

2.9.4 Detection of recombinant proteins

Recombinant protein was analyzed in 1.5% SDS-PAGE. The electrophoresed proteins were transferred to a PVDF membrane (Hybond P; GE Healthcare) (Towbin, 1979). The membrane was washed three times with 1X Tris-buffer saline tween-20 (TBST ; 25 mM Tris, 137 mM NaCl, 2.7 mM KCl and 0.05% tween-20) for 10 minutes, blocked with 20 ml of a blocking buffer (1.0 g of BSA in 20 ml of 1X TBST) and incubated for 1 hour at room temperature with gentle shaking. The membrane was washed three times in 1X TBST and incubated with diluted Mouse Anti-His antibody IgG2a (GE Healthcare; 1 : 5000) in the blocking buffer for 1 hour. The membrane was incubated with diluted goat anti-mouse IgG (H+L) conjugated with alkaline phosphatase (Promega 1 : 10,000) in the blocking buffer for 1 hour. Visualization of immunoreactional signals was carried out by incubating the membrane in NBT/BCIP (Roche) as a substrate. The color reaction was stopped by transferring the membrane into water.

2.9.5 Purification of recombinant proteins

Recombinant protein was purified by using a His GraviTrap kit (GE Healthcare). Initially 1 littre of IPTG-induced cultured at the optimal time and appropriate temperature was harvested by centrifugation at 5,000 rpm for 15 minutes. The pellet was resuspended in the binding buffer (20 mM sodium phosphate, 500 mM NaCl, 20 mM imidazole, pH 7.4), sonicated and centrifuged at 14,000 rpm for 30 minutes. The soluble and insoluble fractions were separated. Soluble fraction composed of the recombinant protein was loaded into column. The column was washed with 10 ml of binding buffer containing 20 mM imidazole (20 mM sodium phosphate, 500 mM NaCl, 20 mM imidazole, pH 7.4), 5 ml of the binding buffer containing 50 mM imidazole (20 mM sodium phosphate, 500 mM NaCl, 50 mM imidazole, pH 7.4) and 5 ml of the binding buffer containing 80 mM imidazole (20 mM sodium phosphate, 500 mM NaCl, 80 mM imidazole, pH 7.4). The recombinant protein was eluted with 6 ml of the elution buffer (20 mM sodium phosphate, 500 mM NaCl, 500 mM imidazole, pH 7.4). Each fraction of the washing and eluting step were

analyzed by SDS-PAGE and western blotting. The purified proteins were stored at 4 ^{o}C or -20 ^{o}C for long term storage.

Proteins separated with SDS-PAGE were transferred onto a PVDF membrane (Hybond P; GE Healthcare) (Towbin, 1979) in 25 mM Tris, 192 mM glycine   (pH 8.3) buffer containing 10% methanol at a constant current of 350 mA for 1 hour. The membrane was treated in the DIG blocking solution (Roche) for 1 hour and incubated with the primary antibody (1 : 100 in the blocking solution) for 1 hour at room temperature with gently shaker. The membrane was washed 3 times with 1X Tris-buffer saline tween-20 (TBST ; 50 mM Tris–HCl, 0.15 M NaCl, pH 7.5, 0.1% Tween-20) and incubated with goat anti rabbit IgG (H+L) conjugated with alkaline phosphatase (Bio-Rad Laboratories) at 1 : 3,000 for 60 minutes and then washed 3 times with 1X TBST. Visualization of immunoreactional signals was carried out by incubating the membrane in NBT/BCIP (Roche) as a substrate. The color reaction was stopped by transferring the membrane into water.

2.9.6 Polyclonal antibody production

Polyclonal antibody against rHOLI-PmNHR96 was immunologically produced from the purified nuclear hormone receptor 96 protein in a rabbit by Faculty of Associated Medical Sciences, Changmai University. Western blot analysis was carried out to examine specificity and sensitivity of the antibody.

2.9.7 Purification of polyclonal antibody

The polyclonal antibody was purified. Briefly, 5 ml of non-purified polyclonal antibody were centrifuge at 10,000 rpm for 10 minutes at 4 °C. The supernatant was transfer to a new microcentrifuge tube and the polyclonal antibody was purified using protein A column according to the protocol recommend from manufacturer (Thermo sciencetific). Protein A column was equilibrated with 3-5 ml of binding buffer. The non-purified rHOLI-PmNHR96 polyclonal antibody (5 ml) were divided to equal aliquots, passed through the column and incubated for 45 and 30 minutes, respectively. The bound IgG was washed with 5-10 ml of the binding buffer. The fractions were collected in aliquots of 2 ml and spectrophotometriclly at 280 nm until the resulting fraction showed the OD close to the blank. After that, the bound

antibody was eluted with 5-10 ml of the elution buffer and aliquots of 2 ml were collected and spectrophotometrically estimated. The eluted fraction was examined by SDS-PAGE.

2.9.8 Determination of the expression patterns on PmNHR96 in ovaries of *P. monodon* using Western blot analysis

2.9.8.1 Total protein extraction

Approximately 0.5 gram of frozen ovaries of *P. monodon* were ground to fine power in the presence of liquid N_2 and suspended in a tree fold-diluted PBS buffer containing protease inhibitor cocktail. After centrifugation at 12,000 rpm for 10 minutes at 4 °C, the supernatant were collected. Trichloroacetic acid in acetone (TCA; 10% w/v) was added and left at -20 ℃ overnight. The mixture was centrifuged at 12,000 rpm for 30 minutes at 4°C. The supernatant was discarded and the pellet was suspended in acetone containing 0.1% dithiothreitol (DTT). The sample was spun at 12,000 rpm for 30 minutes at 4°C. The pellet was air-dried and dissolved in the lysis buffer. The amount of extracted protein was measured by a dye binding assay (Bradford, 1976).

2.9.8.2 Western blot analysis

Twenty micrograms of total ovarian proteins were heated at 100 °C for 5 minutes and immediately cooled on ice. Proteins were size-fractionated on a 15% SDS-PAGE (Laemmli, 1970). Electrophoretically separated proteins were transferred onto a PVDF membrane (Hybond P; GE Healthcare) (Towbin et al., 1979) in 25 mM Tris, 192 mM glycine (pH 8.3) buffer containing 10% methanol at 100 V for 90 minutes. The membrane was treated in the DIG blocking solution (Roche) for 1 hour and incubated with anti-rHOLI-PmNHR96 (1: 500 in the blocking solution) for 1 hour at room temperature. The membrane was washed 3 times with 1× Tris Buffer Saline-Tween20 (TBST; 50 mM Tris–HCl, 0.15 M NaCl, pH 7.5, 0.1% Tween20) and incubated with goat anti rabbit IgG (H+L) conjugated with alkaline phosphatase (Bio-Rad Laboratories) at 1 : 3,000 for 1 hour and washed 3 times with 1× TBST. Immunoreactive signals were visualized using NBT/BCIP (Roche) as the substrate.

CHAPTER III

RESULTS

3.1. Total RNA extraction

Total RNA from ovaries and various tissues of a female wild broodstock including antennal gland, epicuticle, eyestalk, gill, hemocytes, heart, hepatopancreas, lymphoid organs, broodstock ovaries, pleopod, stomach, thoracic ganglia, ovaries of juveniles and testis of male broodstock of *P. monodon* were extracted. The quality and quantity of extracted total RNA were examined by spectrophotometry and integrity of the total RNA was observed by agarose gel electrophoresis. The ratio of RNA extracted were 1.8-2.0 implying that the quality of extracted RNA was acceptable to further applications.

The results from agarose gel electrophoresis (Figure 3.1) showing good quality of extracted RNA with predominated discrete bands along with smeared high molecular weight RNA. The first stand cDNA synthesized from DNA-free total RNA covered the large product sizes (Figure 3.2).
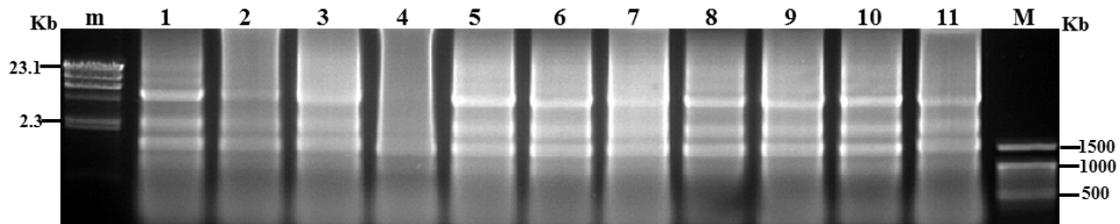
Figure 3.1 A 1.0% Ethidium bromide-stained agarose gel showing the quality of total RNA extracted from female broodstock of *P. monodon*. Lanes m and M are λ-*Hin*d III and a 100 DNA ladder. Lanes 1-11 are total RNA extracted from ovaries of *P. monodon* broodstock.

Figure 3.2 A 1.0% Ethidium bromide-stained agarose gel showing the quality of first stand cDNA synthesized from DNA-free total RNA of female broodstock of *P. monodon*. Lanes M and m are λ-*Hin*d III and a 100 DNA ladder. Lanes 1-11 are the first strand cDNA of each *P. monodon* broodstock.

3.2 Isolation and characterization of the partial cDNA sequences of *nuclear hormone receptor HR96* (*PmNHR96*) and *son of sevenless* (*PmSOS*) of *P. monodon*

3.2.1 The partial cDNA sequence of *PmNHR96*

PmNHR96 (Clone No. LP-S01-0404-LF) was initially obtained from EST analysis of the lymphoid organ cDNA libraly of *P. monodon* (Figures 3.3). This EST significantly matched *nuclear hormone receptor 48* of *Ixodes scapularis* (*E*-value = 2e-37). The primary 5´- and 3´RACE-PCR of this EST was carried out for the possible isolation of the full-length cDNA of this cDNA.

A

ATTTATCTTGGCGTTTCAGCCGGAGTGGAGACAAGACCACAACATCATCTTCCTCTTATCAGCTATTAC
GCTCTTCACGCCCGAGAGGCCTAACATAATCCATGGCGATGCTATTAAACACGAACGGTGCTCATACCT
GTACCTCCTGAAGCGCTACCTGGAGTGCAAGTACGGAGGTTGCGAAGGAAGGACGGTTTACCTCCGGCT
GCTAGAGAGGATTAAGCATCTCAACATCCTCAATGAGAAGCACATTCGTGTCTTTCTAG**ACGTCAATCC
GCAAGAAGTCGAACCAC**TCCTTATAGAAATCTTTGACCTCAAGCATAGG**TGA**CAGTTGTGAATGT**CGTA
CCAGATGCAAAGTGTC**AAAAAAGTCATATGTGATACACATGTCAAGA

B

>   ref|XP_002404556.1| [U][G] nuclear hormone receptor 48, putative [Ixodes scapularis]

 gb|EEC11854.1| [G] nuclear hormone receptor 48, putative [Ixodes scapularis]
Length=412

 GENE ID: 8033479 IscW_ISCW009328 | nuclear hormone receptor 48, putative [Ixodes scapularis]

 Score = 139 bits (351), Expect = 2e-37
 Identities = 63/106 (59%), Positives = 84/106 (79%), Gaps = 0/106 (0%)
 Frame = +2

```
Query   2     FILAFQPEWRQDHNIIFLLSAITLFTPERPNIIHGDAIKHERCSYLYLLKRYLECKYGGC  181
              FI AF+PEWR D NI+ LLSAITLFTPERPN++H D +  E+ +YLYLL+RYL+  Y GC
Sbjct   307   FINAFRPEWRIDENIMLLLSAITLFTPERPNLVHRDVVTFEQDTYLYLLRRYLDTIYTGC  366

Query   182   EGRTVYLRLLERIKHLNILNEKHIRVFLDVNPQEVEPLLIEIFDLK  319
              E R+V+L+L+  ++ +  LNE  + + +D+NP+EVEPLLIEIFDLK
Sbjct   367   ESRSVFLQLIRNLEDMRTLNENQVSILVDLNPREVEPLLIEIFDLK  412
```

Figure 3.3 Nucleotide sequence of an EST significantly matched *nuclear hormone receptor 48* from the lymphoid organ cDNA library of *P. monodon*. The position of sequences primers were illustrated in boldface and underlined. The putative stop codon (TGA) was illustrated in boldface (A). BlastX analysis showing significant similarty of the identified transcript with *nuclear hormone receptor 48* of *Ixodes scapularis* (B).

The 5´- and 3´RACE-PCR of *PmNHR96* generated 800 and 1,600 bp products (Figure 3.4A and B). These fragments were cloned and sequenced for both directions. The 5´RACE-PCR segment significantly matched *Nuclear hormone receptor HR96* of *Camponotus floridanus* (*E*-value = 1e-87). In contrast, the 3´RACE-PCR did not show significant similarity with any sequence previously deposited in GenBank.

Figure 3.4 The 1.5% agarose gel electrophoresis showing 5´- (A) and 3´RACE-PCR (B) products of *PmNHR96* (lane 1). The 100 bp DNA ladder (lane M) was used as the DNA marker**.**

A

AAGCAGTGGTATCAACGCAGAGTCACCAGGAAGATTGGAAGAATTTCAGCGTGCAAGATACCCTGAGAT
TCCTCGAGCCAGGGTGCAAGCAGAGCCCCGGCGCGACGGGGCTGACGATGATGGACTCGATCATGAACA
CCGCCATCAGCGCCGAGTACAGCGCCTTCAGCCTCCTGGGCAGCAACAACCCGAGGGAGCTGAACGAAC
CGGAGAAGATGAAGCTGAACGAACTATCGGAGGCGAACAAGGGCCTTCTGGCGCCGCTCTGCGAGGATT
ATAATTTTAAGGACCTGAGCAACCCGTCGCTTCTCAACATCATCAACCTGACGGAGATCGCCATCCGCC
GCCTCATCAAGATGTCGAAGAGAATATCCGCCTTCAAGAGCCTCTGCCAGGAGGACCAGATCGCGCTGC
TCAAGGGAGGCTGCACGGAGATGATGATCCTGCGGTCCGTCAGCGCCTACGACCCCGATAAGGACTCGT
GGATGATTCAACAGGACCATGACCGTTTCAAGAACATCAAGCTGAAGGTACTAAAGGCCGCCCCAGGGA
ACGTCTATGAGGAACACAAGAGATTTATCTTGGCGTTTCAGCCGGAGTGGAGACAAGACCACAACATCA
TCTTCCTCTTATCAGCTATTACGCTCTTCACGCCCGAGAGGCCTAACATAATCCACGGCGATGCTATTA
AACACGAACGGTGCTCATACCTGTACCTCCTGAAGCGCTACCTGGAGTGCAAGTACGGAGGTTGCGAAG
GAAGGACGGTTTACCTCCGGCTGCTAGAGAGGATTAAGCATCTCAACATCCTCAATGAGAAGCACATTC
GTGTCTTTCTAGACGTCAATCCGCAAGAAGTCGAACCACTCCTTATAGAAATCTTTGACCTCAAGCATA
GGTGACAGTTGTGAATGT**CGTACCAGATGCAAAGTGTC**

B

ACGTCAATCCGCAAGAAGTCGAACCACTCCTTATAGAAATCTTTGACCTCAAGCATAGGTGACAGTTGT
GAATGTCGTACCAGATGCAAAGTGTCAAAAAAAGTCATATGTGATACACATGTCAAGAAAATTATAGAT
ACCTTTCCTTTGTGTTTTAATAACACTTCATTTACTTTCGAAAGAAAAAGGAGAAAATGAAAAAAAAAA
GGTGAAGACGGTAGATATTAATGATCTCTATGCTGTGAACCCAAGGACAGCAACAGTAAAACAGTATTG
AAGTTGCACATTACTCTCCAGAAACAGCTGGAATGTGCAATTGTGAATATGCAGACTTTGTTGTTATGT
TTTATGTATGTATTTGAACCAACATTCTGAAATTATTTAAGGTCTTTTCCTATCTAGATCGTATATGCT
CAAAAGAAGCCATGATTCTTAATTAAGGTATTTGAAAAAAAAAAATGTATAATGCTATTTCTCACAGAG
CTTCATCTTTGACTCTTGAAACCCATTGTATGCAGATTTTTTTATTTATTTTTATTTTTTTTATTAGT
GTAATCTTGTATTTGAATAGAAGACAATTTTCAAGAAGTCCTCTGAATACAAGCAAGACAGTAGAAGTG
CTGTTGGACTCAGGATTAGGATGTAACGACAACATGGGCACTTTTTATTCCTTGATGAAAGATATTATA
TATACAGATAACAGATTTGTAGTTTTCTCTCCGCAGTCTCTTCTCTGGGGGGGGAATGTATTAACATAG
TATTTTATAACGAAAGTAGTTGTATATAAGAGTCACATTTGATGAACATTTTGAGAGTATCTAACGATC
CCTTTGTGTTTTAATAACACTTCATTTACTTTCGAAAGAAAAAGGAGAAAATGAAAAAAAAAAAGGTGAA
GACGGTAGATATTAATGATCTCTATGCTGTGAACCCAAGGACAGCAACAGTAAAACAGTATTGAAGTTG
CACATTACTCTCCAGAAACAGCTGGAATGTGCAATTGTGAATATGCAGACTTTGTTGTTATGTTTTATG
TATGTATTTGAACCAACATTCTGAAATTATTTAAGGTCTTTTCCTATCTAGATCGTATATGCTCAAAAG
AAGCCATGATTCTTAATTAAGGTATTTGAAAAAAAAAAATGTATAATGCTATTTCTCACAGAGCTTCAT
CTTTGACTCTTGAAACCCATTGTATGCAGATTTTTTTATTTATTTTTATTTTTTTTTATTAGTGTAATC
TTGTATTTGAATAGAAGACAATTTTCAAGAAGTCCTCTGAATACAAGCAAGACAGTAGAAGTGCTGTTG
GACTCAGGATTAGGATGTAACGACAACATGGGCACTTTTTATTCCTTGATGAAAGATATTATATATACA
GATAACAGATTTGTAGTTTTCTCTCCGCAGTCTTTTCTCTGGGGGGGGAATGTATTAACATAGTATTTT
ATAACGAAAGTAGTTGTATATAAGAGTCACATTTGATGAACATTTTGAGAGTATCTAACGACTGAAAGA
TGGAGATGCCTTCCTGTCGAAGCATTTATTATTATAGTGTTTATCTTCATTATAATTACCTTTTTAAGT
CATGTCTATAGTATCAGATTGATAACTATTTATGAAAGAACTGAAAATATATTGTATGATGTAAAAAAA
AAAAAAAAAAAAAAAAAAAAAAAAAA**GTACTCTGCGTTGATACCACTGCTT**

Figure 3.5 Nucleotide sequences of 5´- (A) and 3´RACE-PCR fragments of
*PmNHR*96. The positions of sequencing primers are illustrated in boldface (RACE-
PCR primer). The nested UPM primer is italicized and underlined.

Nucleotide sequences of the original EST, 5'RACE and 3'RACE-PCR were assembled and analyzed. Only the partial cDNA of *PmNHR96* was obtained. It was 2436 bp in length with the partial ORF of 879 bp deduced to 292 amino acids with the 3′UTR of 1679 bp (excluding the poly A tail) (Figures 3.6). The closest sequence to *PmNHR96* was *nucler hormone receptor HR96* of *Camponotus floridanus* (E-value = 1e-87). The predicted ligand-binding domain (HOLI) was found at positions 100 – 264 of the deduced amino acid sequence of the partial *PmNHR96* cDNA (Figure 3.6)

A

```
CACCAGGAAGATTGGAAGAATTTCAGCGTGCAAGATACCCTGAGATTCCTCGAGCCAGGG  60
 H   Q   E   D   W   K   N   F   S   V   Q   D   T   L   R   F   L   E   P   G    20
TGCAAGCAGAGCCCCGGCGCGACGGGGCTGACGATGATGGACTCGATCATGAACACCGCC  120
 C   K   Q   S   P   G   A   T   G   L   T   M   M   D   S   I   M   N   T   A    40
ATCAGCGCCGAGTACAGCGCCTTCAGCCTCCTGGGCAGCAACAACCCGAGGGAGCTGAAC  180
 I   S   A   E   Y   S   A   F   S   L   L   G   S   N   N   P   R   E   L   N    60
GAACCGGAGAAGATGAAGCTGAACGAACTATCGGAGGCGAACAAGGGCCTTCTGGCGCCG  220
 E   P   E   K   M   K   L   N   E   L   S   E   A   N   K   G   L   L   A   P    80
CTCTGCGAGGATTATAATTTTAAGGACCTGAGCAACCCGTCGCTTCTCAACATCATCAAC  280
 L   C   E   D   Y   N   F   K   D   L   S   N   P   S   L   L   N   I   I   N    100
CTGACGGAGATCGCCATCCGCCGCCTCATCAAGATGTCGAAGAGAATATCCGCCTTCAAG  340
 L   T   E   I   A   I   R   R   L   I   K   M   S   K   R   I   S   A   F   K    120
AGCCTCTGCCAGGAGGACCAGATCGCGCTGCTCAAGGGAGGCTGCACGGAGATGATGATC  400
 S   L   C   Q   E   D   Q   I   A   L   L   K   G   G   C   T   E   M   M   I    140
CTGCGGTCCGTCAGCGCCTACGACCCCGATAAGGACTCGTGGATGATTCAACAGGACCAT  460
 L   R   S   V   S   A   Y   D   P   D   K   D   S   W   M   I   Q   Q   D   H    160
GACCGTTTCAAGAACATCAAGCTGAAGGTACTAAAGGCCGCCCCAGGGAACGTCTATGAG  520
 D   R   F   K   N   I   K   L   K   V   L   K   A   A   P   G   N   V   Y   E    180
GAACACAAGAGATTTATCTTGGCGTTTCAGCCGGAGTGGAGACAAGACCACAACATCATC  580
 E   H   K   R   F   I   L   A   F   Q   P   E   W   R   Q   D   H   N   I   I    200
TTCCTCTTATCAGCTATTACGCTCTTCACGCCCGAGAGGCCTAACATAATCCATGGCGAT  640
 F   L   L   S   A   I   T   L   F   T   P   E   R   P   N   I   I   H   G   D    220
GCTATTAAACACGAACGGTGCTCATACCTGTACCTCCTGAAGCGCTACCTGGAGTGCAAG  700
 A   I   K   H   E   R   C   S   Y   L   Y   L   L   K   R   Y   L   E   C   K    240
TACGGAGGTTGCGAAGGAAGGACGGTTTACCTCCGGCTGCTAGAGAGGATTAAGCATCTC  760
 Y   G   G   C   E   G   R   T   V   Y   L   R   L   L   E   R   I   K   H   L    260
AACATCCTCAATGAGAAGCACATTCGTGTCTTTCTAGACGTCAATCCGCAAGAAGTCGAA  820
 N   I   L   N   E   K   H   I   R   V   F   L   D   V   N   P   Q   E   V   E    280
CCACTCCTTATAGAAATCTTTGACCTCAAGCATAGG**TGA**CAGTTGTGAATGTCGTACCAG  880
 P   L   L   I   E   I   F   D   L   K   H   R   *                              292
ATGCAAAGTGTCAAAAAAAGTCATATGTGATACACATGTCAAGAAAATTATAGATACCTT  940
TCCTTTGTGTTTTAATAACACTTCATTTACTTTCGAAAGAAAAAGGAGAAAATGAAAAAA  1000
AAAAGGTGAAGACGGTAGATATTAATGATCTCTATGCTGTGAACCCAAGGACAGCAACAG  1060
TAAAACAGTATTGAAGTTGCACATTACTCTCCAGAAACAGCTGGAATGTGCAATTGTGAA  1120
TATGCAGACTTTGTTGTTATGTTTTATGTATGTATTTGAACCAACATTCTGAAATTATTT  1180
AAGGTCTTTTCCTATCTAGATCGTATATGCTCAAAAGAAGCCATGATTCTTAATTAAGGT  1240
ATTTGAAAAAAAAAAATGTATAATGCTATTTCTCACAGAGCTTCATCTTTGACTCTTGAA  1300
ACCCATTGTATGCAGATTTTTTTATTTATTTTTATTTTTTTTTTATTAGTGTAATCTTGTA  1360
TTTGAATAGAAGACAATTTTCAAGAAGTCCTCTGAATACAAGCAAGACAGTAGAAGTGCT  1400
GTTGGACTCAGGATTAGGATGTAACGACAACATGGGCACTTTTTATTCCTTGATGAAAGA  1460
```

```
TATTATATATACAGATAACAGATTTGTAGTTTTCTCTCCGCAGTCTCTTCTCTGGGGGGG 1520
GAATGTATTAACATAGTATTTTATAACGAAAGTAGTTGTATATAAGAGTCACATTTGATG 1580
AACATTTTGAGAGTATCTAACGATCCCTTTGTGTTTTAATAACACTTCATTTACTTTCGA 1640
AAGAAAAAGGAGAAAATGAAAAAAAAAAGGTGAAGACGGTAGATATTAATGATCTCTATG 1700
CTGTGAACCCAAGGACAGCAACAGTAAAACAGTATTGAAGTTGCACATTACTCTCCAGAA 1760
ACAGCTGGAATGTGCAATTGTGAATATGCAGACTTTGTTGTTATGTTTTATGTATGTATT 1820
TGAACCAACATTCTGAAATTATTTAAGGTCTTTTCCTATCTAGATCGTATATGCTCAAAA 1880
GAAGCCATGATTCTTAATTAAGGTATTTGAAAAAAAAAAATGTATAATGCTATTTCTCAC 1940
AGAGCTTCATCTTTGACTCTTGAAACCCATTGTATGCAGATTTTTTTATTTATTTTTATT 2000
TTTTTTTATTAGTGTAATCTTGTATTTGAATAGAAGACAATTTTCAAGAAGTCCTCTGAA 2060
TACAAGCAAGACAGTAGAAGTGCTGTTGGACTCAGGATTAGGATGTAACGACAACATGGG 2120
CACTTTTTATTCCTTGATGAAAGATATTATATATACAGATAACAGATTTGTAGTTTTCTC 2180
TCCGCAGTCTTTTCTCTGGGGGGGAATGTATTAACATAGTATTTTATAACGAAAGTAGT 2240
TGTATATAAGAGTCACATTTGATGAACATTTTGAGAGTATCTAACGACTGAAAGATGGAG 2300
ATGCCTTCCTGTCGAAGCATTTATTATTATAGTGTTTATCTTCATTATAATTACCTTTTT 2360
AAGTCATGTCTATAGTATCAGATTGATAACTATTTATGAAAGAACTGAAAATATATTGTA 2400
TGATGTAAAAAAAAAAAAAAAAAAAAAAAAAAAAAAAAA              2436
```

B

> gb|EFN64539.1| Nuclear hormone receptor HR96 [Camponotus floridanus]
Length=745

```
 Score =  287 bits (735),  Expect = 9e-88
 Identities = 164/300 (55%), Positives = 206/300 (69%), Gaps = 16/300 (5%)
 Frame = +1

Query  10   DWKNFSVQDTLRFLEPGCKQSPGATGLTMMDSIMNTAISAEYSAFSLLGSNN-PRELNEP  186
            DW N + D R +    ++ P A    ++SI+  AI  EYSAFS  G N   RELN+
Sbjct  450  DW-NKNTADVTRDILQDVQRIPIAAN--SIESILCEAIKLEYSAFSSFGGNQISRELNDS  506

Query  187  EKMKLNELSEANKGLLAPL-----------CEDYNFKDlsnpsllniinlTEIAIRRLIK  333
            E+ KLNEL ANK LLAPL           C+  N   S+P LL++INLT IAIRRLIK
Sbjct  507  ERAKLNELIVANKALLAPLDDDITNLVGEECKFKNNSGQSDPMLLDVINLTAIAIRRLIK  566

Query  334  MSKRISAFKSLCQEDQIALLKGGCTEMMILRSVSAYDPDKDSWMIQQDHDRFKNIKLKVL  513
            MSK+I+AFK++CQEDQ+ALLKGGCTEM+ILRS   YDPDKD W I    +  NIK+ VL
Sbjct  567  MSKKINAFKNMCQEDQLALLKGGCTEMLILRSAINYDPDKDMWKIPHSQESMSNIKVDVL  626

Query  514  KAAPGNVYEEHKRFILAFQPEWRQDHNIIFLLSAITLFTPERPNIIHGDAIKHERCSYLY  693
            K A GN+Y EH RF+  F P WR D NII +LSAITLFTP+RP ++H D IK E+ SY Y
Sbjct  627  KEAKGNLYAEHARFVRTFDPRWR-DENIILILSAITLFTPDRPRVVHSDVIKLEQNSYYY  685

Query  694  LLKRYLECKYGGCEGRTVYLRLLERIKHLNILNEKHIRVFLDVNPQEVEPLLIEIFDLKH  873
            LL+RYLE  Y GCE ++ +L+L+++I  L+ LN++ + V+L+VNP  VEPLLIEIFDLKH
Sbjct  686  LLRRYLESVYPGCEAKSTFLKLIQKISELHKLNDEVVGVYLNVNPSSVEPLLIEIFDLKH  745
```

Figure 3.6 The partial cDNA and deduced amino acid sequences of *PmNHR*96 (A) and its blastX result (B) againt previously deposited sequences in the GenBank. Stop codon are illustrated in boldface and underlined.
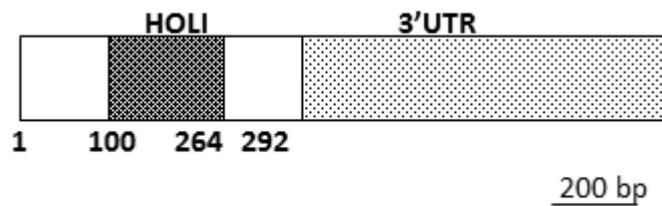
Domain	Position	E-value
HOLI	100-264	3.9e-11

Figure 3.7 Diagram illustrating the partial cDNA of *PmNHR96*. The HOLI domain was found in the deduced protein sequence of this transcript. The scale bar is 200 bp in length.

3.2.2 The partial cDNA sequence of *P. mondon son of sevenless* (*PmSOS*)

An EST representing the partial cDNA sequence of *son of sevenless* (Clone No. AG-N-N01-1056-W) was initially obtained from the antennal gland cDNA libraly of *P. monodon* (Figure 3.8A). This sequence significantly matched *Ras GTP exchange factor, son of sevenless* of *Ixodes scapularis* (*E*-value = 2e-61) (Figure 3.8).

A
```
GTCAGTTAGAACGCACCATACAGAACTCTCCATATGCTCCCTACCTTAAGAGAAAATTAGGAGAAATCA
CTTTACGGCATGGAAGGCAGAGTAGACAACAAACCTTATCTAAAATGAAAGAATTACAACGATCAATAG
ATGGCTGGGAAGGAAAAGTCATCACACAATGTTGCAACGAGTTTGTTTTAGAGGGTGACCTGCTAAAAC
TTGGTGCCACTGGGAAGAAGCCGACGGAGCGGCATGTGTTCCTGTTTGATGGCCTCATAGTCCTCTGCA
AGAGCAATAACCGGCGGTCCTCGGTCACAGGACAGGTTGGAGAGTACAGATTTAAGGAGAAATTTCTTA
TGAGAATGGTAGAAATTTTAGACAGAGAAGATACTGAAGAGATCAAATACTCCTTTGAGATCCGGCCAC
GTGACCAGCCCAGTGTGGTGCTACTTGCAAAGTCTATGGAAGAGAAGAACAATTGGATGGCTGCCCTTG
TTATGCTCAACACTCGGAGTATGTTAGAACGAACCCTAGACAGTATATTATTAGATGAGGAGAAACAGC
ATCCCCTCAATGGCAAAC
```

B
> ref|XP_002435901.1| 🇺🇬 ras GTP exchange factor, son of sevenless, putative [Ixodes scapularis]

 gb|EEC08731.1| 🇬 ras GTP exchange factor, son of sevenless, putative [Ixodes scapularis]
Length=1034

 GENE ID: 8052756 IscW_ISCW006011 | ras GTP exchange factor, son of sevenless, putative [Ixodes scapularis]

 Score = 214 bits (546), Expect = 2e-61

```
 Identities = 106/173 (61%), Positives = 140/173 (81%), Gaps = 3/173 (2%)
 Frame = +3

Query  48    KRKLGEITLR-HGRQSRQQTLSKMKELQRSIDGWEGKVITQCCNEFVLEGDLLKLGATGK   224
             +++ G+++LR H R   R    L K+KELQ+S+DGWEG+ I QCCNE+++EG L K+G+ G+
Sbjct  388   RKRPGDVSLRMHSRDRRAVALHKLKELQKSVDGWEGRDIGQCCNEYLMEGSLGKVGS-GR   446

Query  225   KPTERHVFLFDGLIVLCKSNNRRSSVTG-QVGEYRFKEKFLMRMVEILDREDTEEIKYSF   401
             + TERH+FLFDGL++LCK +++RSSVTG    E+R KE F +R +EI+DREDT+EIK+SF
Sbjct  447   RLTERHLFLFDGLVLLCKHSSKRSSVTGGPTPEFRLKECFFLRRIEIVDREDTDEIKHSF   506

Query  402   EIRPRDQPSVVLLAKSMEEKNNWMAALVMLNTRSMLERTLDSILLDEEKQHPL         560
             EI PRD P ++L AK+ EEK +WMA LVMLN RSMLERTLDSIL DEEK+HPL
Sbjct  507   EIAPRDAPRILLYAKNAEEKCSWMANLVMLNMRSMLERTLDSILSDEEKKHPL         559
```

Figure 3.8 Nucleotide sequence (A) and BlasX result (B) of an EST from the lymphoid organ cDNA libraly of *P. monodon* that significantly matched *son of sevenless* of *Ixodes scapularis*. The position of sequencing primers is illustrated in boldface and underlined. The putative stop codon is illustrated in boldface.

The 5′RACE-PCR of *P. monodon son of sevenless* (*PmSOS*) was further carried out. The resulting product was 1000 bp in length (Figure 3.9). The fragments were cloned and sequenced for both directions. It significantly matched *son of sevenless* of *Ixodes scapularis* (*E*-value = 7e-85).
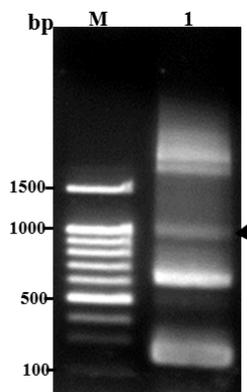
Figure 3.9 The 1.5% agarose gel electrophoresis of 5′RACE-PCR product of *PmSOS* (lane 1). A 100 bp DNA ladder (lane M) was used as the standard marker.

```
AAGATGGGGAGATGAGTGCAGTTGTGGAGGATCCTAACCCTAGACACTTCTGTAACTTATGATGAACTT
GTCAAAGATCTAATACAAGAGGAGAAAGCATATATTAGAGAACTCAATATGATAATTAAGGTGCTTTGC
GACAAGCTTCAGCAGATCCCTGTTTTACAAGGGAGTGGTAGTAGAGAGCTGGAAATTATCTTCTCAAAT
ATCACCGAGATTTATGGCTTCTCTGTAAACTTACTGGGGTCTTTAGAGGACACCCTTGAGGTCACAGAG
GAGAATGAGTCTCCCTTCATAGGCAGCTGTTTTGAGGAATTGGCAGAGGGTGCAGAGTTTGATGTTTAC
GGAAAATATGCCAGCGATGTGTTAAGGCAAGAGTGTGCAGATCAGCTAATGGATGTGGTTAACCAGCCA
CCTGTTAGCGATGCGCTGACAAGTGCTGGACAAGGCTTCAAGGAAGCTGTCAAGTACTACCTGCCAAAG
CTGCTTCTTGTACCTGTTTGTCATGTCTTCACTTATTTTAAATATATAGAGATGATTCTGGGTATGACT
GAGTCAGAAGAAGCTCGAGAGAGCTTAGAACAAGTCAAAGGTCTCTTATGGCCTCTCCAAAGTCAGTTA
GAACGCACCATACAGAACTCTCCATATGCTCCCTACCTTAAGAGAAAATTAGGAGAAATCACTTTACGG
CATGGAAGGCAGAGTAGACAACAAACCTTATCTAAAATGAAAGAATTACAACGATCAATAGATGGCTGG
GAAGGAAAAGTCATCACACAATGTTGCAACGAGTTTGTTTTAGAGGGTGACCTGCTAAAACTTGGTGCC
ACTGCGAAGAAGCCGACGGAGCGGCATGTGTTCCTGTTTGATGGCCTCATAGTCCTCTGCAAGAGCAAT
AACCGGCGGTCCTCGGTCACAGGACAGGTTG
```

Figure 3.10 Nucleotide sequence of 5´RACE-PCR product of *PmSOS*. The positions of sequencing primers are illustrated in boldface and underlined.

Nucleotide sequences of the original EST and 5´RACE-PCR were assembled and analyzed. The partial cDNA sequence of *PmSOS* was obtained. The combined nucleotide sequence of *PmSOS* was 1183 bp in length with the partial ORF of 1183 bp corresponding to to 389 amino acids (Figure 3.11). The closest sequence to *PmSOS* was *Ras GTP exchange factor, son of sevenless* of *Ixodes scapularis* (*E*-value = 8e-125). Functionally important domains including Guanine nucleotide exchange factor for Rho/Rac/Cdc42-like GTPases (RhoGEF) and Pleckstrin homology domain (PH) was found at positions 18-204 and 260–367 in the deduced amino acid of this partial cDNA (Figure 3.12)

A

```
AAGATGGGGAGATGAGTGCAGTTGTGGAGGATCCTAACCCTAGACACTTCTGTAACTTAT  60
            V  Q  L  W  R  I  L  T  L  D  T  S  V  T  Y   15
GATGAACTTGTCAAAGATCTAATACAAGAGGAGAAAGCATATATTAGAGAACTCAATATG  120
D  E  L  V  K  D  L  I  Q  E  E  K  A  Y  I  R  E  L  N  M   35
ATAATTAAGGTGCTTTGCGACAAGCTTCAGCAGATCCCTGTTTTACAAGGGAGTGGTAGT  180
I  I  K  V  L  C  D  K  L  Q  Q  I  P  V  L  Q  G  S  G  S   55
AGAGAGCTGGAAATTATCTTCTCAAATATCACCGAGATTTATGGCTTCTCTGTAAACTTA  220
R  E  L  E  I  I  F  S  N  I  T  E  I  Y  G  F  S  V  N  L   75
CTGGGGTCTTTAGAGGACACCCTTGAGGTCACAGAGGAGAATGAGTCTCCCTTCATAGGC  280
L  G  S  L  E  D  T  L  E  V  T  E  E  N  E  S  P  F  I  G   95
AGCTGTTTTGAGGAATTGGCAGAGGGTGCAGAGTTTGATGTTTACGGAAAATATGCCCGC  340
S  C  F  E  E  L  A  E  G  A  E  F  D  V  Y  G  K  Y  A  R   115
GATGTGTTAAGGCAAGAGTGTGCAGATCAGCTAATGGATGTGGTTAACCAGCCACCTGTT  400
D  V  L  R  Q  E  C  A  D  Q  L  M  D  V  V  N  Q  P  P  V   135
```

```
AGCGATGCGCTGACAAGTGCCGGACAAGGCTTCAAGGAAGCTGTCGAGTACTACCTGCCA  460
 S   D   A   L   T   S   A   G   Q   G   F   K   E   A   V   E   Y   Y   L   P   155
AAGCTGCTTCTTGTACCTGTTTGTCATGTCTTCACTTATTTTAAATATATAGAGATGTTT  520
 K   L   L   L   V   P   V   C   H   V   F   T   Y   F   K   Y   I   E   M   F   175
CTGAGTATGACTGAGTCAGAAGAAGCTCGAGAGAGCTTAGAACAAGTCAAAGGTCTCTTA  580
 L   S   M   T   E   S   E   E   A   R   E   S   L   E   Q   V   K   G   L   L   195
TGGCCTCTCCAAAGTCAGTTAGAACGCACCATACAGAACTCTCCATATGCTCCCTACCTT  640
 W   P   L   Q   S   Q   L   E   R   T   I   Q   N   S   P   Y   A   P   Y   L   215
AAGAGAAAATTAGGAGAAATCACTTTACGGCATGGAAGGCAGAGTAGACAACAAACCTTA  700
 K   R   K   L   G   E   I   T   L   R   H   G   R   Q   S   R   Q   Q   T   L   235
TCTAAAATGAAAGAATTACAACGATCAATAGATGGCTGGGAAGGAAAAGTCATCACACAA  760
 S   K   M   K   E   L   Q   R   S   I   D   G   W   E   G   K   V   I   T   Q   255
TGTTGCAACGAGTTTGTTTTAGAGGGTGACCTGCTAAAACTTGGTGCCACTGGGAAGAAG  820
 C   C   N   E   F   V   L   E   G   D   L   L   K   L   G   A   T   G   K   K   275
CCGACGGAGCGGCATGTGTTCCTGTTTGATGGCCTCATAGTCCTCTGCAAGAGCAATAAC  880
 P   T   E   R   H   V   F   L   F   D   G   L   I   V   L   C   K   S   N   N   295
CGGCGGTCCTCGGTCACAGGACAGGTTGGAGAGTACAGATTTAAGGAGAAATTTCTTATG  940
 R   R   S   S   V   T   G   Q   V   G   E   Y   R   F   K   E   K   F   L   M   315
AGAATGGTAGAAATTTTAGACAGAGAAGATACTGAAGAGATCAAATACTCCTTTGAGATC  1000
 R   M   V   E   I   L   D   R   E   D   T   E   E   I   K   Y   S   F   E   I   335
CGGCCACGTGACCAGCCCAGTGTGGTGCTACTTGCAAAGTCTATGGAAGAGAAGAACAAT  1060
 R   P   R   D   Q   P   S   V   V   L   L   A   K   S   M   E   E   K   N   N   355
TGGATGGCTGCCCTTGTTATGCTCAACACTCGGAGTATGTTAGAACGAACCCTAGACAGT  1120
 W   M   A   A   L   V   M   L   N   T   R   S   M   L   E   R   T   L   D   S   375
ATATTATTAGATGAGGAGAAACAGCATCCCCTCAATGGCAAAC  1183
 I   L   L   D   E   E   K   Q   H   P   L   N   G   K   389
```

B

>ref|XP_002435901.1| ras GTP exchange factor, son of sevenless, putative [Ixodes scapularis]

gb|EEC08731.1| ras GTP exchange factor, son of sevenless, putative [Ixodes scapularis]
Length=1034
GENE ID: 8052756 IscW_ISCW006011 | ras GTP exchange factor, son of sevenless, putative [Ixodes scapularis]

```
 Score = 395 bits (1016),  Expect = 8e-125
 Identities = 207/380 (54%), Positives = 282/380 (74%), Gaps = 13/380 (3%)
 Frame = +1

Query  52    VTYDELVKDLIQEEKAYIRELNMIIKVLCDKLQQIPVLQGS----GSRELEIIFSNITEI  219
             ++YDE VKDLI EE +IRELNM+IKV + L ++    GS        +L++IF N++E+
Sbjct  187   MSYDEEVKDLISEERQHIRELNMVIKVFREPLDKL--FPGSKVPFSPSDLDVIFGNVSEV  244

Query  220   YGFSVNLLGSLEDTLEVTEENESPFIGURESCFEELAEGAEFDVYGKYARDVLRQECADQ  399
             Y FSV+LLGS ED +E+T+E++SP IGSCF E+AE  EFDVY  YAR VL +C ++L
Sbjct  245   YDFSVSLLGSFEDVVEMTDEHQSPAIGSCFYEMAEYDEFDVYEDYARTVLSPDCREKLSQ  304

Query  400   VVNQPPVSDALTSAGQGFKEAVEYYLPKLLLVPVCHVFTYFKYIEMFLSMTESEEARESL  579
             ++ QP V+++L +AG GF  AV+Y LP+LL  PV H F YF+ I++   M  SEE RE+L
Sbjct  305   LLQQPDVANSLQTAGHGFLLAVKYVLPRLLWGPVAHCFQYFEAIKVLQQMAPSEEDRETL  364

Query  580   EQVKGLLWPLQSQLERTIQNSPYAPYLKRKLGEITLR-HGRQSRQQTLSKMKELQRSIDG  756
             EQ +GLL L++QL RT ++        +++ G+++LR H R  R   L K+KELQ+S+DG
Sbjct  365   EQAEGLLRRLRTQLTRTCSDT----LPRKRPGDVSLRMHSRDRRAVALHKLKELQKSVDG  420

Query  757   WEGKVITQCCNEFVLEGDLLKLGATGKKPTERHVFLFDGLIVLCKSNNRRSSVT-GQVGE  933
             WEG+ I QCCNE+++EG L K+G +G++ TERH+FLFDGL++LCK +++RSSVT G   E
Sbjct  421   WEGRDIGQCCNEYLMEGSLGKVG-SGRRLTERHLFLFDGLVLLCKHSSKRSSVTGGPTPE  479

Query  934   YRFKEKFLMRMVEILDREDTEEIKYSFEIRPRDQPSVVLLAKSMEEKNNWMAALVMLNTR  1113
             +R KE F +R +EI+DREDT+EIK+SFEI PRD P ++L AK+ EEK +WMA LVMLN R
Sbjct  480   FRLKECFFLRRIEIVDREDTDEIKHSFEIAPRDAPRILLYAKNAEEKCSWMANLVMLNMR  539
```

```
Query  1114   SMLERTLDSILLDEEKQHPL   1173
              SMLERTLDSIL DEEK+HPL
Sbjct  540    SMLERTLDSILSDEEKKHPL   559
```

Figure 3.11 The partial cDNA and deduced amino acid sequences of *PmSOS* (A) and BlastX result (B) of *PmSOS* against the previously deposited sequences in Genbank. This sequence significantly match *ras GTP exchange factor, son of sevenless* of *Ixodes scapularis*.
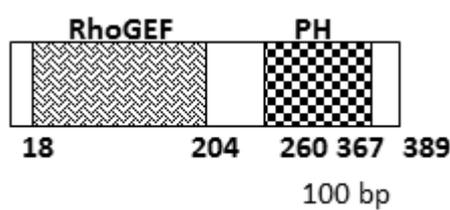
Domain	Position	E-value
RhoGEF	18-204	1.68e-15
PH	260-367	5.66e-13

Figure 3.12 Diagram illustrating the partial cDNA of *PmSOS*. The RhoGEF and PH domains were found in the deduced amino acid sequence of *PmSOS*. The scale bar is 200 bp in length.

3.3 Tissue distribution analysis of functionally reproduction-related genes in this study

Five pairs of primers were designed for amplification of *PmAtNS*, *PmAST*, *Pm-mago nashi*, *PmNHR96* and *PmSOS* in various tissues of *P. monodon*. Tissue expression analysis of each gene was examined in 15 tissues; antennal gland (AN), epicuticle, eyestalk (EP), eyestalk (ES) gill (GL), hemocytes (HC), heart (HE), hepatopancreas (HP), intestine (IN), lymphoid organs (LP), broodstock ovaries (OV), pleopod (PL), stomach (ST) and thoracic ganglia (TG) of female broodstock, juvenile ovaries (OVJ) and testes (TT) of a male broodstock.

3.3.1 *PmAtNS*

PmAtNS was more abundantly expressed in ovaries than other tissues of wild female *P. monodon* broodstock. Lower expression of this transcript was also observed in ovaries of juveniles and testes of wild male broodstock (Figure 3.13)

3.3.2 *PmAST*

PmAST was expressed in all examined tissues of female broodstock, ovaries of juveniles and testes of male broodstock. It was more abundantly expressed in ovaries, heart and pleopods. It was expressed with relatively low levels in intestine and lymphphoid organ of female broodstock and ovaries of juveniles. Moderate expression was observed in the remaining tissues examined (Figure 3.14).
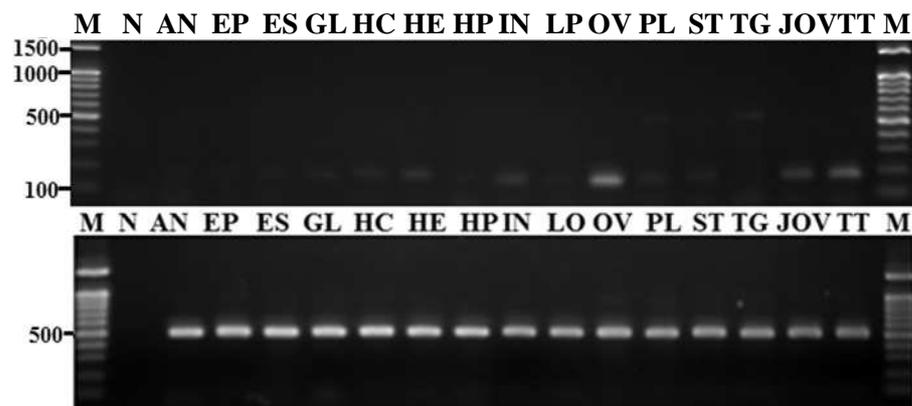
Figure 3.13 The 1.5% ethidium bromide-stained agarose gels showing results from tissue distribution analysis of *PmAtNS* using the first strand cDNA from various tissues of female broodstock and ovaries of juvenile *P. monodon*. Lane M = 100 DNA ladder, Lane N = negative control, AN = antennal gland, EP = epicuticle, ES = eyestalk, GL = gill, HC = hemocytes, HE = heart, HP = hepatopancreas, IN = intestine, LP = lymphoid organs, OV = ovaries of broodstock, PL = pleopod, ST = stomach, TG = thoracic ganglia, OVJ = juvenile ovaries, TT = testis. *EF-1α* was successfully amplified from the same template.
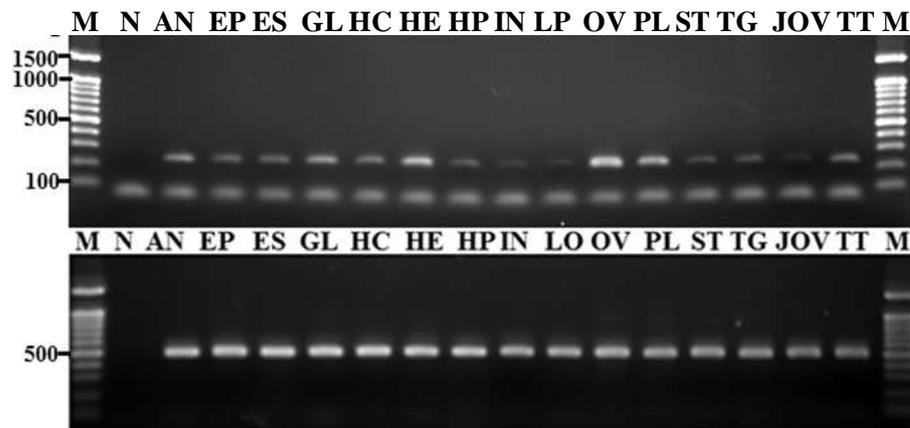
Figure 3.14 The 1.5% ethidium bromide-stained agarose gels showing results from tissue distribution analysis of *PmAST* using the first strand cDNA from various tissues of female broodstock and ovaries of juvenile *P. monodon*. Lane M = 100 DNA ladder, Lane N = negative control, AN = antennal gland, EP = epicuticle, ES = eyestalk, GL = gill, HC = hemocytes, HE = heart, HP = hepatopancreas, IN = intestine, LP = lymphoid organs, OV = ovaries of broodstock, PL = pleopod, ST = stomach, TG = thoracic ganglia, OVJ = juvenile ovaries, TT = testis. *EF-1α* was successfully amplified from the same template.

3.3.3 *Pm-mago nashi*

Pm-mago nashi seemed to be abundantly expressed in gonads of both male and female *P. monodon*. Lower expression was observed in other tissues. Low expression levels were found in antennal gland, hepatopancreas and pleopods of female broodtock (Figure 3.15).

3.3.4 *PmNHR96*

PmNHR96 was expressed in all examined tissues of female broodstock and juvenile ovaries and testes of male broodstock of *P. monodon*. It was abundantly expressed in heart, gills and lymphoid organs. Moderate expression levels were observed in other tissues where limited expression was found in hemocytes (Figure 3.16).
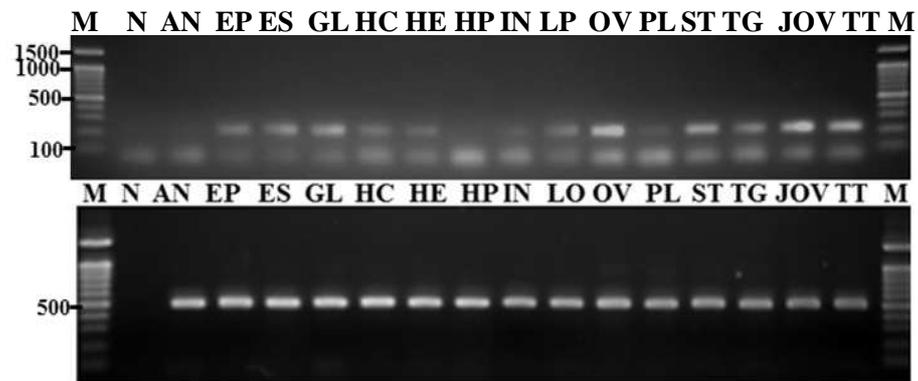
Figure 3.15 The 1.5% ethidium bromide-stained agarose gels showing results from tissue distribution analysis of *Pm-mago nashi* using the first strand cDNA from various tissues of female broodstock and ovaries of juvenile *P. monodon*. Lane M = 100 DNA ladder, Lane N = negative control, AN = antennal gland, EP = epicuticle, ES = eyestalk, GL = gill, HC = hemocytes, HE = heart, HP = hepatopancreas, IN = intestine, LP = lymphoid organs, OV = ovaries of broodstock, PL = pleopod, ST = stomach, TG = thoracic ganglia, OVJ = juvenile ovaries, TT = testis. *EF-1α* was successfully amplified from the same template.
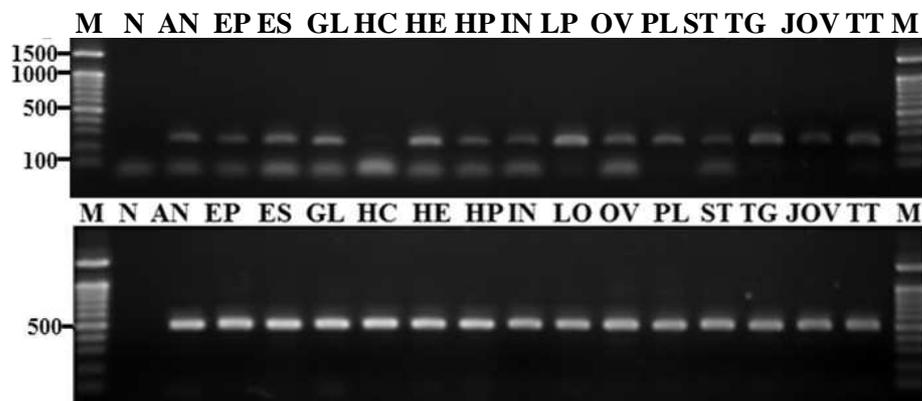
Figure 3.16 The 1.5% ethidium bromide-stained agarose gels showing results from tissue distribution analysis of *PmNHR96* using the first strand cDNA from various tissues of female broodstock and ovaries of juvenile *P. monodon*. Lane M = 100 DNA ladder, Lane N = negative control, AN = antennal gland, EP = epicuticle, ES = eyestalk, GL = gill, HC = hemocytes, HE = heart, HP = hepatopancreas, IN = intestine, LP = lymphoid organs, OV = ovaries of broodstock, PL = pleopod, ST = stomach, TG = thoracic ganglia, OVJ = juvenile ovaries, TT = testis. *EF-1α* was successfully amplified from the same template.

3.3.5 *PmSOS*

PmSOS was abundantly expressed in ovaries. Lower expression was found in hemocytes of female broodstock, juvenile ovaries and testes of male broodstock. Very low expression of this transcript was observed in the remaining tissues (Figure 3.17).
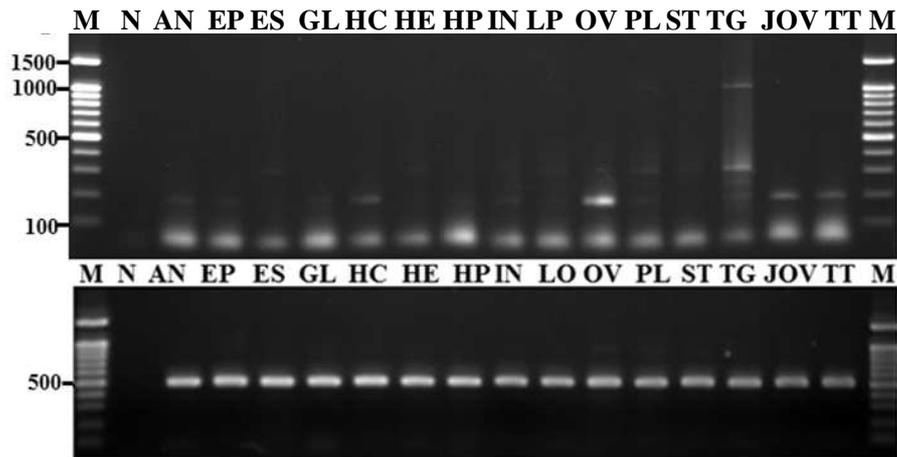
Figure 3.17 The 1.7% ethidium bromide-stained agarose gels showing results from tissue distribution analysis of *PmSOS* using the first strand cDNA from various tissues of female broodstock and ovaries of juvenile *P. monodon*. Lane M = 100 DNA ladder, Lane N = negative control, AN = antennal gland, EP = epicuticle, ES = eyestalk, GL = gill, HC = hemocytes, HE = heart, HP = hepatopancreas, IN = intestine, LP = lymphoid organs, OV = ovaries of broodstock, PL = pleopod, ST = stomach, TG = thoracic ganglia, OVJ = juvenile ovaries, TT = testis. *EF-1α* was successfully amplified from the same template.

3.4 Determination of the expression of reproduction-related genes in ovaries and testes of *P. monodon* using RT-PCR

RT-PCR was used for determining the expression profiles of various reproduction-related genes in ovaries and testes of cultured juveniles and wild broodstock of *P. monodon* (Figure 3.18).

PmAtNS, *Pm-mago nashi* and *PmSOS* were more preferentially expressed in ovaries than testes of *P. monodon*. No obvious difference was observed between the expression of this transcript in juveniles and broodstock of shrimp with the same sexes. More abundant expression of *PmAST* in ovaries of broodstock than that in ovaries of juveniles and testes of both male juveniles and broodstock was observed.

In contrast, *PmNHR96* did not revealed differential expression profiles between ovaries and testes in both juvenile and broodstock of *P. monodon*.
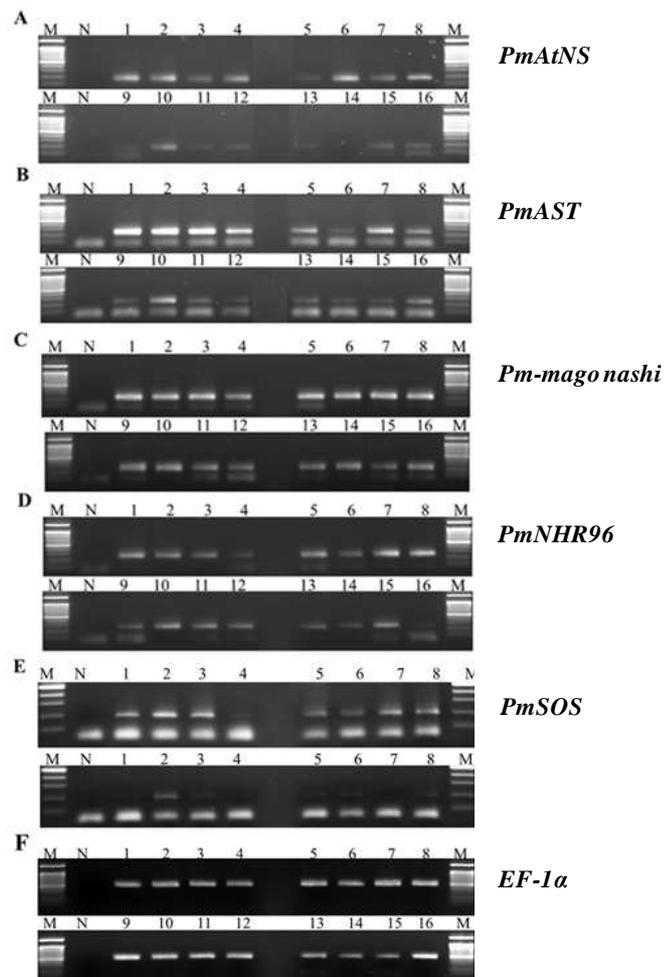
Figure 3.18 RT-PCR of *PmAtNS* (A)*, PmAST* (B)*, Pm-mago nashi* (C)*, PmNHR96* (D) and *PmSOS* (E) using the first stand cDNA of ovaries (lanes 1-8) of wild broodstock (lanes 1-4) and cultured juveniles (Lanes 5-8) and testes (lanes 9-16) of wild broodstock (lanes 9-12) and cultured juveniles (Lane 13-16) of *P. monodon*. *EF-1∞* was successfully amplified from the same template (F).

Table 3.1 Expression profiles of gene homologues in various tissues of a female and testis of a male *P. monodon* broodstock

Gene	Expression level														
	AN	**EP**	**ES**	**GL**	**HC**	**HE**	**HP**	**IN**	**LP**	**OV**	**PL**	**ST**	**TG**	**JOV**	**TT**
1. *Aparaginyl tRNA synthetase*	+	+	+	+	++	++	+	++	+	+++	+	+	-	++	++
2. *Aspartate amino transferase*	++	++	++	++	++	+++	+	+	+	+++	+++	+	+	+	++
3. *Mago nashi*	-	++	++	++	+	+	-	+	++	+++	+	++	++	+++	+++
4. *Nuclear hormone receptor*	+	+	++	++	+	+++	+	+	+++	++	++	+	++	++	++
5. *Son of sevenless*	+	+	-	+	++	-	+	+	+	+++	+	-	+	++	++

*- = not expressed, + = low level of expression, ++ = moderate level of expression, +++ = abundant level of expression

3.5 Quantitative real-time PCR analysis of *PmAtNS, PmAST, Pm-mago nashi, PmNHR96* in ovaries of *P. monodon*

The expression levels of *PmAtNS, PmAST, Pm-mago nashi* and *PmNHR96* during ovarian development of *P. monodon* were examined by quantitative real-time PCR analysis. The standard curve of each target gene and the control *(EF-1α)* were constructed from 10-fold dilutions covering 10^3- 10^8 copy numbers of dsDNA of these genes. High R^2 vules and efficiency of amplification of the examined transcripts were found (Figure 3.19). Therefore, these standard curves were acceptable to be used for quantitative estimation of all genes.
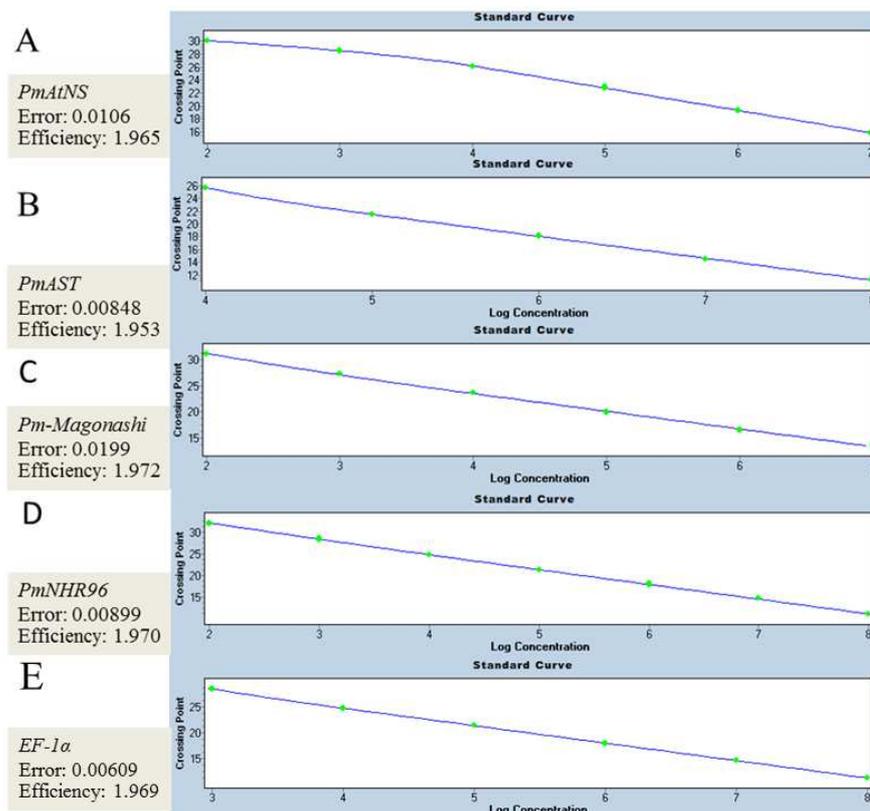
Figures 3.19 The standard amplification curves of various genes examine by quantitative real-time PCR. The standard curve of *PmAtNS* (A; efficiency for the amplification = 1.965, error = 0.0106), *PmAST* (B; efficiency for the amplification = 1.953, error = 0.00848,), *Pm-magonashi* (C; efficiency for the amplification = 1.972, error = 0.0199)*, PmNHR96* (D; efficiency for the amplification = 1.970, error = 0.00899), and *EF-1α* (E; efficiency for the amplification = 1.969, error = 0.00609).

3.5.1 The expression level of *PmAtNS, PmAST, Pm-mago nashi, PmNHR96* in intact and eyestalk-ablated broodstock of wild *P. monodon*

-*PmAtNS*

Results from quantitative real-time PCR revealed that the expression level of *PmAtNS* in juveniles and intact broodstock was not significantly different ($P > 0.05$). In intact broodstock, its expression level in different ovarian stages of intact broodstock was not significantly different ($P > 0.05$). A non-differential expression pattern was also observed in eyestalk-ablated broodstock ($P > 0.05$) (Figure 3.20A and B). When the data from both groups were analyzed together, the expression level of *PmAtNS* in stage II ovaries of intact broodstock was significantly greater than that in the same ovarian stage in eyestalk-ablated broodstock ($P < 0.05$) (Figure 3.20C).

-*PmAST*

The expression level of *PmAST* in ovaries of juveniles was significantly lower than that in intact broodstock ($P < 0.05$). In intact broodstock, its expression level was significantly increased in stage IV ovaries. In contrast, the expression level of *PmAST* was not significantly different during ovarian development of eyestalk-ablated shrimp ($P < 0.05$) (Figures 3.21A and B). The expression levels of this transcript in stages II ovaries of eyestalk-ablated broodstock were significantly greater than those in similar ovarian stages in intact broodstock ($P < 0.05$) (Figure 3.21C).

Pm-mago nashi

The expression level of *Pm-mago nashi* in juveniles and intact broodstock was not significantly different ($P > 0.05$). In intact broodstock, its expression level in different ovarian stages of intact broodstock was not significantly different ($P > 0.05$). A non-differential expression pattern was also observed during ovarian development in eyestalk-ablated broodstock ($P > 0.05$) (Figure 3.22A and B). When the data from both groups were analyzed together, the expression level of *Pm-mago nashi* in stage I-IV ovaries of eyestalk-ablated broodstock was significantly greater than that in the same ovarian stage in intact broodstock ($P < 0.05$) (Figure 3.22C).

A

B

C

Ovarian stage	GSI	Relative expression level Intactbroodstock	N	Relative expression level Eyestalk-ablated broodstock	N
Juvenile	-	0.0346 ± 0.01479^{ab}	6	-	
Stage I	(< 1.5)	0.0320 ± 0.01453^{ab}	9	0.0354 ± 0.03177^{ab}	4
Stage II	(< 2.0 - 4.0)	0.0497 ± 0.01704^{b}	7	0.0244 ± 0.01656^{a}	7
Stage III	(< 4.0 - 6.0)	0.0322 ± 0.01709^{ab}	6	0.0307 ± 0.00823^{ab}	10
Stage IV	(> 6.0)	0.0416 ± 0.02264^{ab}	9	0.0261 ± 0.00740^{a}	10
Post-spowning	(1.86 - 3.49)	0.0430 ± 0.01090^{ab}	5	-	

Figure 3.20 Histograms showing relative expression levels of *PmAtNS* during ovarian development of intact (A) and unilateral eyestalk-ablated (B) wild *P. monodon* broodstock. Data of intact and eyestalk-ablated broodstock were also analyzed together (C). Expression level were measured as the absolute copy number of *PmAtNS* mRNA (50 ng template) and normalized by that of *EF-1α* mRNA (0.5 ng template).

A

B

C

Ovarian stage	GSI	Relative expression level Intactbroodstock	N	Relative expression level Eyestalk-ablated broodstock	N
Juvenile	-	0.1491 ± 0.0597^{a}	5	-	
Stage I	(< 1.5)	0.3506 ± 0.18137^{abc}	9	0.4553 ± 0.20709^{bcd}	4
Stage II	($< 2.0 - 4.0$)	0.2890 ± 0.15203^{ab}	7	0.5249 ± 0.23072^{cd}	7
Stage III	($< 4.0 - 6.0$)	0.4357 ± 0.16003^{bcd}	6	0.6034 ± 0.12642^{d}	10
Stage IV	(> 6.0)	0.5448 ± 0.5584^{cd}	10	0.5584 ± 0.26341^{cd}	10
Post-spowning	($1.86 - 3.49$)	0.3703 ± 0.15374^{bc}	6	-	
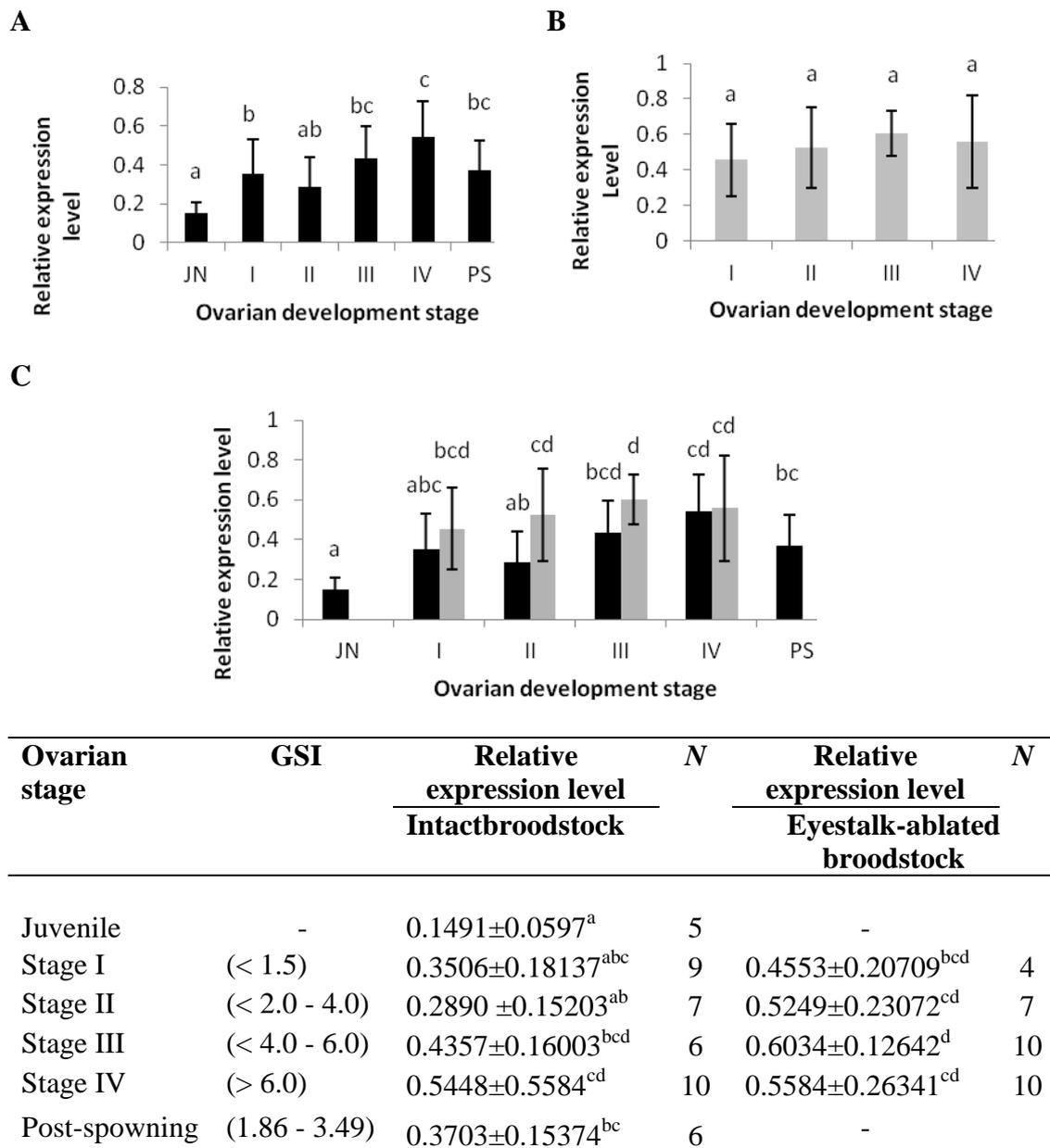
Figure 3.21 Histograms showing relative expression levels of *PmAST* during ovarian development of intact (A) and unilateral eyestalk-ablated (B) wild *P. monodon* broodstock. Data of intact and eyestalk ablated broodstock were also analyzed together (C). Expression level were measured as the absolute copy number of *PmAST* mRNA (50 ng template) and normalized by that of *EF-1α*mRNA (0.5 ng template).

A

B

C
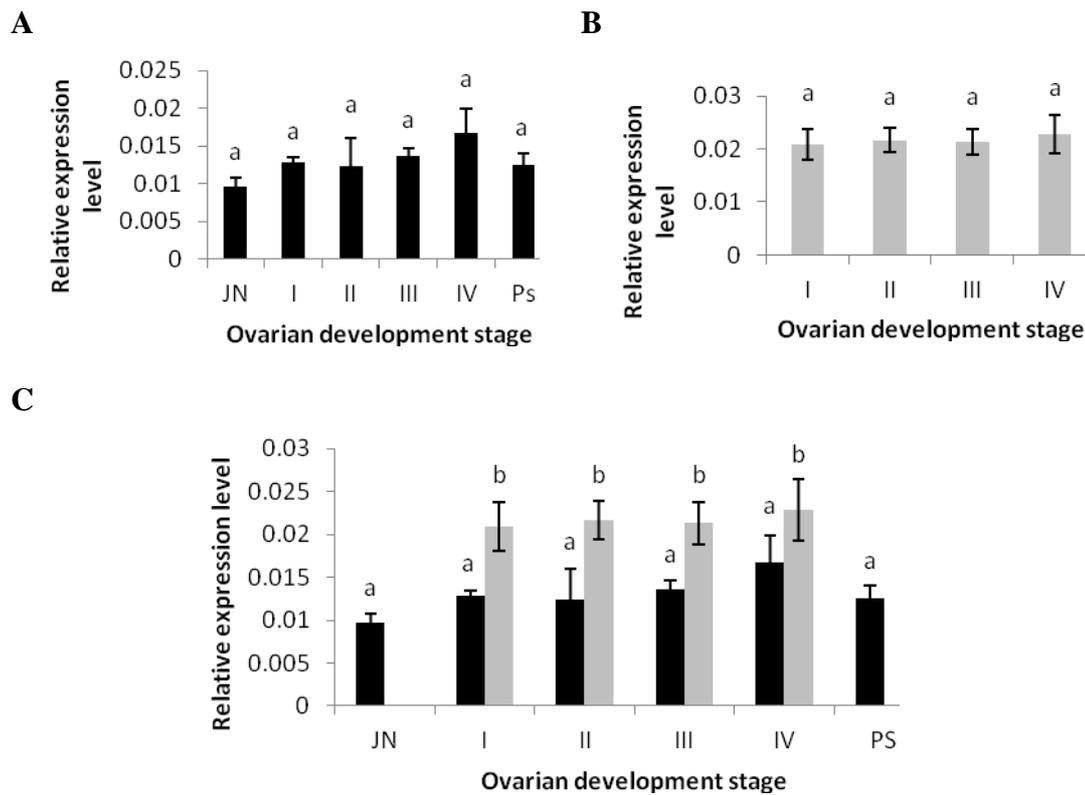
Ovarian stage	GSI	Relative expression level	N	Relative expression level	N
		Normal broodstock		Eyestalk-ablated broodstock	
Juvenile	-	0.0097 ± 0.00112^a	6	-	
Stage I	(< 1.5)	0.0128 ± 0.00069^a	4	0.0209 ± 0.00286^b	5
Stage II	(< 2.0 - 4.0)	0.0124 ± 0.00107^a	4	0.0217 ± 0.00226^b	8
Stage III	(< 4.0 - 6.0)	0.0136 ± 0.00107^a	5	0.0213 ± 0.00249^b	9
Stage IV	(> 6.0)	0.0168 ± 0.00313^a	9	0.0228 ± 0.00356^b	5
Post-spowning	(1.86 - 3.49)	0.0125 ± 0.00152^a	5	-	

Figure 3.22 Histograms showing relative expression levels of *Pm-mago nashi* during ovarian development of intact (A) and unilateral eyestalk-ablated (B) wild *P. monodon* broodstock. Data of intact and eyestalk ablated broodstock were also analyzed together (C). Expression level were measured as the absolute copy number of *Pm-magonashi* mRNA (50 ng template) and normalized by that of *EF-1α* mRNA (0.5 ng template).
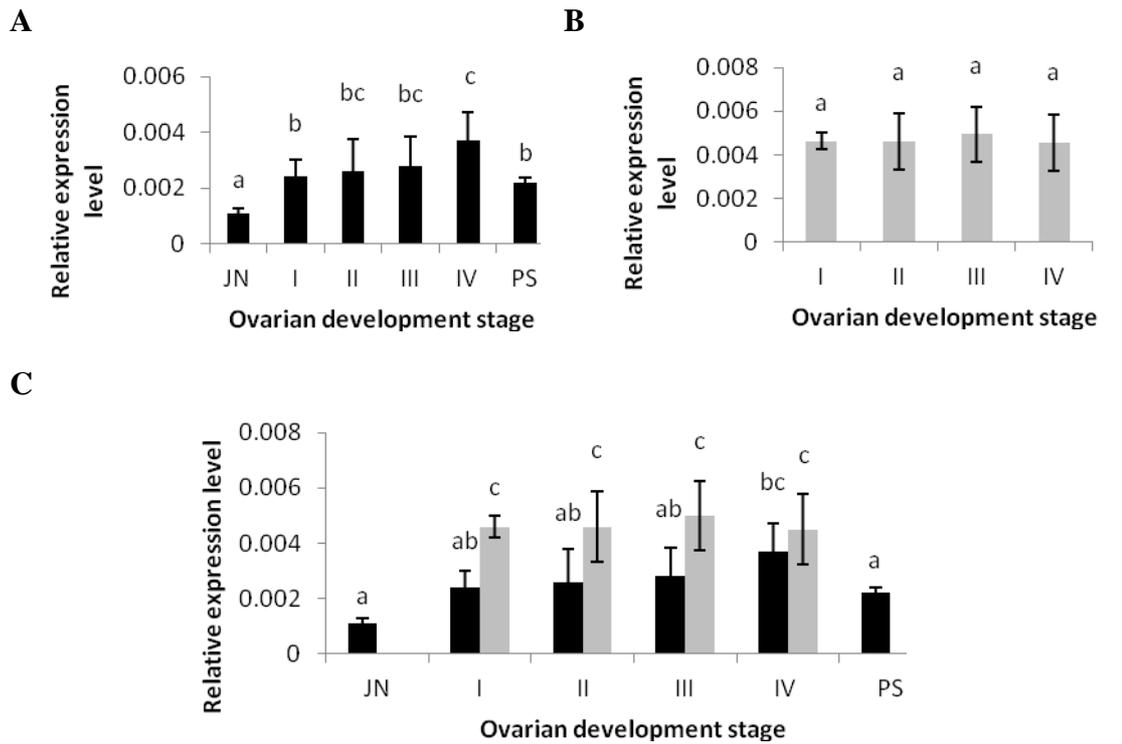
A

B

C

Ovarian stage	GSI	Relative expression level Intactbroodstock	N	Relative expression level Eyestalk-ablated broodstock	N
Juvenile	-	0.0011 ± 0.00017^a	5	-	
Stage I	(< 1.5)	0.0024 ± 0.0046^{ab}	4	0.00460 ± 0.00038^c	5
Stage II	(< 2.0 - 4.0)	0.0026 ± 0.00117^{ab}	5	0.00117 ± 0.00127^c	8
Stage III	(< 4.0 - 6.0)	0.0028 ± 0.00105^{ab}	5	0.00500 ± 0.00126^c	9
Stage IV	(> 6.0)	0.0037 ± 0.00101^{cd}	8	0.00450 ± 0.00127^c	5
Post-spowning	(1.86 - 3.49)	0.0022 ± 0.00018^a	5	-	

Figure 3.23 Histograms showing relative expression levels of *PmNHR96* during ovarian development of intact (A) and unilateral eyestalk-ablated (B) wild *P. monodon* broodstock. Data of intact and eyestalk ablated broodstock were also analyzed together (C). Expression level were measured as the absolute copy number of *PmNHR96* mRNA (50 ng template) and normalized by that of *EF-1α* mRNA (0.5 ng template).

-PmNHR96

The expression level of *PmNHR96* in ovaries of juveniles was significantly lower than that of intact broodstock ($P < 0.05$). Its expression level in intact broodstock was increased in stage IV ovaries (Figure 3.23A). In eyestalk-ablated broodtock, the expression level of *PmNHR96* was comparable (Figure 3.23B). When the data from both groups were analyzed together, the expression level of *Pm NHR96* in stage I-III ovaries of eyestalk-ablated broodstock was significantly greater than that in the same ovarian stage in intact broodstock ($P < 0.05$, Figure 3.23C).

3.5.2 The expression level of *PmAtNS, PmAST, Pm-mago nashi* and *PmNHR96* in domesticated *P. monodon*

In domesticated shrimp, the expression level of *PmAtNS* in5-month-old shrimp was not different from that of 9-month-old shrimp ($P > 0.05$) but significantly greater than that in 14-month-old shrimp ($P < 0.05$). Its expression was increased to be comparable with juvenile shrimp in 19-month-old shrimp (Figure 3.24 and Table 3.2).

The expression level of *PmAST* in 5, 9 and 14-month-old shrimp was not different ($P > 0.05$) but its expression was significantly increases in 19-month-old shrimp ($P < 0.05$, Figure 3.25 and Table 3.3).
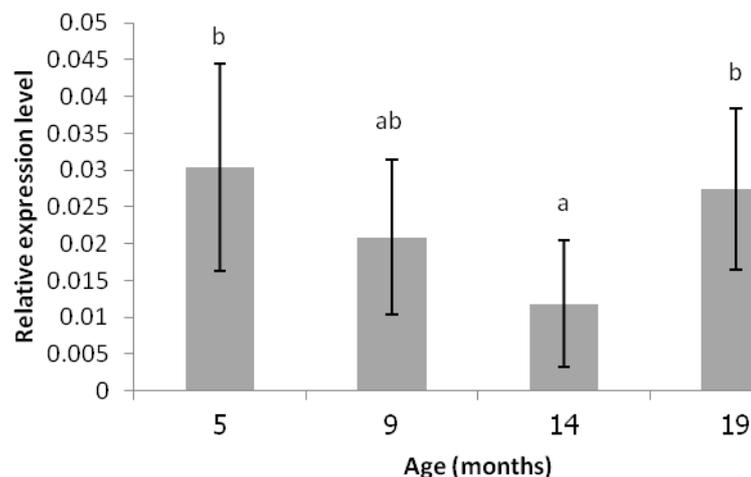
Figure 3.24 Histograms showing relative expression levels of *PmAtNS* in domesticate 5-, 9-, 14- and 19- month-old shrimp.

Table 3.2 Relative expression levels of *PmAtNS* in domesticated *P. monodon* female broodstock

Age of shrimp	Relative expression level	N
5-month-old	0.0304 ± 0.01411^{b}	5
9-month-old	0.0209 ± 0.01059^{ab}	7
14-month-old	0.0118 ± 0.00858^{a}	8
19-month-old	0.0274 ± 0.01098^{b}	5

In contrast, the expression level of *Pm-mago nashi* in 5-, 9-, 14- and 19-month old shrimp was comparable ($P < 0.05$, Figure 3.26 and Table 3.4).

The expression level of *PmNHR96* in 5-, 9-and 19-month-old shrimp was not different ($P > 0.05$). Its expression was significantly increased in 14-month-old shrimp and reduced to be comparable with juveniles and 9-month-old shrimp in 19-month-old shrimp (Figure 3.27 and Table 3.5).
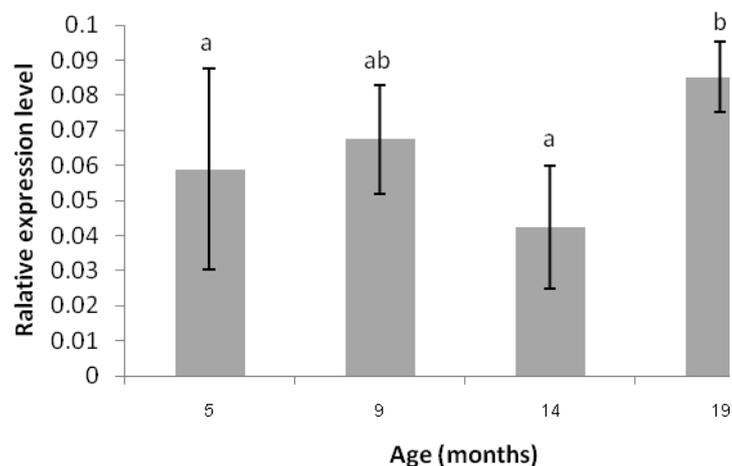
Figure 3.25 Histograms showing relative expression levels of *PmAST* in domesticated 5-, 9-, 14- and 19- month-old shrimp.

Table 3.3 Relative expression levels of *PmAST* in domesticated *P. monodon* female broodstock

Age of shrimp	Relative expression level	N
5-month-old	0.0589±0.02867[a]	5
9-month-old	0.0674±0.01541[ab]	6
14-month-old	0.0424±0.01743[a]	6
19-month-old	0.0852±0.01002[b]	5
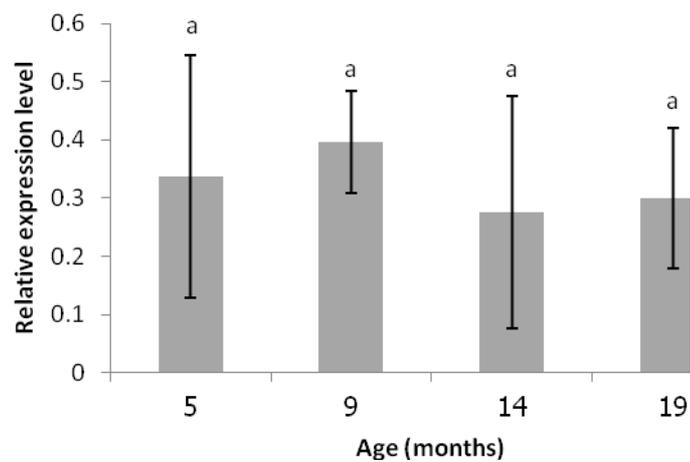
Figure 3.26 Histograms showing relative expression levels of *Pm-mago nashi* in domesticated 5-, 9-, 14- and 19- month-old shrimp.

Table 3.4 Relative expression levels of *Pm-magonashi* in domesticated *P. monodon* female broodstock.

Age of shrimp	Relative expression level	N
5-month-old	0.3374±0.20818[a]	5
9-month-old	0.3963±0.08737[a]	6
14-month-old	0.2750 ±0.19976[a]	8
19-month-old	0.2998±0.12066[a]	5
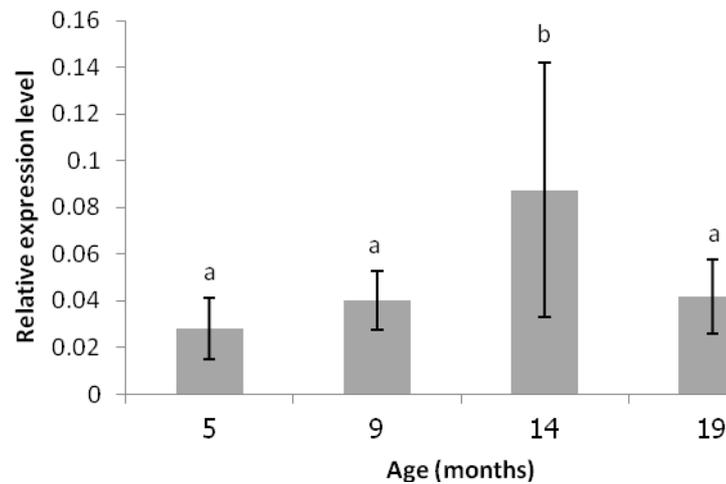
Figure 3.27 Histograms showing relative expression levels of *PmNHR96* in domesticated 5-, 9-, 14- and 19- month-old shrimp.

Table 3.5 Relative expression levels of *PmNHR96* in domesticated *P. monodon* female broodstock

Age of shrimp	Relative expression level	*N*
5-month-old	0.0282 ± 0.01317^{a}	5
9-month-old	0.0400 ± 0.0126^{a}	7
14-month-old	0.0874 ± 0.05454^{b}	8
19-month-old	0.0418 ± 0.0158^{a}	5

3.5.3 Effects of 17β-estradiol injection on expression of reproduction-related gene in ovaries of domesticated *P. monodon*

Effects of 17β-estradiol on expression of *PmAtNS, PmAST, Pm-mago nashi* and *PmNHR96* in 14-month-old domesticated *P. monodon* were examined at 7, 14 and 28 days post injection.

The expression level of ovarian *PmAtNS* was significantly reduced from the vehicle control at 7 days post injection but the effects of 17β-estradiol was not significant at 14 and 28 days post injection. Eyestalk ablation resulted in an increase expression level of *PmAtNS* at 28 days post treatment but results was not significant when compared with the negative control ($P > 0.05$) (Figure 3.28 and Table 3.6).

The injection of 17β-estradiol did not affect the expression level of ovarian *PmAST* at all time intervals ($P > 0.05$). Eyestalk ablation resulted in an increase expression level of *PmAST* at 28 days of the experiment ($P < 0.05$) (Figure 3.29 and Table 3.7).

The injection of 17β-estradiol did not affect the expression level of ovarian *Pm-mago nashi* at all time intervals ($P > 0.05$). Eyestalk ablation resulted in an increase expression level of *Pm-mago nashi* at 7 day of the experiment ($P < 0.05$) (Figure 3.30 and Table 3.8).

The expression level of ovarian *PmNHR96* after treatment with 17β-estradiol seemed to increase from that in the vehicle control at 7 days after injection but the result was not significant due to large standard deviation between groups of samples. The injection of 17β-estradiol did not affect the expression level of this transcript at 14 and 28 days post treatment ($P > 0.05$). Eyestalk ablation resulted in a significant increase of *PmNHR96* from that of the negative control at 14 days of the experiment ($P < 0.05$) (Figure 3.31 and Table 3.9).
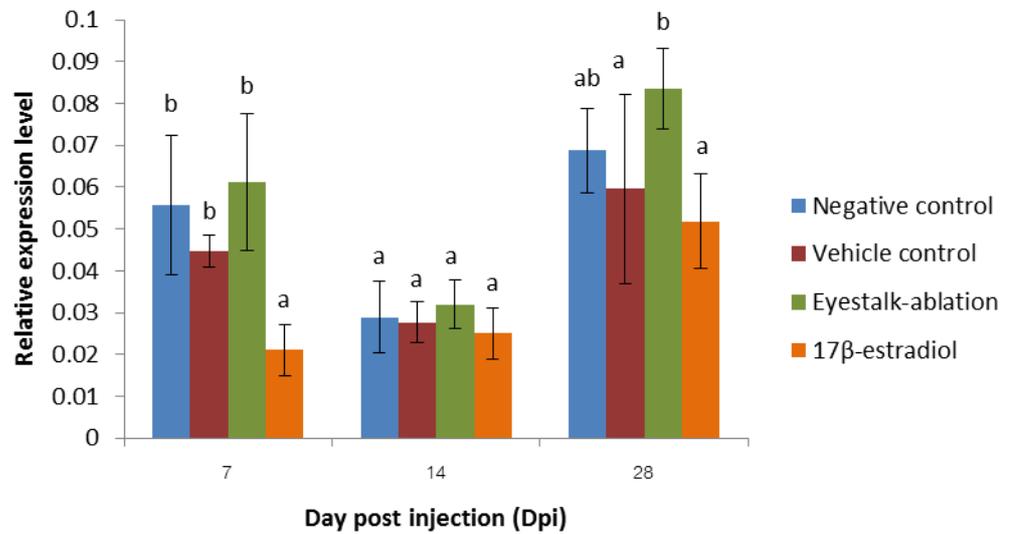
Figure 3.28 Histograms showing relative expression levels of *PmAtNS* in 14-month-old shrimp following 17β-estradiol injection for 7, 14 and 28 days.

Table 3.6 Relative expression levels of *PmAtNS* in 14-month-old shrimp following 17β-estradiol injection for 7, 14 and 28 days

Group	Relative expression	*N*
7 days		
Negative control	0.0556±0.01669[b]	6
Vehicle control	0.0447±0.00371[b]	5
Eyestalk ablation	0.0612±0.0163[db]	9
17β-estradiol	0.0210 ±0.00611[a]	5
14 days		
Negative control	0.0289±0.00849[a]	5
Vehicle control	0.0277±0.00482[a]	5
Eyestalk ablation	0.0320 ±0.0057[a]	6
17β-estradiol	0.0251±0.00613[a]	6
28 days		
Negative control	0.0687±0.01017[ab]	5
Vehicle control	0.0596±0.0227[a]	5
Eyestalk ablation	0.0835±0.0096[b]	8
17β-estradiol	0.0518±0.01134[a]	6
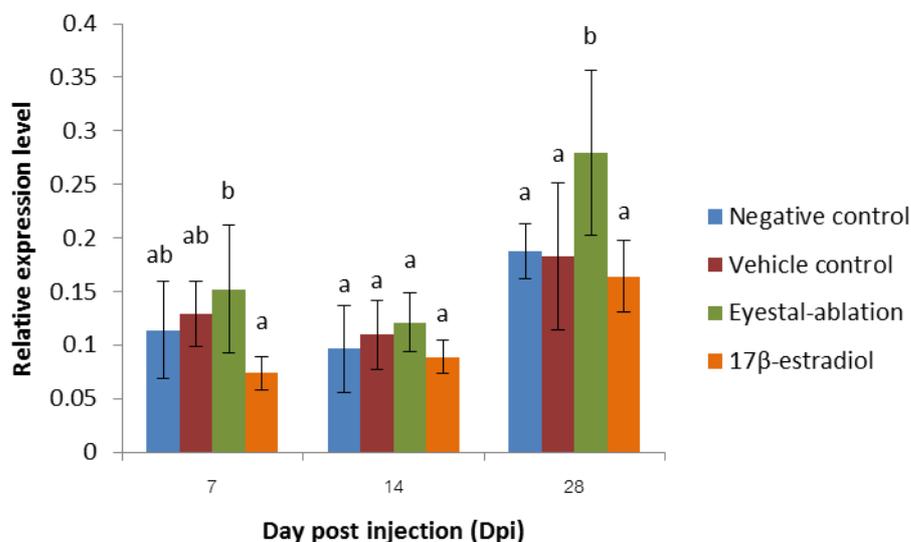
Figure 3.29 Histograms showing relative expression levels of *PmAST* in 14-month-old shrimp following 17β-estradiol injection for 7, 14 and 28 days.

Table 3.7 Relative expression levels of *PmAST* in 14-month-old shrimp following 17β-estradiol injection for 7, 14 and 28 days

Group	Relative expression	*N*
7 days		
Negative control	0.1137 ± 0.04551^{ab}	6
Vehicle control	0.1290 ± 0.03066^{ab}	6
Eyestalk ablation	0.1521 ± 0.05961^{b}	9
17β-estradiol	0.0737 ± 0.05961^{a}	5
14 days		
Negative control	0.0962 ± 0.04028^{a}	5
Vehicle control	0.1095 ± 0.03235^{a}	5
Eyestalk ablation	0.1211 ± 0.02732^{a}	6
17β-estradiol	0.0887 ± 0.01572^{a}	6
28 days		
Negative control	0.1874 ± 0.02568^{a}	5
Vehicle control	0.1826 ± 0.06855^{a}	5
Eyestalk ablated shrimp	0.2790 ± 0.07712^{b}	8
17β-estradiol	0.1642 ± 0.03373^{a}	5
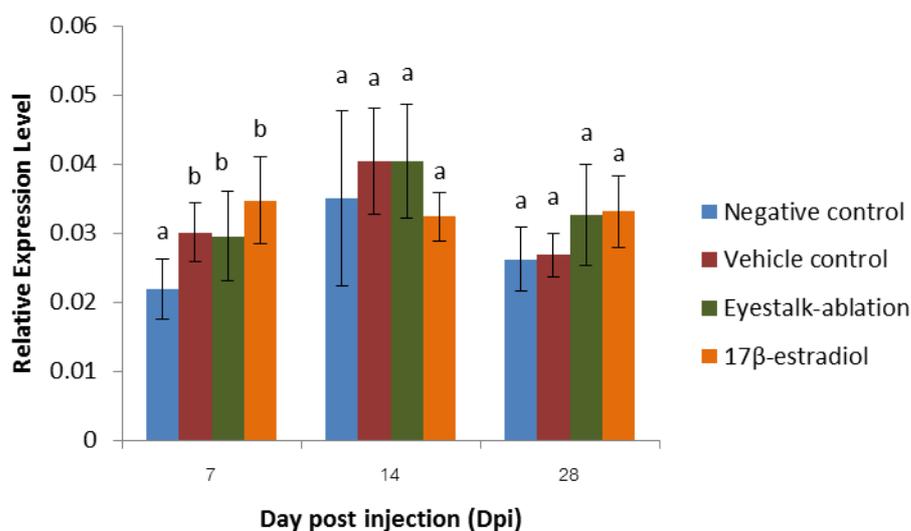
Figure 3.30 Histograms showing relative expression levels of *Pm-mago nashi* in 14-month-old shrimp following 17β-estradiol injection for 7, 14 and 28 days.

Table 3.8 Relative expression levels of *Pm-magonashi* in 14-month-old shrimp following 17β-estradiol injection for 7, 14 and 28 days

Group	Relative expression	*N*
7 days		
Negative control	0.0218 ± 0.00435^a	6
Vehicle control	0.0301 ± 0.00426^b	6
Eyestalk ablation	0.0295 ± 0.00646^b	9
17β-estradiol	0.0347 ± 0.00646^b	5
14 days		
Negative control	0.0351 ± 0.0127^a	5
Vehicle control	0.0404 ± 0.00777^a	5
Eyestalk ablation	0.0404 ± 0.00827^a	6
17β-estradiol	0.0324 ± 0.00353^a	6
28 days		
Negative control	0.0262 ± 0.00467^a	4
Vehicle control	0.0268 ± 0.00315^a	4
Eyestalk ablation	0.0326 ± 0.00737^a	8
17β-estradiol	0.0331 ± 0.00514^a	6
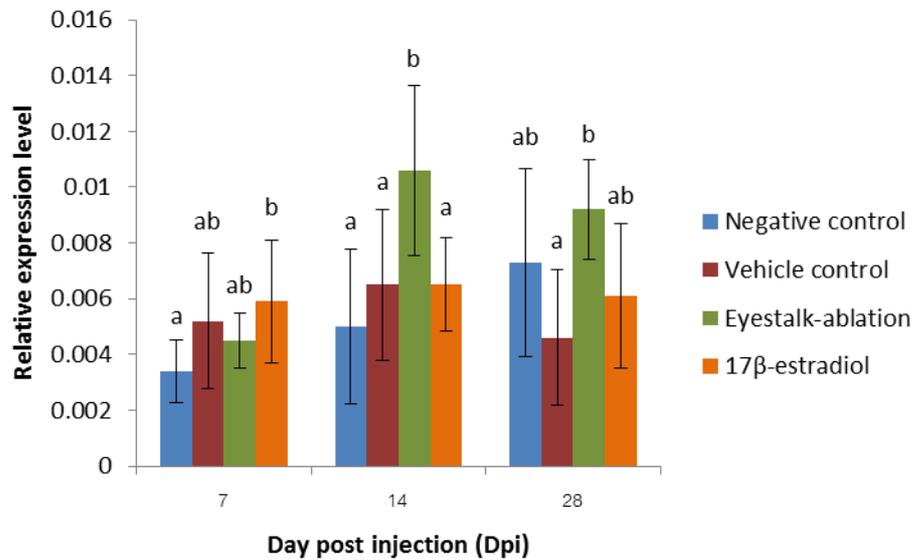
Figure 3.31 Histograms showing relative expression levels of *PmNHR96* in 14-month-old shrimp following 17β-estradiol injection for 7, 14 and 28 days.

Table 3.9 Relative expression levels of *PmNHR96* in 14-month-old shrimp following 17β-estradiol injection for 7, 14 and 28 days

Group	Relative expression	*N*
7 days		
Negative control	0.0034±0.00111[a]	5
Vehicle control	0.0052±0.00242[ab]	6
Eyestalk ablation	0.0045±0.00097[ab]	9
17β-estradiol	0.0059±0.0022[b]	5
14 days		
Negative control	0.0050±0.00276[a]	5
Vehicle control	0.0065±0.00271[a]	5
Eyestalk ablation	0.0106±0.00304[b]	6
17β-estradiol	0.0065±0.00168[a]	6
28 days		
Negative control	0.0073±0.00336[ab]	5
Vehicle control	0.0046±0.00244[a]	5
Eyestalk ablation	0.0092±0.00177[b]	8
17β-estradiol	0.0061±0.00261[ab]	6

3.5.4 Effects of diets supplemented with 17β-estradiol on expression of reproduction-related genes in ovaries of 18-monnth-old *P. monodon*

At the end of the experiment, the remaining 17β-estradiol in diets was kindly analyzed by the Hormonal Analysis Laboratory in Wildlife, Chaingmai Zoo. The results using competitive ELISA indicated that 17β-estradiol was not found in the control diet while 29.9% and 40.9% were found in diets originally supplemented with 1 and 10 mg/kg 17β-estradiol (Table 3.10).

Table 3.10 Analysis of the remaining 17β-estradiol in the artificial diets

Diet	Amount 17β-estradiol in diet (mg/kg)
Control	0.000
1 mg/kg estradiol	0.299 (29.9%)
10 mg/kg estradiol	4.090 (40.9%)

Effects of 17β-estradiol-supplemented diets on expression of *PmAtNS, PmAST, Pm-mago nashi* and *PmNHR96* in 18-month-old domesticated *P. monodon* were examined at 7, 14 28 and 35 days post treatment.

The expression level of *PmAtNS* after feeding with the diet supplemented with 1 and 10 mg/kg of 17β-estradiol for 7 days were significantly lower than that of the control ($P < 0.05$). However, prolonged treatment 17β-estradiol did not affect the expression level of this gene disregarding the doses of 17β-estradiol. In eyestalk-ablated shrimp, the expression level of *PmAtNS* at 7 days was significantly lower than that of the control and was significantly increased at 28 days after treatment ($P < 0.05$) (Figure 3.32 and Table 3.11).

The expression level of *PmAST* after feeding with the diet supplemented with 10 mg/kg of 17β-estradiol for 7 days was significantly lower than that of the control ($P < 0.05$). However, the contradictory result was obtained from the treatment with 1 mg/kg of 17β-estradiol as an increase expression level of *PmAST* was observed at 35 days post treatment ($P < 0.05$). Eyestalk ablation resulted in an increased

expression level of this gene at 35 days post treatment ($P < 0.05$) (Figure 3.33 and Table 3.12).

The expression level of *Pm-mago nashi* after feeding with the diet supplemented with 10 mg/kg of 17β-estradiol for 7 days was significantly greater than that of the control ($P < 0.05$). The results were also significant at 14 days post treatment as the expression level of *Pm-mago nashi* in treated shrimp was lower than that of the control for both 1 and 10 mg/kg of 17β-estradiol ($P < 0.05$). Eyestalk ablation did not resulted in changes of the expression level of this gene during the experimental period (Figure 3.34 and Table 3.13).
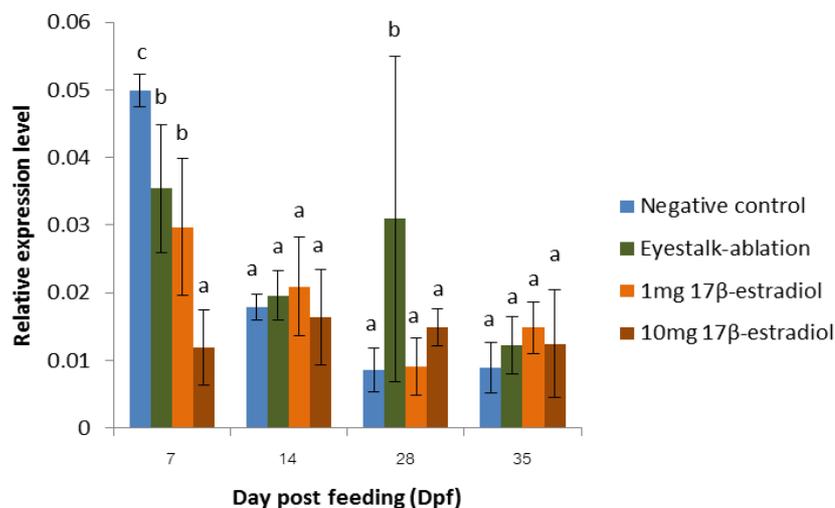
Figure 3.32 Histograms showing relative expression levels of *PmAtNS* after feeding with diets supplemented with 17β-estradiol. Non-treated shrimp and eyestalk-ablated shrimp were included as the negative and positive control.

Table 3.11 Relative expression levels of *PmAtNS* after feeding with diets supplemented with 17β-estradiol.

Group	Relative expression	N
7 days		
Normal shrimp	0.0499 ± 0.00242^c	4
Eyestalk ablation	0.0354 ± 0.00945^b	3
1 mg 17β-estradiol	0.0297 ± 0.01015^b	6
10 mg 17β-estradiol	0.0119 ± 0.00553^a	6
14 days		
Normal shrimp	0.0178 ± 0.00193^a	6
Eyestalk ablation	0.0196 ± 0.00367^a	3
1 mg 17β-estradiol	0.0209 ± 0.00727^a	6
10 mg 17β-estradiol	0.0164 ± 0.0071^a	5
28 days		
Normal shrimp	0.0085 ± 0.00322^a	6
Eyestalk ablation	0.0309 ± 0.02405^b	3
1 mg 17β-estradiol	0.0090 ± 0.00422^a	4
10 mg17β-estradiol	0.0149 ± 0.00269^a	4
35 days		
Normal	0.0089 ± 0.00372^a	8
Eyestalk ablation	0.0122 ± 0.00419^a	4
1 mg 17β-estradiol	0.0148 ± 0.00382^a	6
10 mg17β-estradiol	0.0124 ± 0.00797^a	5
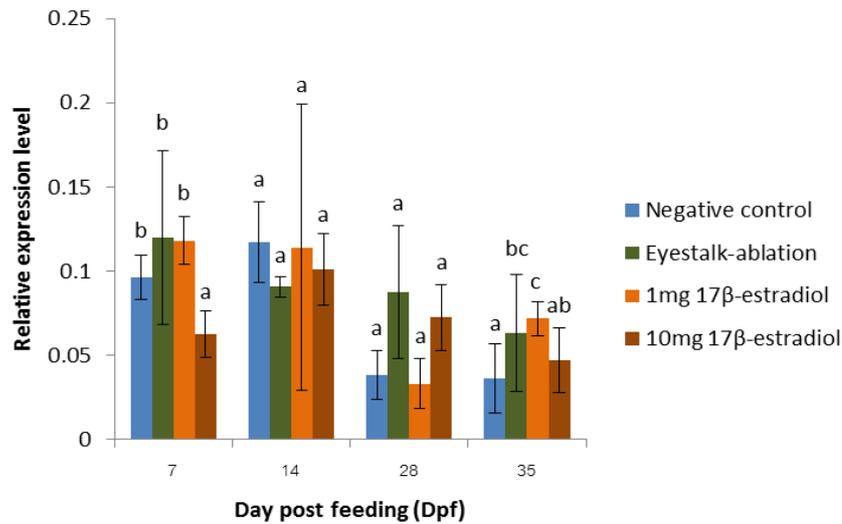
Figure 3.33 Histograms showing relative expression levels of *PmAST* after feeding with diets supplemented with 17β-estradiol. Non-treated shrimp and eyestalk-ablated shrimp were included as the negative and positive control.

Table 3.12 Relative expression levels of *PmAST* after feeding with diets supplemented with 17β-estradiol.

Group	Relative expression	*N*
7 days		
Normal	0.0962 ± 0.01307^b	6
Eyestalk ablation	0.1200 ± 0.02396^b	3
1 mg 17β-estradiol	0.1182 ± 0.0143^b	6
10 mg17β-estradiol	0.0625 ± 0.0143^a	6
14 days		
Normal	0.1170 ± 0.05149^a	6
Eyestalk ablation	0.0908 ± 0.00597^a	3
1 mg 17β-estradiol	0.1142 ± 0.03926^a	6
10 mg17β-estradiol	0.1009 ± 0.03461^a	5
28 days		
Normal	0.0383 ± 0.01417^a	6
Eyestalk ablation	0.0877 ± 0.08521^a	5
1 mg 17β-estradiol	0.0332 ± 0.01466^a	4
10 mg17β-estradiol	0.0726 ± 0.0102^a	4
35 days,		
Normal	0.0363 ± 0.01382^a	8
Eyestalk ablation	0.0634 ± 0.02117^{ab}	4
1 mg 17β-estradiol	0.0719 ± 0.01973^c	6
10 mg17β-estradiol	0.0469 ± 0.01914^{ab}	5
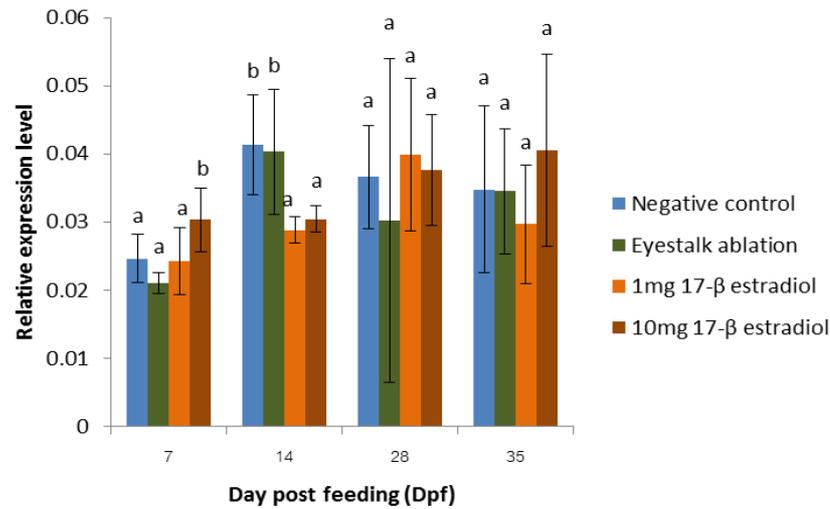
Figure 3.34 Histograms showing relative expression levels of *Pm-mago nashi* after feeding with diets supplemented with 17β-estradiol. Non-treated shrimp and eyestalk-ablated shrimp were included as the negative and positive control.

Table 3.13 Relative expression levels of *Pm-magonashi* after feeding with diets supplemented with 17β-estradiol.

Group	Relative expression	*N*
7 days		
Normal	0.0246±0.00353[a]	6
Eyestalk ablation	0.0211±0.00153[a]	3
1 mg 17β-estradiol	0.0242±0.00492[a]	6
10 mg17β-estradiol	0.0303±0.00462[b]	6
14 days		
Normal	0.0413±0.00738[b]	6
Eyestalk ablation	0.0403±0.00917[b]	3
1 mg 17β-estradiol	0.0288±0.00191[a]	6
10 mg17β-estradiol	0.0304±0.00193[a]	5
28 days		
Normal	0.0366±0.00761[a]	6
Eyestalk ablation	0.0302±0.0237[a]	5
1 mg 17β-estradiol	0.0399±0.01114[a]	5
10 mg17β-estradiol	0.0376±0.00811[a]	4
35 days		
Normal	0.0348±0.01232[a]	7
Eyestalk ablation	0.0345±0.00919[a]	4
1 mg 17β-estradiol	0.0297±0.00869[a]	5
10 mg17β-estradiol	0.0405±0.01405[a]	5

The expression level of *PmNHR96* after feeding with the diet supplemented with 1 mg/kg and 10 mg/kg of 17β-estradiol was not significantly different at all time of the experiment ($P > 0.05$). In eyestalk-ablated shrimp, the expression level of *PmNHR96* was significantly increased at 14 days but not different at 7, 28 and 35 after treatment (Figure 3.35 and Table 3.14).
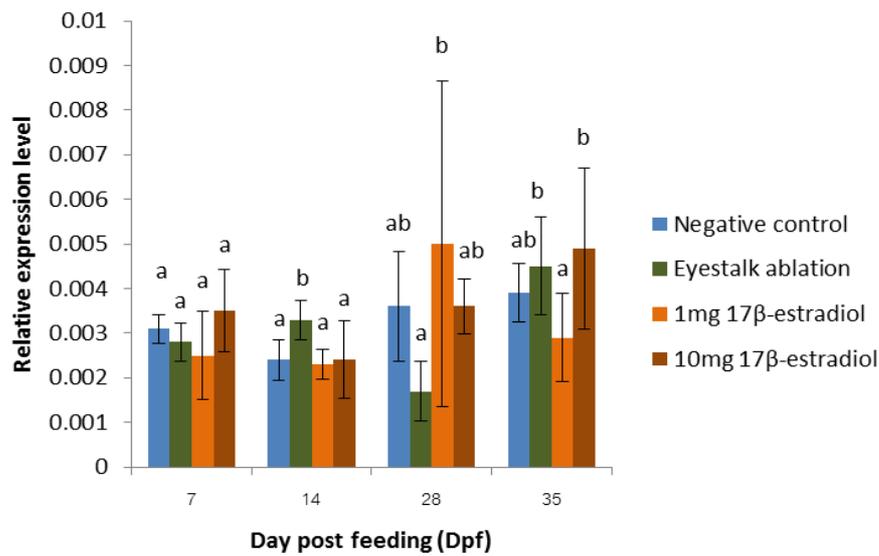
Figure 3.35 Histograms showing relative expression levels of *PmNHR96* after feeding with diets supplemented with 17β-estradiol. Non-treated shrimp and eyestalk-ablated shrimp were included as the negative and positive control.

Table 3.14 Relative expression levels of *PmNHR96* after feeding with diets supplemented with 17β-estradiol.

Group	Relative expression	N
7 days		
Normal	0.0031 ± 0.00032^a	6
Eyestalk ablation	0.0028 ± 0.00043^a	3
1 mg 17β-estradiol	0.0025 ± 0.001^a	6
10 mg17β-estradiol	0.0035 ± 0.00093^a	6
14 days		
Normal	0.0024 ± 0.00046^a	6
Eyestalk ablation	0.0033 ± 0.00044^b	3
1 mg 17β-estradiol	0.0023 ± 0.00034^a	6
10 mg17β-estradiol	0.0024 ± 0.00087^a	5
28 days		
Normal	0.0036 ± 0.00123^{ab}	6
Eyestalk ablation	0.0017 ± 0.00068^a	4
1 mg 17β-estradiol	0.0050 ± 0.00364^b	6
10 mg17β-estradiol	0.0036 ± 0.00062^{ab}	4
35 days		
Normal	0.0039 ± 0.00066^{ab}	6
Eyestalk ablation	0.0045 ± 0.0011^b	4
1 mg 17β-estradiol	0.0029 ± 0.00098^a	6
10 mg17β-estradiol	0.0049 ± 0.0018^b	5

3.6 *In vitro* expression of recombinant PmNHR96 using the bacterial expression system

3.6.1 Construction of recombinant plasmids

Recombinant plasmids carrying the ligand-binding domain of PmNHR96 was successfully constructed for *in vitro* expression of the corresponding protein domain. A primer pair overhung with *Bam*HI and *Xho*I-6XHis was designed to amplify fragment of 660 bp in length corresponding to 213 amino acids.

Subsequently, the amplified ligand binding domain of hormone receptor (HOLI) of PmNHR96 was amplified by *Pfu* (Figure 3.36A) and digested with *Bam*HI and *Xho*I. The gel-eluted product (Figure 3.36B) was ligated with pET-29a expression vector and transformed into *E. coli* JM109. For examining the orientation of recombinant plasmid pHOLI-PmNHR96, the positive plasmid DNA was sequenced for both directions. Nucleotide sequence was analyzed by BlastX and the correct orientation of pHOLI-PmNHR96 was confirmed (Figure 3.37B).
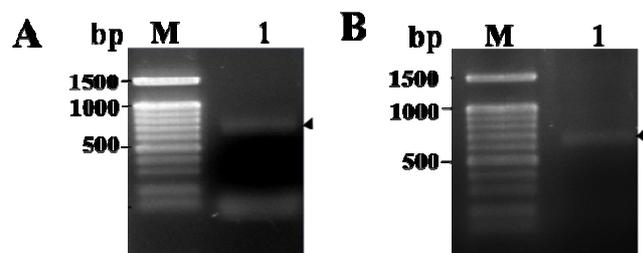
Figure 3.36 (A) Gel electrophoresis showing the PCR fragment of ligand-binding domain (HOLI) of *PmNHR96* amplified by domain-specific primer overhang with *Bam*HI and *Xho*I-6XHis using the first strand cDNA from ovaries as the template. (B) The purified PCR fragment was digested with *Ban*HI and *Xho*I. Lane M = a 100 bp DNA ladder.

A.

```
GGATCCATGCTATCGGAGGCGAACAAGGGCCTTCTGGCGCCGCTCTGCGAGGATTATAATTTTAAGGAC
CTGAGCAACCCGTCGCTTCTCAACATCATCAACCTGACGGAGATCGCCATCCGCCGCCTCATCAAGATG
TCGAAGAGAATATCCGCCTTCAAGAGCCTCTGCCAGGAGGACCAGATCGCGCTGCTCAAGGGAGGCTGC
ACAGAGATGATGATCCTGCGGTCCGTCAGCGCCTACGACCCCGATAAGGACTCGTGGATGATTCAACAG
GACCATGACCGTTTCAAGAACATCAAGCTGAAGGTACTAAAGGCCGCCCCAGGGAACGTCTATGAGGAA
CACAAGAGATTTATCTTGGCGTTTCAGCCGGAGTGGAGACAAGACCACAACATCATCTTCCTCTTATCA
GCTATTACGCTCTTCACGCCCGAGAGGCCTAACATAATCCATGGCGATGCTATTAAACACGAACGGTGC
TCATACCTGTACCTCCTGAAGCGCTACCTGGAGTGCAAGTACGGAGGTTGTGAAGGAAGGACGGTTTAC
CTCCGGCTGCTAGAGAGGATTAAGCATCTCAACATCCTCAATGAGAAGCACATTCGTGTCTTTCTAGAC
GTCAATCCGCAAGAAGTCGAACCACATCATCATCATCATCATTAACTCGAG
```

B.

> ☐ ref|XP_002404556.1| U G nuclear hormone receptor 48, putative [Ixodesscapularis]
gb|EEC11854.1| G nuclear hormone receptor 48, putative [Ixodesscapularis]
Length=412

GENE ID: 8033479 IscW_ISCW009328 | nuclear hormone receptor 48, putative [Ixodesscapularis]

```
 Score =  229 bits (584),  Expect = 7e-70
 Identities = 110/180 (61%), Positives = 142/180 (79%), Gaps = 2/180 (1%)
 Frame = +1

Query  100  TEIAIRRLIKMSKRISAFKSLCQEDQIALLKGGCTEMMILRSVSAYDPDKDSWMIQQDHD  279
            T+ AIRRLIKMSKRI+AFKSLCQEDQ+ALLKGG TE+M+LRSV +YD ++D W  +
Sbjct  226  TDHAIRRLIKMSKRITAFKSLCQEDQVALLKGGSTELMLLRSVMSYDAERDCW--KGPDP  283

Query  280  RFKNIKLKVLKAAPGNVYEEHKRFILAFQPEWRQDHNIIFLLSAITLFTPERPNIIHGDA  459
R  +IKL +LK A GNVYEEHKRFI AF+PEWR D NI+ LLSAITLFTPERPN++H D
Sbjct  284  RLMSIKLDILKEARGNVYEEHKRFINAFRPEWRIDENIMLLLSAITLFTPERPNLVHRDV  343

Query  460  IKHERCSYLYLLKRYLECKYGGCEGRTVYLRLLERIKHLNILNEKHIRVFLDVNPQEVEP  639
+  E+ +YLYLL+RYL+   Y GCE R+V+L+L+  ++ +  LNE  + + +D+NP+EVEP
Sbjct  344  VTFEQDTYLYLLRRYLDTIYTGCESRSVFLQLIRNLEDMRTLNENQVSILVDLNPREVEP  403
```

Figure 3.37 (A) Nucleotide sequence of the recombinant plasmid covering the ligand-binding domain, HOLI) of *PmNHR96*. (B) the Blast X result of nucleotide sequence ofthe recombinant plasmid.

3.6.2 *In vitro* expression of recombinant protein

In vitro expression of rHOLI-PmNHR96 (ligand-binding hormone domain) after induction with 0.4 mM IPTG at 0, 2, 4, 6, 12, 24 hr at 37 °C was examined. The recombinant protein of 25.7 kDa was found after induced with IPTG for 2-4 hr. The extent period from 6 hr to overnight gradually reduced the expression of rHOLI-PmNHR96 (Figure 3.38).
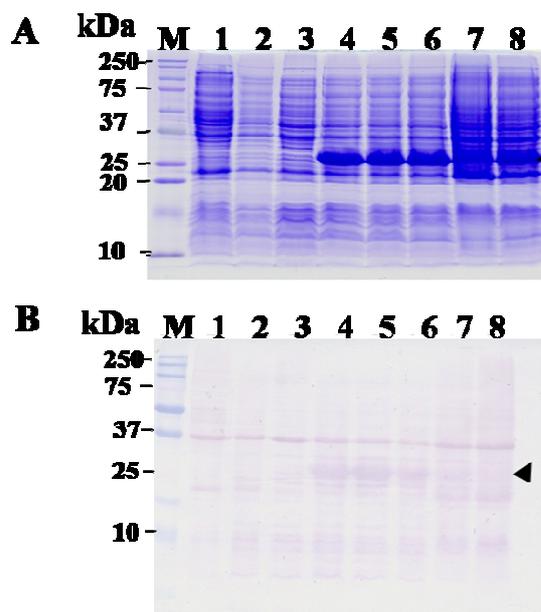
Figure 3.38 SDS-PAGE (A) and Western blot analysis (B) showing *in vitro* expression of the ligand-binding domain, HOLI of PmNHR96 after induction with 0.4mM. Lanes 1-2 =*E. coli* BL 21-CodonPlus (DE3)-RIPL and that containing pET-29a vector, lanes 3-8 = *E. coli* BL 21-CodonPlus (DE3)-RIPL containing recombinant plasmid after induced with 0.4 mM IPTG for 0, 2, 4, 6, 12 and 24 hours respectively.

In addition, cell localization of PmNHR96 protein was examined. Aliquots of the IPTG-induced culture (OD = 1) of rHOLI-PmNHR96 protein cultured at 37°C for 2 hour after IPTG induction was collected. The soluble and insoluble protein fractions of this recombinant protein were analyzed by 15% SDS-PAGE.

The rHOLI-PmNHR96 protein was expressed in the insoluble fraction but not in the soluble fraction when the recombinant clone was cultured at 37 °C for 2 hour (Figure 3.39A). Results were consistent when cultured at 15 °C after induction with 0.4 mM IPTG (Figure 3.39B).
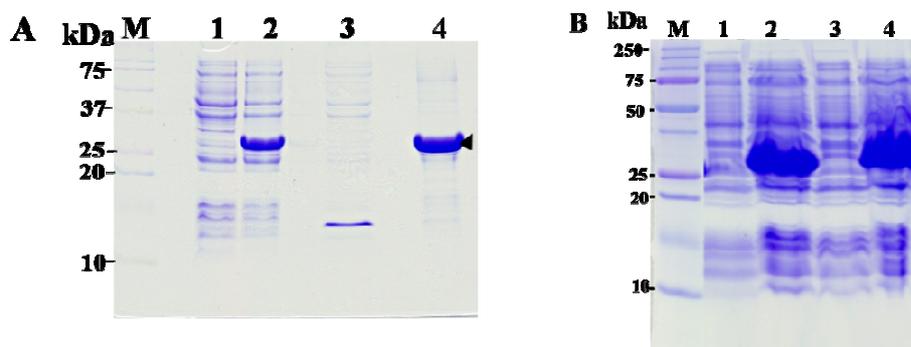
Figure 3.39 15% SDS-PAGE showing *in vitro* expression of recombinant clone of the ligand-binding domain, HOLI of PmNHR96 cultured at 37 °C (A) and 15 °C (B) for 2 hours after induction with 0.4 mM IPTG. Lane 1 is whole cells before IPTG induction, lane 2 is whole cells after IPTG induction, lane 3 = the soluble protein fraction, lane 4 = the insoluble fraction. Lane M = the protein standard marker.

3.6.3 Purification of recombinant protein

The rHOLI-PmNHR96 protein was purified from insoluble fractions under the denaturing conditions. Initially, the washed and eluted fractions were analyzed by SDS-PAGE (Figure 3.40). After purification, eluted proteins fractions were kept at -20 °C overnight.

The discrete band of approximately 25.7 kDa was found in both the washed fractions and the eluted fractions. Fractions containing the purified recombinant protein were pooled, concentrated and size-fractionated through SDS-PAGE (Figure 3.41).

The expected 25.7 kDa band of recombinant protein were excised and electro-eluted. After concentrated, the purified rHOLI-PmNHR96 was sent to Faculty of Medical Technology for the production of polyclonal antibody in rabbit.
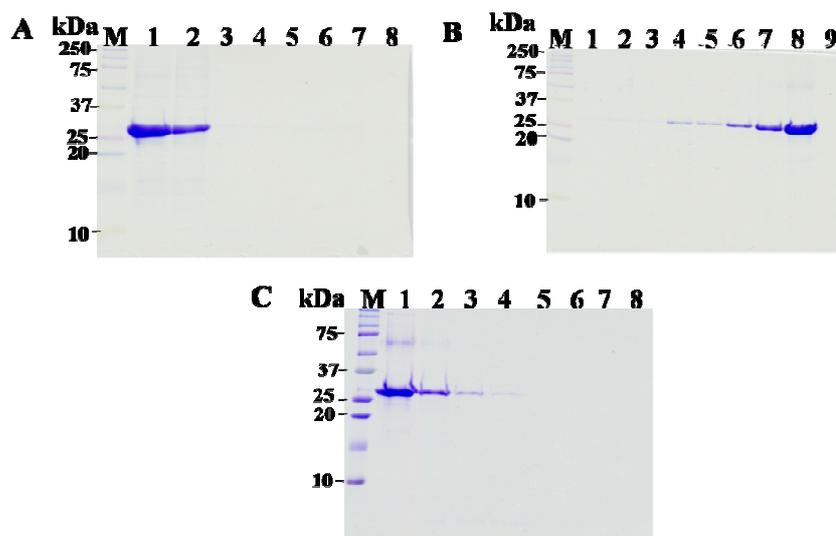
Figure 3.40 15 % SDS-PAGE showing of the purification of rHOLI-PmNHR96 under the denaturing conditions. **A** : lane 1 = whole cells, lane 2 = the insoluble fraction after pass through the column, Lanes 3-6 = the first wash fractions, Lanes 7-8 = the second wash fractions. **B** : lanes 1-3 = the second wash fractions, lanes 4-9 = third wash fractions. **C**: lanes 1-8 = the eluted fractions. Lane M = the protein standard marker.
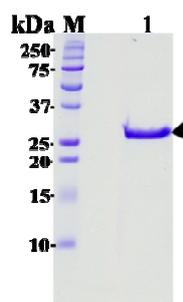
Figure 3.41 15 % SDS-PAGE showing of purified rHOLI-PmNHR96 after concentrated. Lane M = the protein standard marker.

Anti-rHOLI-PmNHR polyclonal antibody (PcAb) was successfully produced in rabbit after the third immunization (Table 3.15). Rabbits were sacrificed and their serum was collected, filtrated through 0.22 μM membrane and kept at -20 ℃.

Table 3.15 Titers of polyclonal antibody using indirect ELISA assay after rabbits were immunized with recombinant NHR96 for 3 times

Dilution of serum	Polyclonal antibody	
	Pre-immunized serum(OD_{450})*	Immunized serum (OD_{450})**
1:500	0.062	2.310
1:2000	0.031	1.259
1:8000	0.018	0.494
1:32000	0.016	0.148

*Preimmunized serum = serum of a rabbit before immunization.
**Immunized serum = serum from rabbit injected with rHOLI-PmNHR96

3.6.4 Western blot analysis of PmNHR96 protein during ovarian development of *P. monodon*

Anti-rHOLI-PmNHR96 was analyzed by Western blot using total protein extracted from ovaries of intact broodstock (juveniles ovaries and stages I, II, III, IV and post-spawning ovaries of broodtock). The intense band of approximately 75 kDa and several additional bands were observed. Based on the fact that the actual molecular size of ovarian PmNHR96 is not available, further analysis of the positive bands should be examined using mass spectrometry (e.g LC-MS/MS) (Figure 3.42).
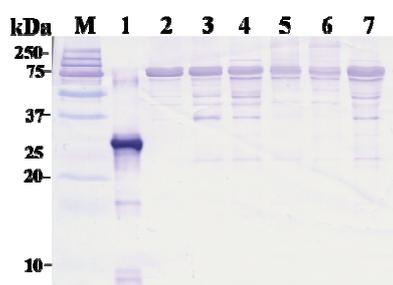
Figure 3.42 Western blot analysis of anti-rHOLI-PmNHR96 (1:200, expected MW ~ 80 kDa) using total protein extracted from ovaries (20 µg) of intact broodstock. Lane 1 = rHOLI-PmNHR96, lanes 2 -7 =ovarian proteins of juvenile and broodstock with

stages I, II, III, IV and V (post-spawning) ovaries, respectively. Lane M = the protein standard marker.

The polyclonal antibody against rHOLI-PmNHR was immunochromatographic purified (protein A) and western blot was carried out. Like results from non-purified polyclonal antibody, non-specific patterns were obtained. Therefore, the determination of expression profile of PmNHR96 was not further carried out (Figure 3.43).
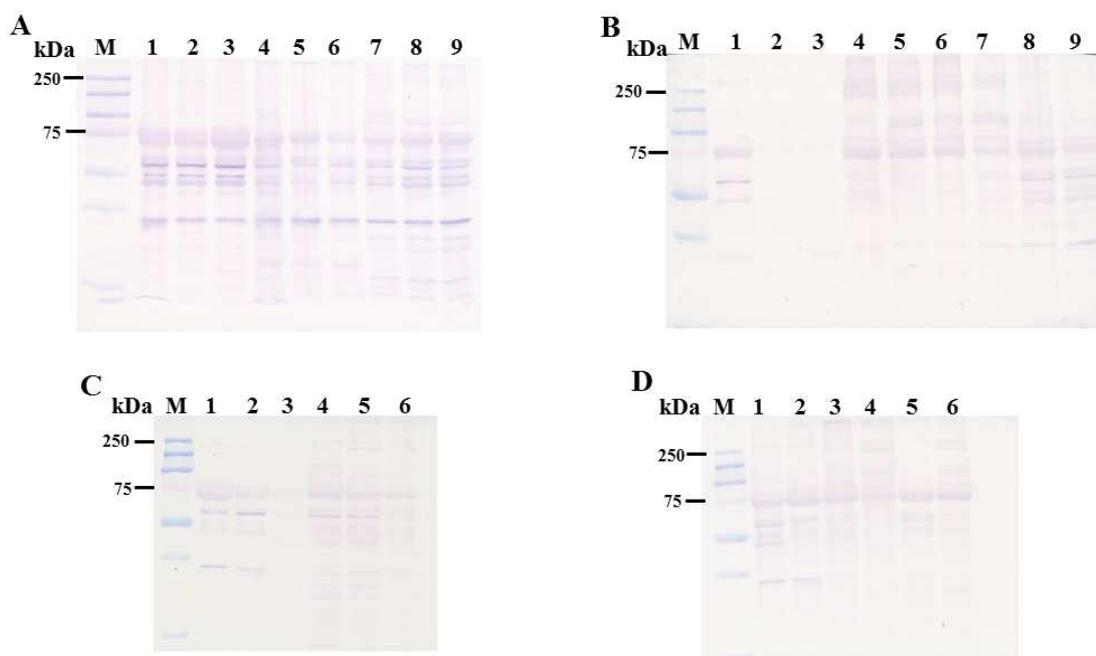
Figure 3.43 Western blot analysis of anti-rHOLI-PmNHR96 (1 : 200) using total protein extracted from ovaries (20 µg) of intact (A and B) and eyestalk-ablated (C and D) broodstock. A : lanes 1-3 = juveniles, lanes = 4-6 =stage I ovaries with GSI of 0.67, 1.26 and 0.81, lanes 7-9 = stage II ovaries with GSI of 2.95, 2.58 and 2.24; B : lanes 1-3 = stage III ovaries with GSI of 5.0, 5.91 and 6.23, lanes 4-6 = stage IV ovaries with GSI of 7.46, 10.414 and 11.213, lanes 7-9 = stage V (post-spawning) ovaries with GSI of 1.86, 3.49 and 3.27; C: lanes 1-3 = stage I ovaries with GSI of 0.76, 1.41 and 1.45, lanes 4-6 = stages II ovaries with GSI of 2.72, 2.32 and 2.71; D : lanes 1-3 = stages III ovaries with GSI of 5.79, 4.64 and 4.29, lanes 4-6 = stages IV ovaries with GSI of 10.94, 7.17 and 9.09 ; Lane M = the protein standard marker.

CHAPTER IV

DISCUSSION

There have been many studies on characterization of vitellogenin/vitellin and the elucidation of the process of vitellogenesis in penaeid shrimp (Tsutsui *et al*., 2000; Okumura *et al*., 2006) as well as molecular endocrinology of shrimp reproduction, particularly on GIH and methylfarnosoate (MF) (Silva Gunawardene *et al*., 2001; Gu *et al*.,2002; Yamano *et al*., 2004). Although these studies begin to reveal a better picture of the endocrine control of ovarian maturation in shrimp, reproductive maturation of penaeid shrimp is still not well understood.

Different biotechnological approaches, for example; injection of vertebrate steroid hormones and neurotransmitters and the use of specially formulated feed can be applied to induce ovarian maturation of female penaeid shrimp.

Yano and Hoshino (2006) determined the effects of 17β-estradiol on vitellogenin synthesis and oocyte development were investigated in previtellogenic ovaries of *M. japonicus* incubated with Medium 199. After three days incubation ofthe ovarian tissue, Vitellogenin concentrations in media containing 3.6 nM, 36.7 nM, 367 nm and 3671 nM 17β-estradiol were significantly ($P< 0.01$) greater than that of the control. A more advanced stage of oocyte development at primary vitellogenic stage, which is surrounded by round and greatly expanded follicle cells, was observed in previtellogenic ovarian pieces incubated in media containing 17β-estradiol. The results suggested that 17 β-estradiol induces Vg-itellogenin synthesis and appearance of primary vitellogenic oocytes in the ovaries of immature *M. japonicus*.

In this study, effects of 17β-estradiol on expression of several reproduction-related genes were examined for the possible use of this sex steroid hormone for stimulation of ovarian development in *P. monodon*.

Isolation and characterization of *PmNHR96* and *PmSOS*

The actions of sex steroid are mediated through the nuclear receptor, a member of the steroid/thyroid hormone receptor superfamily, as the classical pathway.

Recently, the full-length cDNAs of *progestin membrane receptor component 1* (*Pgmrc1*) were isolated from both testes (Leelatanawit *et al*., 2008) and ovaries (Preechaphol et al., 2010) of *P. monodon*. Unilateral eyestalk ablation resulted in a greater expression of *PmPgmrc1* in vitellogenic, early cortical rod and mature ovaries compared to that in the same ovarian stages of intact broodstock (*P*< 0.05). Immunohistochemistry revealed the positive signals of the PmPgmrc1 protein in the follicular layers and cell membrane of follicular cells and various stages of oocytes (Preechaphol *et al*., 2010). However, no nuclear hormone receptor has been identified and characterized in *P. monodon*.

In the present study, the partial ORF (879 bp, 292 amino acids) and 3′UTR of 1679 bp (excluding the poly A tail) of *PmNHR96* was isolated. Nevertheless, the full-length cDNA of this transcript was not obtained after RACE-PCR was carried out for several times.

Nuclear hormone receptor proteins is recognized as a class of ligand activated proteins that, when bound to specific sequences of DNA, serve as on-off switches for transcription within the cell nucleus as well as the continual regulation of reproductive tissues. Nuclear hormone receptors regulate gene expression by interacting with specific DNA sequences upstream of their target genes.

In addition, the partial cDNA of *PmSOS* (928 bp) was also isolated. The deduced amino acid sequence contained the predicted guanine nucleotide exchange factor for Rho/Rac/Cdc42-like GTPases (RhoGEF) and Pleckstrin homology domain (PH) domins. Like *PmNHR96*, the full-length cDNA of *PmSOS* was not obtained after RACE-PCR was carried out for several times.

Son of sevenless (SOS) is a dual specificity guanine nucleotide exchange factor (GEF) that regulates both Ras and Rho family GTPases and thus is uniquely poised to integrate signals that affect both gene expression and cytoskeletal

reorganization (Yang, 2006)**.** The *SOS* gene functions in signaling pathways initiated by the sevenless and epidermal growth factor receptor tyrosine kinases (Bonfini, 1992).

Expression levels of of *PmAtNS*, *PmAST*, *Pm-mago nashi PmNHR96* and *Pmson of sevenless* transcripts functionally involved in reproductive development and maturation of *P. monodon*

Transcription in germ cells during oogenesis follows carefully regulated programs corresponding to a series of developmental events in oocytes**.** RT-PCR analysis across various tissues of female and testes of male broodstock indicated that *PmAtNS*, *PmAST*, *Pm-mago nashi, PmNHR96* and *PmSOS* were not specifically expressed in ovaries or gonads but were observed in a variety of tissues of *P. monodon* broodstock. The results suggested that they should be multifunctional proteins playing the role in several physiological and biological processes.

These genes were more abundantly expressed in ovaries than testes of *P. monodon* broodstock. The information suggested that they should play more important role in ovarian than testicular development.

Expression analysis of *PmAtNS*, *PmAST*, *Pm-mago nashi* and *PmNHR96* in ovaries of *P. monodon* broodstock

Quantitative real-time PCR indicated that the expression level of *PmAtNS* and *Pm-mago nashi* was not significantly different during ovarian development in both intact and eyestalk-ablated broodstock. The expression level of both *PmAST* was significantly increased in stage II and *PmNHR96* was significantly increased in stage IV ovaries in intact *P. monodon* broodstock.

Unilateral eyestalk ablation is used in practice to induce ovarian maturation in penaeid shrimp. Eyestalk ablation caused an increase in the mRNA levels of *vitellogenin* and *cortical rod protein* in ovaries of *M. japonicas* (Tsutsui et al., 2005; Okumura et al., 2006).

Eyestalk ablation resulted in significant greater expression levels of *PmAST* in stages II ovaries, *Pm-mago nashi* in stages I-IV and *PmNHR96* in stages I-III ovaries compared to those in intact broodstock. The increase in mRNA of these genes during

ovarian development in eyestalk-ablated female broodstock suggests that gonad inhibiting hormone (GIH; Meusy and Payen, 1988) affects *PmAST, Pm-mago nashi* and *PmNHR96* transcription.

The expression levels of *PmAtNS*, *PmAST*, *Pm-mago nashi* and *PmNHR96* in ovarian of *P. monodon* following the injection of 17β-estradiol

The presence of vertebrate-type steroids has been documented in almost all invertebrate groups including crustaceans (Cardosa et al., 1997). The conversion of progesterone into 17β-estradiol was reported in *M. japonicus* (Summavielleet al., 2003). 17β-estradiol levels in the hemolymph were shown to fluctuate closely with that of the serum vitellogenin level during ovarian maturation stages of *P. monodon* (Quinitio et al.,1994) implying its controlling role in vitellogenesis.

In this study, 17β-estradiol injection was carried out and resulted in significantly reduced of ovarian *PmAtNS* at 7 days post injection but did not affect the expression level of *PmAST* and *Pm-mago nashi*. Nevertheless, the expression level of ovarian *PmNHR96* seemed to be increased at 7 days after injection.

Eyestalk ablation resulted in the significant increase in the expression of *PmATS* at 28 days after unilateral eyestalk ablation. Similarly, an induction of *Pm-mago nashi* and *PmNHR96* in domesticated 14-month-old shrimp was observed at 7 days and 14 days after ablation, respectively.

Considering effects of the expression of various genes under 17β-estradiol treatment and eyestalk ablation, it is proposed that 17β-estradiol inhibits the transcription of *PmAtNS* and not expression of, *PmAST* and *Pm-mago nashi PmNHR96*. Therefore, 17β-estradiol injection, at least at the concentration used in this study, may inhibit ovarian development of *P. monodon*.

The expression levels of *PmAtNS*, *PmAST*, *Pm-mago nashi* and *PmNHR96* in ovarian of *P. monodon* after feeding with the diet supplemented with 17β-estradiol

Subsequently, the feeding experiment using diets supplemented with 1 and 10 mg/kg of 17β-estradiol was carried out. The remaining 17β-estradiol in the diets was

analyzed and 25.9% and 40.9% resulting in the actual amount of 0.259 and 4.09 mg/kg diets were found.

The expression level of *PmAtNS* and *Pm-mago nashi* after feeding with the diet supplemented both with 1 and 10 mg/kg of 17β-estradiol for 7 and 14 days, respectively was significantly lower than that of the control ($P < 0.05$) and *PmAST* after feeding with the diet supplemented 10 mg/kg of 17β-estradiol for 7 days was significantly lower than that of the control ($P < 0.05$). In contrast, feeding with 1 mg/kg of 17β-estradiol resulted in an increase expression level of ovarian *PmAST* at 35 days post treatment ($P < 0.05$). Likewise, feeding of 10 mg/kg of 17β-estradiol supplemented diets resulted in a greater level of *Pm-mago nashi* than that of the control at 7 days post treatment ($P < 0.05$). The expression level of *PmNHR96* after feeding with the diet supplemented was not significantly than that of the control ($P < 0.05$). Apparently, results from both injection and diet supplementation of 17β-estradiol on expression of reproduction-related genes in this study were similar.

Yano and Hoshino (2006) illustrated that 17β-estradiol induces vitellogenin synthesis and oocyte development in ovaries of immature *M. japonicus in vitro*. In lobster (*Homarusamericanus*), 17β-estradiol was found in vitellogenic ovary, although it was undetectable inprevitellogenic ovary (Couch *et al*., 1987). Based on the information in various species, it is proposed that 17β-estradiol induces vitellogenin synthesis and may act as an ovarian vitellogenesis-stimulating hormone (OVSH) in immature females of decapod crustaceans.

Demonstrating the effects of hormones or neurotransmitters on ovarian development of *P. monodon* is rather difficult in immature females. The reason is that immature females are strongly affected by GIH from the X organ-sinus gland complex of the eyestalk compared to maturing females. It should be noted that, domesticated shrimp with an immature ovarian stage were used in the present study.

Like results in this study, significant ovarian development was not observed in the tiger prawn, *P.esculentus* with undeveloped ovaries after injection of 17β-estradiol (0.01 μg/g body weights) alone or in combination with prostaglandin E_2 (PGE_2) under tank-reared conditions during the tri at of 5 weeks (Koskela *et al*., 1992).

It is possible that the effects of injected 17β-estradiol in shrimp with undeveloped ovaries are influenced by the GIH level or by numerous stresses originating from handling or the culture condition in tanks. Accordingly, *in vitro* effects of 17β-estradiol on expression of various reproduction-related genes should be carried out.

Molecular mechanisms involving gonadal development of *P. monodon* have long been of interest by aquaculture industries. Considering all information in this study, *PmAtNS*, *PmAST*, *Pm-magonashi* and *PmNHR96* should play the role during ovarian development and maturation of *P. monodon*. The expression levels of their protein during ovarian development and/or oogenesis should be further examined for an unambiguous conclusion on the functions of these gene products. The basic knowledge obtained allows functional characterization of *PmAtNS*, *PmAST*, *Pm-magonashi* and *PmNHR96* genes and proteins on ovarian and oocyte development for better understanding of the reproductive maturation of female *P. monodon* in captivity.

CHAPTER V

CONCLUSIONS

1. The partial cDNA sequences of *PmNHR96* and *PmSOS* were isolated. They were 2436 and 1183 bp containing the ORFs of 879 and 1183 bp, respectively.

2. Tissue distribution analysis of *PmAtNS, PmAST, Pm-mago nashi*, *PmNHR96* and *PmSOS* were examined and these transcripts were abundantly expressed in ovaries of *P. monodon* broodstock. *PmAtNS, PmAST* and *PmSOS* were more preferentially expressed in ovaries than testes of *P. monodon*.

3. Quantitative real-time PCR indicated that the expression level of *PmAtNS* was not significantly different during ovarian development in both intact and eyestalk-ablated broodstock. Its expression in stage II ovaries of intact broodstock was significantly greater than that in the same ovarian stage in eyestalk-ablated broodstock ($P < 0.05$).

4. The expression level of ovarian *PmAST* was significantly increased in stage IV ovaries in intact broodstock but was not differentially expressed in eyestalk-ablated shrimp. Its expression in stages II ovaries of eyestalk-ablated broodstock was significantly greater than that in the same ovarian stage in intact broodstock ($P < 0.05$).

5. *Pm-mago nashi* was not differentially expressed during ovarian development in both intact and eyestalk-ablated broodstock ($P > 0.05$). The expression level of *Pm-mago nashi* in stage I-IV ovaries of eyestalk-ablated broodstock was significantly greater than that in the same ovarian stages in intact broodstock ($P < 0.05$).

6. The expression level of *PmNHR96* in intact broodstock was increased in stage IV ovaries but was not differentially expressed in eyestalk-ablated broodstock. Its expression in stages I-III ovaries of eyestalk-ablated broodstock was significantly greater than that in the same ovarian stages in intact broodstock ($P < 0.05$).

7. Exogenous injection of 17β-estradiol resulted in significantly reduction of ovarian *PmAtNS* at 7 days post injection but did not affect the expression level of *PmAST* and *Pm-mago nashi*. Nevertheless, the expression level of ovarian *PmNHR96* seemed to be increased at 7 days after injection.

8. The expression level of *PmAtNS* after feeding with the diets supplemented both with 1 and 10 mg/kg of 17β-estradiol for 7 days was significantly lower than that of the control ($P < 0.05$).

9. Similar results were also found for *PmAST*. Shrimp fed with 10 mg/kg of 17β-estradiol for 7 days had a significantly lower expression of *PmAST* than that of the control ($P < 0.05$). However, the treatment with 1 mg/kg of 17β-estradiol resulted in an increase expression level of *PmAST* at 35 days post treatment ($P < 0.05$).

10. For *Pm-mago nashi*, its expression level was induced after feeding with the diet supplemented with 10 mg/kg of 17β-estradiol for 7 days. In contrast, feeding of diets supplemented both with 1 and 10 mg/kg of 17β-estradiol resulted in the expression level of *Pm-mago nashi* lower than that of the control at 14 days post treatment ($P < 0.05$).

11. The expression level of *PmNHR96* after feeding with the diet supplemented with both with 1 and 10 mg/kg of 17β-estradiol was not significantly than that of the control ($P < 0.05$).

REFERENCES

Benzie, J.A.H. (1998). Penaeid genetics and biotechnology. *Aquaculture*, 164: 23–47.

Bell, T. A., and Lightner, D. V. (1988). A handbook of normal penaeid shrimp histology. *World Aquaculture Society*, Baton Rouge, LA.

Bradford, M.M. (1976). A rapid and sensitive method for the quantitation of microgram quantities of protein utilizing the principle of protein-dye binding, *Anal. Biochemistry*, 72: 248-254.

Brown, M.R., Sieglaff, D.H., and Rees, H.H. (2009). Gonadal ecdysteroidogenesis in arthropoda: occurrence and regulation. *Annu. Rev. Entomol*, 54: 105-125.

Cardoso, A.M., Cristina, M.F., and Correia, A.J. 1997. Identification of vertebrate type steroid hormones in the shrimp *Penaeus japonicus* by tandem mass spectrometry and sequential product ion scanning. *Journal of the American Society for Mass Spectrometry*, 8(4): 365–370.

Clark Jr, W.H., Yudin, A.I., Lynn, J.W., Griffin, F.J., and Pillai, M.C. (1990). Jelly layer formation in Penaeoide an shrimp eggs. *Biol. Bull*, 178: 295–299.

Clifford, H. C., and Preston, N. P. (2006). Genetic improvement in operating procedures for shrimp farming global shrimp OP survey results and recommendations. *Global Aquaculture Alliance*, pp 73-77. St. Louis: USA.

Coman, G.J., Arnold, S.J., Peixoto, S., Crocos, P.J., Coman, F.E., and Preston, N.P. (2006). Reproductive performance of reciprocally crossed wild-caught and tank-reared *Penaeus monodon* broodstock. *Aquaculture*, 252: 372-384.

Couch, E.F., Hagino, N., and Lee, J.W. (1987). Changes in estradiol and progesterone immunoreactivity in tissues of the lobster *Homarus americanus* with developing and immature ovaries. *Comp. Biochem. Physiol*, 87A: 765-770.

Diwan, A. D. (2005). Current progress in shrimp endocrinology-A review. *Ind J Exp Biol*, 43: 209-223.

Donahue, J. K., and Jennings, E. D. (1937). The occurrence of estrogenic substance in the ovaries of echinoderms. *Endocrinology*, 21(5): 690-691.

Dube´ F, Amireault P. (2007). Local serotonergic signaling in mammalian follicles oocytes and early embryos. *Life Sci*, 81:1627-1637.

Fairs, N. J., Quinlan, P.T., and Goad, L. J., 1990. Changes in ovarian unconjugated and conjugated steroid titers during vitellogenesis in *Penaeus monodon*. *Aquaculture*, 89: 83-99.

Fingerman, M., Nagabhushanam, R., and Sarojini, R. (1993). Vertebrate type hormones in crustaceans localization identification and functional significance. *Zool Sci*, 18: 13-29.

Goodwin, T.W. (1978). Ecdysteroids a new generic term. *Nature*, 272: 122.

Gu, P.L., Tobe, S.S., Chow. B.K.C., Chu K.H., He J.G., and Chan S.M. (2002). Characterization of an additional molt inhibiting hormone-like neuropeptide from the shrimp *Metapenaeus ensis*. *Peptides*, 23: 1875-1883.

Gunamalai, V., Kirubagaran, R., and Subramoniam, T. (2006). Vertebrate steroids and the control of female reproduction in two decapods crustaceans, *Emerita asiatica* and *Macrobrachium rosenbergii*. *Curr Sci*, 90 (1): 119-123.

Jalabert, B. (2005). Particularities of reproduction and oogenesis in teleost fish compared to mammals. *Reprod. Nutr. Develop*, 45: 261-279.

Kanchana, S. (2006). Isolation and characterization of gene involving ovarian development of the black tiger shrimp Penaeus monodon. M.Sc. Thesis. Chulalongkorn University, Bangkok, Thailand.

Kenway, W., Macbeth, M., Salmon, M., McPhee, C., Benzie, J., Wilson, K., and Knibb, W. (2006). Heritability and genetic correlations of growth and survival in black tiger prawn *Penaeus monodon* reared in tanks. *Aquaculture*, 259: 138-145.

Khamnamtong, B., Klinbunga, S., Menasveta, P. (2005). Species identification of five penaeid shrimps using PCR-RFLP and SSCP analyses of 16S ribosomal DNA. *J Biochem Mol Biol*, 38: 491-499.

Kim, Y.K., Kawazoe, I., Jasmaani, S., Ohira, T., Wilder, M.N., Kaneko T., and Aida, K. 2007. Molecular cloning and characterization of cortical rod protein in the giant freshwater prawn *Macrobrachium resenbergii*, a species not forming cortical rod structures in the oocytes. *Comp. Biochem. Physiol,* B 148: 184-191.

Klinbunga, S., Penman, D.J., McAndrew, B.J., and Tassanakajon, A. (1999). Mitochondrial DNA diversity in three populations of the giant tiger shrimp *Penaeus monodon. Marine. Biotechnol*, 1: 113-121.

Koskela, R.W., Greenwood, J.G., and Rothlisberg, P.C., (1992). The influence of prostaglandin E2 and the steroid hormones, 17a-hydroxyprogesterone and 17β-estradiol on moulting and ovarian development in the tiger prawn, *Penaeus esculentus* Haswell, 1879 (Crustacea: Decapoda). *Comp. Biochem. Physiol*, 101: 295-299.

Kruevaisayawan, H., Vanichviriyakit, R., Weerachatyanukul, W., Withyachumnarnkul, W., and Sobhon, P. (2007). Biochemical characterization and physiological role of cortical rods in black tiger shrimp, *Penaeus monodon. Aquaculture*, 270: 289-298.

Kyozuka, K., Deguchi, R., Yoshida, N., and Yamashita, M. (1997). Change in intracellular Ca2q is not involved in serotonin induced meiosis reinitiation from the first prophase in oocytes of the marine bivalve *Crassostrea gigas. Dev. Biol*, 182: 33-41.

Lafont, R., and Mathieu, M. (2007). Steroids in aquatic invertebrates. *Ecotoxicol*, 16: 109-130.

Leelatanawit, R., Klinbunga, S., Hirono, I., Aoki, T., and Menasveta, P. (2008). Suppression subtractive hybridization (SSH) for isolation and characterization of genes related with testicular development of the giant tiger *Penaeus monodon*. *BMB Rep*, 41: 796-802.

Martins, J., K. Ribeiro, T. Rangel-Figueiredo, and J. Coimbra. (2007). Reproductive cycle ovarian development, and vertebrate-type steroids profile in the freshwater prawn *Macrobrachium rosenbergii*. *J Crustacean Biol*, 27: 220-228.

Medina, A., Y. Vila, G. Mourente, and A. Rodriguez. (1996). A comparative study of the ovarian development in wild and pond-reared shrimp, *Penaeus kerathurus*. *Aquaculture*, 148: 63-75

Meunpol O, Iam-Pai S, Suthikrai W, and Piyatiratitivorakul S. (2007). Identification of progesterone and 17a-hydroxyprogesterone in polychaetes (Perinereis sp.) and the effects of hormone extracts on penaeid oocyte development *in vitro*. *Aquaculture*, 270: 485-492.

Meusy, J.J., and Payen, G.G. (1988). Female reproduction in malacostracan Crustacea. *Zool. Sci*, 5: 217-265.

Mishra, A., Joy, and K. P. (2006). 2-hydroxyestradiol-17β induced oocyte maturation: involvement of cAMP–protein kinase A and okadaic acid-sensitive protein phosphatases, and their interplay in oocyte maturation in the catfish *Heteropneustes fossilis*. *J Expe Biol*, 209: 2567-2575.

Okumura, T. and K. Sakiyama. (2004). Hemolymph levels of vertebrate-type steroid hormones in female kuruma prawn *Marsupenaeus japonicus* during natural

reproductive cycle and induced ovarian development by eyestalk ablation. *Fish. Sci*, 70: 372-386.

Okumura, T., Kim, Y. K., Kawazoe, I., Yamano, K., Tsutsui, N. and Aida, K. (2006). Expression of vitellogenin and cortical rod proteins during induced ovarian development by eyestalk ablation in the kuruma prawn, *Marsupenaeus japonicus. Comp. Biochem. Physiol*, 143: 246-253.

Okumura, T. 2004. Review Perspectives on hormonal manipulation of shrimp reproduction. *JARQ*, 38 (1): 49-54.

Palacios, E., Ibarra, A.M. and Racotta, I.S. (2003). Tissue biochemical composition in relation to multiple spawning in wild and pond-reared *Penaeus vannamei* broodstock. *Aquaculture*, 185: 353-371.

Parida, M. M., Sathosl S. R., Dash P. K. and Thipatri N. K. (2006) Rapid and real-time detection of chikungunya virus by reverse transcription loop-mediated isothermal amplification assay**.** *J clini microbial*, 45(2): 351-357.

Platon, R. R. (1978). Design, operation and economics of a small-scale hatchery for the larval rearing of sugpo, Penaeus monodon Fab. *Aquaculture Department, Southeast Asian Fisheries Development Center*. Tigbauan, Iloilo: Philippines

Preechaphol, R. (2008). Identification of genes related to ovarian development of the giant tiger shrimp *Penaeus monodon*. Ph.D. Thesis. Chulalongkorn University, Bangkok: Thailand.

Preechaphol, R., Leelatanawit1, R., Sittikankeaw1, K., Klinbunga, S., Khamnamtong, B., Puanglarp, N. and Menasveta, P. (2007). Expressed sequence tag analysis for identification and characterization of sex-related genes in the giant tiger shrimp *Penaeus monodon*, *JBMB*, 40: 501-510.

Preechaphol, R., Klinbunga, S., Yamano, K., and Menasveta, P. (2010). Molecular cloning and expression of progestin membrane receptor component 1(Pgmrc1)

of the giant tiger shrimp *Penaeus monodon*. *Gen Comp Endocrinol*, 168: 440-449.

Quackenbush, L.S. (2001). Yolk synthesis in the marine shrimp, *Penaeus vannamei*. *Am. Zool*, 41: 458-464.

Qiu, G-F. and Yamano, K. (2005). Three forms of cyclin B transcripts in the ovary of the kuruma prawn *Marsupenaeus japonicus*: Their molecular characterizations and expression profiles during oogenesis. *Comp. Biochem. Physiol. Part B*, 141: 186-195.

Quinitio, E. T., A. Hara, K. Yamauchi, and S. Nakao. (1994). Changes in the steroid hormone and vitellogenin levels during the gametogenic cycle of the giant tiger shrimp, *Penaeus monodon*. *Comp. Biochem. Physiol*, 109: 21–26.

Rosenberry, B. (2003) World shrimp farming 2003. Shrimp News International, San Diego: CA.

Rowley, A.F., Vogan, C.L., Taylor, G.W., Clare, A.S. (2005). Prostaglandins in non-insectan invertebrates recent insights and unsolved problems. *J. Exp Biol*, 208: 3-14.

Sambrook, J., and Russell, D.W. (2001). Molecular Cloning: A Laboratory Manual, 3rd edition. Cold Spring Harbor, NY: Cold Spring Habor Laboratory Press.

Stanley, D.W., 2006. Prostaglandins and other eicosanoids in insects: Biological significance. *Biol Control Insects Res*, 51: 25-44.

Styrishave, B., Lund, T., Andersen, O., 2008. Ecdysteroids in female shore crabs *Carcinus maenas* during the moulting cycle and oocyte. *Development*, 88(3) : 575-581.

Subramoniam, T. (2000) Crustacean ecdysteriods in reproduction and embryogenesis. *Comp. Biochem. Physiol*, 125(2) : 135-156.

Summavielle, T., Monteiro, P.R.R., Reis-Henriques, M.A., and Coimbra, J. (2003). *In vitro* metabolism of steroid hormones by ovary and hepatopancreas of the crustacean Penaeid shrimp *Marsupenaeus japonicus*. *Sci. Mar*, 67: 299-306.

Sun, Y.-D., Zhao, X.-F., Kang, C.-J., and Wang, J.-X. (2006). Molecular cloning and characterization of Fc-TSP from Chinese shrimp *Fenneropenaeus chinensis*. *Mol. Immuol*, 43: 1202–1210.

Tsutsui, N., Kawazoe, I., Ohira, T.S.J., Yang, W.-J., Wilder, M., and Aida, K. (2000). Molecular Characterization of a cDNA encoding vitellogenin and its expression in the hepatopancreas and ovary during vitellogenesis in the Kuruma prawn, *Penaeus japonicus*. *Zool. Sc*, 17: 651-660.

Tsutsui, N., Katayama, H., Ohira, T., Nagasawa, H., Wilder, M.N., and Aida, K. (2005). The effects of crustacean hyperglycemic hormone-family peptides on vitellogenin gene expression in the kuruma prawn, *Marsupenaeus japonicus*. *Gen. Comp. Endocrinol*, 144: 232-239.

Warrier, S. R., R. Tirumalai, and T. Subramoniam. (2001). Occurrence of vertebrate steroids, estradiol-17_ and progesterone in the reproducing females of the mud crab *Scylla serrata*. *Comp. Biochem. Physiol*, 130: 283-294.

Withyachumnarnkul, B., Boonsaeng, V., Flegel, T. W., Panyim, S. and Wongteerasupaya C. (1998). Domestication and selective breeding of *Penaeus monodon* in Thailand, in: Proceedings to the Special Session on Advances in Shrimp Biotechnology, Felgel, T.(ed.) :73-77,. The Fifth Asian Fisheries Forum: International Conference on Fisheries and Food Security Beyond the Year 2000. 11-14 November 1998. Chiangmai: Thailand.

Wongprasert, K. (2006). Serotonin stimulates ovarian maturation and spawning in black tiger shrimp *Penaeus monodon*. *Aquaculture*, 261(4): 1447-1454.

Yamano, K., Qiu, G.-F., and Unuma, T. (2004). Molecular cloning and ovarian expression profiles of thrombospondin, a major component of cortical rods in

mature oocytes of penaeid shrimp, *Marsupenaeus japonicus*. *Biol,* 70: 1670-1678.

Yano, I. (1995). Final oocyte maturation, spawning and mating in penaeid shrimp. *J Exp Marine Biol Ecol*, 193: 113 -118.

Yano, I., and Hoshino, R. (2006). Effects of 17β-estradiol on the vitellogenin synthesis and oocyte development in the ovary of kuruma prawn (*Marsupenaeus japonicus*). *Comp. Biochem. Physiol, Part A* 144: 18-23.

Ye, H.H., Huang, H.Y., Li, S.J., and Wang, G. Z. (2008). Immunorecognition of estrogen and androgen receptors in the brain and thoracic ganglion mass of mud crab, *Scylla paramamosain*. *Prog in Nat Sci*, 18(6): 691-695.

APPENDICES

Appendix A

Table A1 The percentage of GSI and related data of wild broodstock of *P. monodon* used in this study

No.	Body weight (g.)	Gonad weight (g.)	GSI (%)	Total length (cm.)	Original codes	Gonad color	Remark
1	115.28	0.32	0.27	23.5	BUFOV03	light white	Stage I
2	76.37	0.47	0.61	23.0	BUFOV06	light white	Stage I
3	105.70	0.70	0.66	24.5	BUFOV04	light white	Stage I
4	99.96	0.77	0.77	23.5	AGYLOV03	white	Stage I
5	170.28	1.46	0.86	-	PMBF2	white	Stage I
6	112.35	1.00	0.89	23.0	BUFOV07	light yellow	Stage I
7	82.71	0.90	1.08	21.5	BUFOV05	turbid white	Stage I
8	157.33	1.73	1.10	27.0	AGYLOV01	white + light pink	Stage I
9	104.97	1.18	1.12	23.0	AGYLOV04	white	Stage I
10	120.58	1.60	1.33	23.5	AGYLOV02	white	Stage I
11	186.69	2.69	1.44	26.0	BFNOV32	yellow	Stage I
12	188.30	2.76	1.47	-	PMBF1	light yellow	Stage I
13	218.71	4.70	2.15	28.0	BFNOV38	light green + yellow	Stage II
14	205.67	4.61	2.24	27.5	BFNOV33	light yellow	Stage II
15	128.74	2.25	2.25	24.5	ASPOV10	light yellow	Stage II
16	205.05	5.29	2.58	28.0	BFNOV35	light yellow	Stage II
17	149.64	2.68	2.68	26.7	ASPOV06	light yellow	Stage II
18	208.54	6.16	2.95	26.0	BFNOV31	light green	Stage II
19	181.30	6.00	3.31	28.5	BFNOV04/1	yellow + green	Stage II

Table A1 (Cont.)

No.	Body weight (g.)	Gonad weight (g.)	GSI (%)	Total length (cm.)	Original codes	Gonad color	Remark
20	159.80	6.40	4.01	27.7	BFNOV07	light green	Stage III
21	187.10	8.27	4.42	30.0	BFNOV18	green + yellow	Stage III
22	173.40	8.00	4.61	28.0	BFNOV03	green	Stage III
23	164.50	7.60	4.64	27.5	BFNOV04	green	Stage III
24	230.93	12.12	5.28	32.0	BFNOV23	green + yellow	Stage III
25	235.98	12.69	5.37	33.0	BFNOV24	green	Stage III
26	172.30	9.90	5.75	28.0	BFNOV05	green	Stage III
27	172.60	10.20	5.91	28.0	BFNOV01	green	Stage III
28	136.40	8.40	6.16	26.5	BFNOV09	dark green	Stage IV
29	133.20	8.30	6.23	26.0	BFNOV08	green	Stage IV
30	176.20	12.90	7.32	29.0	BFNOV06	dark green	Stage IV
31	272.20	20.30	7.46	32.0	BFNOV02	green	Stage IV
32	152.20	12.80	8.42	27.0	BFNOV14	green	Stage IV
33	139.90	13.10	9.36	25.5	BFNOV10	dark green	Stage IV
34	162.20	16.20	9.99	28.0	BFNOV12	dark green	Stage IV
35	166.90	16.70	10.01	27.5	BFNOV11	light green	Stage IV
36	239.86	24.98	10.41	33.0	BFNOV21	green	Stage IV
37	207.40	23.20	11.19	30.5	BFNOV15	dark green	Stage IV
38	232.57	26.08	11.21	30.0	BFNOV20	green	Stage IV
39	156.10	18.20	11.66	27.0	BFNOV16	dark green	Stage IV
40	252.11	31.30	12.41	30.0	BFNOV17	green	Stage IV
41	158.60	19.90	12.55	27.5	BFNOV13	dark green	Stage IV

Table A1 (Cont.)

No.	Body weight (g.)	Gonad weight (g.)	GSI (%)	Total length (cm.)	Original codes	Gonad color	Remark
42	300.12	10.47	3.49	32.5	BFNOV30	light green + yellow	post-spawn
43	194.49	3.61	1.86	27.5	BFNOV36	light yellow + little green	post-spawn
44	256.40	8.39	3.27	29.5	BFNOV34	light yellow	post-spawn
45	264.70	7.66	2.89	30.0	BFNOV37	light yellow	post-spawn
46	285.97	8.30	2.90	32.0	BFNOV39	yellow	post-spawn
47	200.79	5.18	2.58	28.0	BFNOV40	light yellow	post-spawn
48	236.51	1.79	0.76	27.50	BFEAOV18	white	Eyestalk-ablated; Stage I
49	111.00	1.00	0.90	24.50	YLBOV01	white + light yellow	Eyestalk-ablated; Stage I
50	163.00	2.00	1.22	25.00	YLBOV06	white	Eyestalk-ablated; Stage I
51	272.20	3.71	1.36	30.00	BFEAOV15	yellow	Eyestalk-ablated; Stage I
52	125.00	2.00	1.60	24.50	YLBOV05	white + light yellow	Eyestalk-ablated; Stage II
53	118.00	2.00	1.69	24.50	YLBOV08	white	Eyestalk-ablated; Stage II
54	173.37	4.72	2.72	25.50	BFEAOV19	light green + yellow	Eyestalk-ablated ;Stage II
55	252.03	7.16	2.84	29.50	BFEAOV17	green + yellow	Eyestalk-ablated ;Stage II
56	151.00	5.00	3.31	25.00	YLBOV07	lihgt green	Eyestalk-ablated ;Stage II
57	291.39	10.31	3.54	30.50	BFEAOV16	green	Eyestalk-ablated ;Stage II
58	164.00	6.00	3.66	26.00	YLBOV04	light green	Eyestalk-ablated ;Stagw II

Table A1 (Cont.)

No.	Body weight (g.)	Gonad weight (g.)	GSI (%)	Total length (cm.)	Original codes	Gonad color	Remark
59	193.65	8.82	4.55	27.00	BFEAOV21	dark green	Eyestalk-ablated ;Stage III
60	153.00	7.00	4.57	25.50	YLBOV02	light green	Eyestalk-ablated ;Stage III
61	125.00	6.00	4.80	25.00	YLBOV03	light green	Eyestalk-ablated ;Stage III
62	118.80	5.90	4.97	24.50	BFEAOV08	green	Eyestalk-ablated ;Stage III; BIOTEC shrimp
63	186.50	9.40	5.04	27.50	BFEAOV05	light green	Eyestalk-ablated ;Stage III
64	196.90	10.00	5.08	29.50	BFEAOV02	light green + yellow	Eyestalk-ablated ;Stage III
65	96.20	4.90	5.09	23.30	BFEAOV11	green	Eyestalk-ablated ;Stage III; BIOTEC shrimp
66	182.70	9.40	5.15	28.00	BFEAOV03	yellow + little green	Eyestalk-ablated ;Stage III
67	278.23	14.37	5.16	29.50	BFEAOV20	dark green + little yellow	Eyestalk-ablated ;Stage III
68	197.40	10.80	5.47	29.50	BFEAOV04	light green + yellow	Eyestalk-ablated ;Stage III
69	229.60	14.60	6.36	30.00	BFEAOV01	green + yellow	Eyestalk-ablated ;Stage IV
70	220.10	14.00	6.36	28.50	BFEAOV07	light green + yellow	Eyestalk-ablated ;Stage IV
71	170.20	11.60	6.82	27.00	BFEAOV06	light green + yellow	Eyestalk-ablated; StgIV
72	365.38	25.08	6.86	33.00	BFEAOV24	Green	Eyestalk-ablated ;Stage IV
73	116.40	8.00	6.87	25.50	BFEAOV10	dark green	Eyestalk-ablated; StgIV; BIOTEC shrimp

Table A1 (Cont.)

No.	Body weight (g.)	Gonad weight (g.)	GSI (%)	Total length (cm.)	Original codes	Gonad color	Remark
75	188.20	13.80	7.35	27.50	BFEAOV13	dark green	Eyestalk-ablated ; Stage IV
76	167.54	14.33	8.55	25.00	BFEAOV22	dark green	Eyestalk-ablated ;Stage IV
77	256.34	22.41	8.74	29.50	BFEAOV23	dark green	Eyestalk-ablated ;Stage IV
78	249.50	22.30	8.94	31.50	BFEAOV09	light green	Eyestalk-ablated ;Stage IV

Table A2 The percentage of GSI and related data of domesticated of *P. monodon* used for the feeding experiments of 17β-estradiol-supplented diets

No.	Body weight (g.)	Gonad weight (g.)	GSI (%)	Total length (cm.)	Original codes	Gonad color	Remark
1	61.49	0.48	0.78	20.1	7CBUFOV1	light white	Stage I
2	73.3	0.51	0.70	20.9	7CBUFOV2	light white	Stage I
3	61.79	0.33	0.53	19	7CBUFOV3	light white	Stage I
4	61.41	0.5	0.81	17	7CBUFOV4	light white	Stage I
5	60.13	0.43	0.72	20.4	7CBUFOV5	light white	Stage I
6	57.03	0.56	0.98	19.8	7CBUFOV6	light white	Stage I
7	78.3	0.67	0.86	19.1	7CBUFEAOV1	light white	Stage I
8	71.39	0.52	0.73	21.6	7CBUFEAOV2	light white	Stage I
9	60.66	0.31	0.51	15.4	7CBUFEAOV3	light white	Stage I
10	55.99	0.5	0.89	19	7ES1BUFOV1	light white	Stage I
11	58.67	0.2	0.34	20.1	7ES1BUFOV2	light white	Stage I
12	70.64	0.26	0.37	20.5	7ES1BUFOV3	light white	Stage I
13	82.34	0.7	0.85	21.5	7ES1BUFOV4	light white	Stage I
14	70.21	0.51	0.73	19.5	7ES1BUFOV5	light white	Stage I
15	57.83	0.61	1.05	17.5	7ES1BUFOV6	light white	Stage I
16	69.32	0.49	0.71	20.5	7ES10BUFOV1	light white	Stage I
17	70.3	0.62	0.88	18.4	7ES10BUFOV2	light white	Stage I
18	73.14	0.57	0.78	20.4	7ES10BUFOV3	light white	Stage I
19	58.46	0.49	0.84	19.7	7ES10BUFOV4	light white	Stage I
20	81.6	0.6	0.74	20	7ES10BUFOV5	light white	Stage I
21	73.08	0.34	0.47	19.9	7ES10BUFOV6	light white	Stage I
22	56.37	0.16	0.28	18	14CBUFOV1	light white	Stage I
23	59.2	0.25	0.42	18.5	14CBUFOV2	light white	Stage I
24	77.27	0.68	0.88	20	14CBUFOV3	light white	Stage I
25	72.26	0.45	0.62	19	14CBUFOV4	light white	Stage I
26	62.24	0.42	0.67	18.7	14CBUFOV5	light white	Stage I
27	73.45	0.39	0.53	20.3	14CBUFOV6	light white	Stage I
28	65.25	0.48	0.74	19	14CBUFEAOV1	light white	Stage I
29	71.04	0.46	0.65	19	14CBUFEAOV2	light white	Stage I
30	61.5	0.38	0.62	-	14CBUFEAOV3	light white	Stage I
31	67.86	0.51	0.75	18.5	14ES1BUFOV1	light white	Stage I
32	58.16	0.61	1.05	17.5	14ES1BUFOV2	light white	Stage I
33	72.07	0.98	1.36	16.5	14ES1BUFOV3	light white	Stage I
34	66.63	0.44	0.66	18	14ES1BUFOV4	light white	Stage I
35	79.89	0.53	0.66	20.3	14ES1BUFOV5	light white	Stage I
36	77.53	0.52	0.67	19.4	14ES1BUFOV6	light white	Stage I
37	73.37	0.43	0.59	19	14ES10BUFOV1	light white	Stage I
38	75.38	0.76	1.01	19.6	14ES10BUFOV3	light white	Stage I
39	61.93	0.43	0.69	18.5	14ES10BUFOV4	light white	Stage I
40	70.9	0.56	0.79	19.2	14ES10BUFOV5	light white	Stage I

Table A2 (Cont.)

No.	Body weight (g.)	Gonad weight (g.)	GSI (%)	Total length (cm.)	Original codes	Gonad color	Remark
41	71.42	0.51	0.71	19.5	14ES10BUFOV6	light white	Stage I
42	72.32	0.49	0.68	19.6	28CBUFOV1	light white	Stage I
43	61.94	0.4	0.65	17.4	28CBUFOV2	light white	Stage I
44	64.04	0.28	0.44	18.2	28CBUFOV3	light white	Stage I
45	66.87	0.3	0.45	19.2	28CBUFOV4	light white	Stage I
46	64.02	0.44	0.69	17	28CBUFOV5	light white	Stage I
47	72.57	0.4	0.55	19.6	28CBUFOV6	light white	Stage I
48	72.63	0.67	0.92	19.2	28CBUFEAOV1	light white	Stage I
49	82.13	0.83	1.01	19.5	28CBUFEAOV2	light white	Stage I
50	71.38	0.39	0.55	18.1	28CBUFEAOV3	light white	Stage I
51	62.44	0.38	0.61	17.8	28CBUFEAOV5	light white	Stage I
52	50.23	0.35	0.70	15.7	28CBUFEAOV6	light white	Stage I
53	69.89	0.51	0.73	18.7	18ES1BUFOV1	light white	Stage I
54	62.13	0.28	0.45	17.6	18ES1BUFOV2	light white	Stage I
55	75.39	0.5	0.66	20.3	18ES1BUFOV3	light white	Stage I
56	63.48	0.27	0.43	16.6	18ES1BUFOV4	light white	Stage I
57	63.43	0.33	0.52	17.6	18ES1BUFOV5	light white	Stage I
58	63.51	0.37	0.58	19	18ES1BUFOV6	light white	Stage I
59	73.94	0.6	0.81	19.8	35ES10BUFOV3	light white	Stage I
60	67.96	0.51	0.75	19.6	35ES10BUFOV4	light white	Stage I
61	68.72	0.65	0.95	18.3	35ES10BUFOV5	light white	Stage I
62	72.31	0.43	0.59	19.5	35ES10BUFOV6	light white	Stage I
63	71.54	0.39	0.55	19.2	35CBUFOV1	light white	Stage I
64	56.91	0.32	0.56	14.5	35CBUFOV2	light white	Stage I
65	57.5	0.34	0.59	16.4	35CBUFOV3	light white	Stage I
66	62.58	0.29	0.46	17.6	35CBUFOV4	light white	Stage I
67	58.7	0.33	0.56	18.1	35CBUFOV5	light white	Stage I
68	67.67	0.38	0.56	19.4	35CBUFOV6	light white	Stage I
69	67.77	0.55	0.81	17.8	35CBUFOV7	light white	Stage I
70	62.95	0.31	0.49	18.5	35CBUFOV8	light white	Stage I
71	80.71	0.95	1.18	17.6	35CBUFEAOV1	light yellow	Stage I
72	66.63	0.56	0.84	18.5	35CBUFEAOV2	light white	Stage I
73	52.96	0.37	0.70	17.4	35CBUFEAOV3	light white	Stage I
74	65.46	0.57	0.87	16.6	35CBUFEAOV4	light white	Stage I
75	86.56	0.78	0.90	20.2	35ES1BUFOV1	light white	Stage I
76	85.63	0.56	0.65	20	35ES1BUFOV2	light white	Stage I
77	64.65	0.37	0.57	18.7	35ES1BUFOV3	light white	Stage I
78	54.17	0.36	0.66	17.9	35ES1BUFOV4	light white	Stage I
79	60.27	0.52	0.86	15.3	35ES1BUFOV5	light white	Stage I
80	71.88	0.66	0.92	18.4	35ES1BUFOV6	light white	Stage I
81	71	0.61	0.86	18.8	35ES10BUFOV1	light white	Stage I
82	76.12	0.53	0.70	18.7	35ES10BUFOV2	light white	Stage I
83	63.19	0.96	1.52	15.1	35ES10BUFOV3	light white	Stage I

Table A2 (Cont.)

No.	Body weight (g.)	Gonad weight (g.)	GSI (%)	Total length (cm.)	Original codes	Gonad color	Remark
84	64.07	0.42	0.66	17.8	35ES10BUFOV4	light white	Stage I
85	54.38	0.39	0.72	16.2	35ES10BUFOV5	light white	Stage I

Appendix B

Table B1. Relative expression levels of *PmAtNS* in different ovarian developmental stages of wild broodstock of *P. monodon* based on quantitative real-time PCR analysis

Sample group		Mean conc.		Ratio	Average	SD
		PmAtNS	*EF-1α*	(target/*EF-1α*)		
Junvenile	JNOV05	1.62E+04	6.03E+05	2.68E-02	0.0346	0.01479
	JNOV06	3.14E+04	1.25E+06	2.51E-02		
	JNOV07	5.64E+04	2.28E+06	2.48E-02		
	JNOV08	3.24E+04	6.75E+05	4.80E-02		
	JNOV09	7.29E+04	1.25E+06	5.83E-02		
	JNOV10	4.18E+04	1.72E+06	2.43E-02		
N-BD-Stage I	BUFOV03	5.61E+04	2.08E+06	2.70E-02	0.032	0.01453
	BUFOV06	1.51E+04	2.80E+05	5.39E-02		
	BUFOV04	7.11E+04	1.84E+06	3.86E-02		
	BUFOV07	2.08E+04	3.93E+05	5.31E-02		
	BUFOV05	1.17E+04	3.42E+05	3.43E-02		
	AGYLOV01	5.16E+04	4.54E+06	1.14E-02		
	AGYLOV04	6.58E+04	3.53E+06	1.86E-02		
	AGYLOV02	5.42E+04	2.09E+06	2.60E-02		
	BUFOV32	3.68E+04	1.48E+06	2.49E-02		
N-BD-Stage II	ASPOV10	8.22E+04	1.10E+06	7.50E-02	0.0497	0.01704
	ASPOV06	8.36E+04	1.83E+06	4.57E-02		
	BFNOV38	3.89E+04	7.45E+05	5.21E-02		
	BFN0V33	2.07E+04	1.06E+06	1.96E-02		
	BRNOV35	3.85E+04	6.53E+05	5.89E-02		
	BFNOV31	4.08E+04	7.46E+05	5.47E-02		
	BFNOV4/1	2.70E+04	6.49E+05	4.17E-02		
N-BD-Stage III	BFNOV18	1.21E+04	3.74E+05	3.22E-02	0.0322	0.01709
	BFNOV04	1.67E+04	6.17E+05	2.71E-02		
	BFNOV23	1.40E+04	6.58E+05	2.13E-02		
	BFNOV24	2.39E+04	3.64E+05	6.58E-02		
	BFNOV05	1.27E+04	6.47E+05	1.96E-02		
	BFNOV01	1.47E+04	5.48E+05	2.69E-02		
N-BD-Stage IV	BFNOV02	1.05E+04	1.35E+05	7.78E-02	0.0416	0.02264
	BFNOV14	7.52E+03	3.08E+05	2.44E-02		
	BFNOV10	8.38E+03	3.89E+05	2.16E-02		
	BFNOV12	1.00E+04	4.38E+05	2.29E-02		
	BFNOV21	9.03E+03	4.85E+05	1.86E-02		
	BFNOV15	9.59E+03	2.53E+05	3.79E-02		
	BFNOV20	1.16E+04	1.95E+05	5.93E-02		
	BFNOV16	6.89E+03	1.71E+05	4.04E-02		
	BFNOV17	6.79E+03	9.51E+04	7.14E-02		

Table B1. (Cont.)

Sample group		Mean conc.		Ratio	Average	SD
		PmAtNS	*EF-1α*	(target/*EF-1α*)		
N-BD-Stage PS	BFNOV30	3.44E+04	7.76E+05	4.43E-02	0.043	0.0109
	BFNOV36	2.80E+04	6.93E+05	4.05E-02		
	BFNOV34	3.92E+04	6.43E+05	6.10E-02		
	BFNOV37	2.13E+04	6.11E+05	3.49E-02		
	BFNOV39	2.76E+04	8.06E+05	3.42E-02		
EA-BD-Stage I	BFEAOV18	1.69E+04	6.93E+05	2.43E-02	0.0354	0.03177
	YLBOV01	2.28E+05	2.77E+06	8.25E-02		
	YLBOV06	8.13E+03	6.16E+05	1.32E-02		
	BFEAOV15	1.40E+04	6.54E+05	2.15E-02		
EA-BD-Stage II	YLBOV05	4.98E+04	3.19E+06	1.56E-02	0.0244	0.01656
	YLBOV08	3.19E+04	1.60E+06	1.99E-02		
	BFEAOV19	1.25E+04	8.77E+05	1.42E-02		
	BFEAOV17	1.68E+04	6.21E+05	2.71E-02		
	YLBOV07	6.19E+03	5.81E+05	1.06E-02		
	BFEAOV16	2.87E+04	4.81E+05	5.97E-02		
	YLBOV04	2.65E+04	1.13E+06	2.35E-02		
EA-BD-Stage III	BFEAOV21	2.24E+04	7.48E+05	3.00E-02	0.0307	0.00823
	YLBOV02	1.74E+04	6.17E+05	2.81E-02		
	YLBOV03	1.49E+04	7.07E+05	2.11E-02		
	BFEA08	3.51E+04	1.02E+06	3.44E-02		
	BFEAOV05	4.39E+04	1.03E+06	4.26E-02		
	BFEAOV02	2.67E+04	6.10E+05	4.37E-02		
	BFEAOV11	1.81E+04	5.28E+05	3.42E-02		
	BFEAOV03	2.87E+04	1.34E+06	2.15E-02		
	BFEAOV20	9.89E+03	3.25E+05	3.05E-02		
	BFEAOV04	1.39E+04	6.53E+05	2.13E-02		
EA-BD-Stage IV	BFEAOV01	1.28E+04	8.43E+05	1.52E-02	0.0261	0.0074
	BFEAOV07	3.54E+04	1.12E+06	3.15E-02		
	BFEAOV06	1.44E+04	5.05E+05	2.85E-02		
	BFEAOV24	1.77E+04	5.79E+05	3.05E-02		
	BFEAOV10	1.32E+04	7.22E+05	1.82E-02		
	BFEAOV12	1.09E+04	4.98E+05	2.19E-02		
	BFEAOV13	3.23E+04	8.59E+05	3.76E-02		
	BFEAOV22	7.58E+03	2.48E+05	3.05E-02		
	BFEAOV09	7.88E+03	4.54E+05	1.74E-02		
	BFEAOV14	3.13E+03	1.06E+05	2.96E-02		

Table B2. Relative expression levels of *PmAST* in different ovarian developmental stages of wild broodstock of *P. monodon* based on quantitative real-time PCR analysis

Sample group		Mean conc.		Ratio	Average	SD
		PmAST	*EF-1α*	(target/*EF-1α*)		
Junvenile	JNOV05	1.17E+05	6.03E+05	1.93E-01	0.1491	0.0597
	JNOV06	1.54E+05	1.25E+06	1.23E-01		
	JNOV07	3.05E+05	2.28E+06	1.34E-01		
	JNOV08	3.46E+04	6.75E+05	5.13E-02		
	JNOV09	2.72E+05	1.25E+06	2.18E-01		
	JNOV10	3.02E+05	1.72E+06	1.75E-01		
N-BD-Stage I	BUFOV03	5.72E+05	2.08E+06	2.76E-01	0.3506	0.18137
	BUFOV06	1.68E+05	2.80E+05	5.99E-01		
	BUFOV04	5.72E+05	1.84E+06	3.11E-01		
	BUFOV07	2.25E+05	3.93E+05	5.73E-01		
	BUFOV05	1.90E+05	3.42E+05	5.56E-01		
	AGYLOV01	7.10E+05	4.54E+06	1.56E-01		
	AGYLOV04	5.49E+05	3.53E+06	1.55E-01		
	AGYLOV02	3.92E+05	2.09E+06	1.88E-01		
	BUFOV32	5.05E+05	1.48E+06	3.41E-01		
N-BD-Stage II	ASPOV10	1.83E+05	1.10E+06	1.67E-01	0.289	0.15203
	ASPOV06	2.88E+05	1.83E+06	1.57E-01		
	BFNOV38	1.99E+05	7.45E+05	2.67E-01		
	BFN0V33	1.50E+05	1.06E+06	1.43E-01		
	BRNOV35	3.35E+05	6.53E+05	5.13E-01		
	BFNOV31	2.26E+05	7.46E+05	3.02E-01		
	BFNOV4/1	3.07E+05	6.49E+05	4.74E-01		
N-BD-Stage III	BFNOV18	6.51E+04	3.74E+05	1.74E-01	0.4357	0.16003
	BFNOV04	2.77E+05	6.17E+05	4.48E-01		
	BFNOV23	3.91E+05	6.58E+05	5.94E-01		
	BFNOV24	2.03E+05	3.64E+05	5.59E-01		
	BFNOV05	2.09E+05	6.47E+05	3.23E-01		
	BFNOV01	2.83E+05	5.48E+05	5.16E-01		
N-BD-Stage IV	BFNOV02	5.26E+04	1.35E+05	3.89E-01	0.5448	0.18047
	BFNOV14	1.85E+05	3.08E+05	6.01E-01		
	BFNOV10	1.82E+05	3.89E+05	4.68E-01		
	BFNOV12	1.39E+05	4.38E+05	3.18E-01		
	BFNOV21	1.51E+05	4.85E+05	3.11E-01		
	BFNOV15	1.25E+05	2.53E+05	4.96E-01		
	BFNOV20	1.33E+05	1.95E+05	6.81E-01		
	BFNOV16	1.02E+05	1.71E+05	5.98E-01		
	BFNOV17	6.99E+04	9.51E+04	7.35E-01		
	BFNOV13	2.04E+05	2.40E+05	8.51E-01		
N-BD-Stage PS	BFNOV30	1.20E+05	7.76E+05	1.54E-01	0.3703	0.15374
	BFNOV36	2.83E+05	6.93E+05	4.09E-01		

Table B2. (Cont.)

Sample group		Mean conc.		Ratio	Average	SD
		PmAST	*EF*-1α	(target/*EF*-1α)		
	BFNOV34	3.06E+05	6.43E+05	4.76E-01		
	BFNOV37	2.18E+05	6.11E+05	3.56E-01		
	BFNOV39	2.00E+05	8.06E+05	2.48E-01		
	BFNOV40	4.37E+05	7.54E+05	5.79E-01		
EA-BD-Stage I	BFEAOV18	4.27E+05	6.93E+05	6.16E-01	0.4553	0.20709
	YLBOV01	4.23E+05	2.77E+06	1.53E-01		
	YLBOV06	3.40E+05	6.16E+05	5.53E-01		
	BFEAOV15	3.26E+05	6.54E+05	4.99E-01		
EA-BD-Stage II	YLBOV05	9.12E+05	3.19E+06	2.86E-01	0.5249	0.23072
	YLBOV08	9.07E+05	1.60E+06	5.68E-01		
	BFEAOV19	2.80E+05	8.77E+05	3.19E-01		
	BFEAOV17	2.70E+05	6.21E+05	4.35E-01		
	YLBOV07	3.06E+05	5.81E+05	5.27E-01		
	BFEAOV16	4.73E+05	4.81E+05	9.82E-01		
	YLBOV04	6.28E+05	1.13E+06	5.57E-01		
EA-BD-Stage III	BFEAOV21	3.90E+05	7.48E+05	5.20E-01	0.6034	0.12642
	YLBOV02	4.50E+05	6.17E+05	7.29E-01		
	YLBOV03	3.52E+05	7.07E+05	4.97E-01		
	BFEA08	7.73E+05	1.02E+06	7.55E-01		
	BFEAOV05	7.00E+05	1.03E+06	6.78E-01		
	BFEAOV02	4.24E+05	6.10E+05	6.95E-01		
	BFEAOV11	3.27E+05	5.28E+05	6.20E-01		
	BFEAOV03	4.91E+05	1.34E+06	3.68E-01		
	BFEAOV20	2.20E+05	3.25E+05	6.77E-01		
	BFEAOV04	3.23E+05	6.53E+05	4.95E-01		
EA-BD-Stage IV	BFEAOV01	2.96E+05	8.43E+05	3.52E-01	0.5584	0.26341
	BFEAOV07	4.53E+05	1.12E+06	4.03E-01		
	BFEAOV06	2.85E+05	5.05E+05	5.64E-01		
	BFEAOV24	3.91E+05	5.79E+05	6.76E-01		
	BFEAOV10	4.77E+05	7.22E+05	6.62E-01		
	BFEAOV12	3.28E+05	4.98E+05	6.60E-01		
	BFEAOV13	5.31E+05	8.59E+05	6.18E-01		
	BFEAOV22	2.11E+03	2.48E+05	8.51E-03		
	BFEAOV09	2.81E+05	4.54E+05	6.20E-01		
	BFEAOV14	1.07E+05	1.06E+05	1.02E+00		

Table B3. Relative expression levels of *Pm-mago nashi* in different ovarian developmental stages of wild broodstock of *P. monodon* based on quantitative real-time PCR analysis

Sample group		Mean conc.		Ratio	Average	SD
		Pm-mago nashi	*EF*-1α	(target/*EF*-1α)		
Junvenile	JNOV4	5.72E+04	6.06E+06	9.42E-03	0.0097	0.00112
	JNOV5	3.06E+04	3.34E+06	9.16E-03		
	JNOV6	4.49E+04	5.40E+06	8.32E-03		
	JNOV7	7.20E+04	6.39E+06	1.13E-02		
	JNOV14	6.63E+04	6.54E+06	1.01E-02		
N–BD-Stage I	BU14OV8	8.68E+04	6.91E+06	1.26E-02	0.0128	0.00069
	BU14OV15	7.15E+04	5.20E+06	1.38E-02		
	BU14OV18	7.01E+04	5.67E+06	1.24E-02		
	BFN0V22	5.12E+04	4.17E+06	1.23E-02		
N–BD-Stage II	BFN0V25	4.15E+04	2.60E+06	1.59E-02	0.0124	0.0036
	BFN0V31	6.42E+04	4.67E+06	1.38E-02		
	BFN0V33	4.68E+04	3.75E+06	1.25E-02		
	BFN0V38	5.11E+04	6.87E+06	7.44E-03		
N–BD-Stage III	BFN0V01	2.12E+04	1.40E+06	1.51E-02	0.0136	0.00107
	BFN0V07	1.95E+04	1.43E+06	1.37E-02		
	BFN0V18	3.08E+04	2.54E+06	1.21E-02		
	BFN0V23	3.33E+04	2.42E+06	1.38E-02		
	BFN0V24	2.97E+04	2.22E+06	1.34E-02		
N–BD-Stage IV	BFN0V08	1.09E+04	7.56E+05	1.43E-02	0.0168	0.00313
	BFN0V09	1.61E+04	6.93E+05	2.33E-02		
	BFN0V10	8.13E+03	5.59E+05	1.46E-02		
	BFN0V11	1.06E+04	7.12E+05	1.49E-02		
	BFN0V14	1.48E+04	8.84E+05	1.68E-02		
	BFN0V15	1.20E+04	6.56E+05	1.83E-02		
	BFN0V16	1.07E+04	8.09E+05	1.33E-02		
	BFN0V17	1.05E+04	6.50E+05	1.62E-02		
	BFN0V20	1.32E+04	6.81E+05	1.94E-02		
N–BD-Stage PS	BFN0V30	5.05E+04	4.97E+06	1.02E-02	0.0125	0.00152
	BFN0V34	7.80E+04	6.43E+06	1.21E-02		
	BFN0V37	7.51E+04	5.27E+06	1.43E-02		
	BFN0V39	8.14E+04	6.26E+06	1.30E-02		
	BFN0V40	4.86E+04	3.73E+06	1.30E-02		
EA-BD-Stage I	YLBOV06	2.51E+04	1.38E+06	1.82E-02	0.0209	0.00286
	EFEAOV15	5.35E+04	2.10E+06	2.54E-02		
	EFEAOV18	1.51E+04	7.75E+05	1.95E-02		
	WFEAOV04	3.70E+04	1.89E+06	1.95E-02		
	WFEAOV33	2.05E+04	9.31E+05	2.20E-02		
EA-BD-Stage II	WFEAOV27U	3.77E+04	2.11E+06	1.78E-02	0.0217	0.00226
	WFEAOV06	3.11E+04	1.54E+06	2.02E-02		

Table B3. (Cont.)

Sample group	Mean conc.			Ratio (target/*EF*-1α)	Average	SD
	Pmmago nashi		*EF*-1α			
	WFEAOV01	3.08E+04	1.53E+06	2.02E-02		
	WFEAOV29	2.70E+04	1.20E+06	2.25E-02		
	WFEAOV05	2.68E+04	1.23E+06	2.19E-02		
	WFEAOV20	4.01E+04	1.59E+06	2.52E-02		
	WFEAOV30U	2.60E+04	1.13E+06	2.31E-02		
	WFEAOV30L	2.45E+04	1.07E+06	2.28E-02		
EA-BD-Stage III	WFEAOV18	2.41E+04	1.27E+06	1.90E-02	0.0213	0.00249
	WFEAOV19	3.55E+04	1.64E+06	2.16E-02		
	WFEAOV28	2.79E+04	1.25E+06	2.22E-02		
	WFEAOV26	3.12E+04	1.29E+06	2.42E-02		
	WFEAOV32	1.75E+04	6.71E+05	2.61E-02		
	WFEAOV9	1.54E+04	7.51E+05	2.05E-02		
	WFEAOV31U	1.52E+04	7.65E+05	1.99E-02		
	WFEAOV31L	1.09E+04	5.62E+05	1.93E-02		
	WFEAOV12	2.07E+04	1.09E+06	1.90E-02		
EA-BD-Stage IV	WFEAOV13	1.72E+04	6.87E+05	2.51E-02	0.0228	0.00356
	WFEAOV11	1.78E+04	7.78E+05	2.28E-02		
	WFEAOV14	1.60E+04	7.18E+05	2.22E-02		
	WFEAOV16	2.34E+04	8.84E+05	2.65E-02		
	WFEAOV15	9.74E+03	5.65E+05	1.72E-02		

Table B4 Relative expression levels of *PmNHR96* in different ovarian developmental stage of wild broodstock of *P. monodon* based on quantitative real-time PCR analysis

Sample group	Mean conc.		EF-1α	Ratio (target/*EF*-1α)	Average	STDEV
		PmNHR96	*EF*-1α			
Junvenile	JNOV4	6.21E+03	6.06E+06	1.02E-03	0.0011	0.00017
	JNOV5	3.20E+03	3.34E+06	9.56E-04		
	JNOV6	7.01E+03	5.40E+06	1.30E-03		
	JNOV7	6.09E+03	6.39E+06	9.53E-04		
	JNOV14	8.35E+03	6.54E+06	1.28E-03		
N-BD-Stage I	BU14OV8	1.52E+04	6.91E+06	2.20E-03	0.0024	0.00061
	BU14OV15	1.28E+04	5.20E+06	2.46E-03		
	BU14OV18	9.91E+03	5.67E+06	1.75E-03		
	BFN0V22	1.34E+04	4.17E+06	3.21E-03		
N-BD-Stage II	BFN0V25	9.88E+03	2.60E+06	3.80E-03	0.0026	0.0026
	BFN0V31	9.01E+03	4.67E+06	1.93E-03		
	BFN0V33	1.22E+04	3.75E+06	3.24E-03		
	BFN0V38	8.67E+03	6.87E+06	1.26E-03		
N-BD-Stage III	BFN0V01	2.71E+03	1.40E+06	1.93E-03	0.0028	0.00105
	BFN0V07	6.50E+03	1.43E+06	4.56E-03		
	BFN0V18	6.64E+03	2.54E+06	2.61E-03		
	BFN0V23	6.04E+03	2.42E+06	2.50E-03		
	BFN0V24	4.77E+03	2.22E+06	2.15E-03		
N-BD-Stage IV	BFN0V08	3.03E+03	7.56E+05	4.01E-03	0.0037	0.00101
	BFN0V09	2.28E+03	6.93E+05	3.30E-03		
	BFN0V10	1.84E+03	5.59E+05	3.29E-03		
	BFN0V11	3.91E+03	7.12E+05	5.49E-03		
	BFN0V14	2.58E+03	8.84E+05	2.92E-03		
	BFN0V15	1.55E+03	6.56E+05	2.36E-03		
	BFN0V16	2.35E+03	8.09E+05	2.91E-03		
	BFN0V17	3.15E+03	6.50E+05	4.84E-03		
	BFN0V20	2.80E+03	6.81E+05	4.11E-03		
N-BD-Stage PS	BFN0V30	9.57E+03	4.97E+06	1.93E-03	0.0022	0.00018
	BFN0V34	1.43E+04	6.43E+06	2.22E-03		
	BFN0V37	1.28E+04	5.27E+06	2.44E-03		
	BFN0V39	1.42E+04	6.26E+06	2.27E-03		
	BFN0V40	8.40E+03	3.73E+06	2.25E-03		
EA-BD-Stage I	YLBOV06	6.63E+03	1.38E+06	4.81E-03	0.004616	0.0003794
	EFEAOV15	9.46E+03	2.10E+06	4.50E-03		
	EFEAOV18	3.18E+03	7.75E+05	4.10E-03		
	WFEAOV04	8.63E+03	1.89E+06	4.55E-03		
	WFEAOV33	4.77E+03	9.31E+05	5.12E-03		
EA-BD-Stage II	WFEAOV27U	8.14E+03	2.11E+06	3.86E-03	0.004629	0.0012724
	WFEAOV06	7.61E+03	1.54E+06	4.94E-03		
	WFEAOV01	6.88E+03	1.53E+06	4.51E-03		

Table B4 (Cont.)

Sample group		Mean conc.		Ratio (target/*EF*-1α)	Average	STDEV
		PmNHR96	*EF*-1α			
	WFEAOV29	5.56E+03	1.20E+06	4.62E-03		
	WFEAOV05	2.61E+03	1.23E+06	2.13E-03		
	WFEAOV20	7.70E+03	1.59E+06	4.83E-03		
	WFEAOV30U	7.20E+03	1.13E+06	6.38E-03		
	WFEAOV30L	6.18E+03	1.07E+06	5.76E-03		
EA-BD-Stage III	WFEAOV18	7.78E+03	1.27E+06	6.12E-03	0.004964	0.0012562
	WFEAOV19	6.64E+03	1.64E+06	4.04E-03		
	WFEAOV28	5.61E+03	1.25E+06	4.47E-03		
	WFEAOV26	6.18E+03	1.29E+06	4.78E-03		
	WFEAOV32	3.61E+03	6.71E+05	5.38E-03		
	WFEAOV9	2.71E+03	7.51E+05	3.61E-03		
	WFEAOV31U	3.76E+03	7.65E+05	4.91E-03		
	WFEAOV31L	4.26E+03	5.62E+05	7.57E-03		
	WFEAOV12	4.13E+03	1.09E+06	3.80E-03		
EA-BD-Stage IV	WFEAOV13	2.92E+03	6.87E+05	4.26E-03	0.004544	0.0012702
	WFEAOV11	5.25E+03	7.78E+05	6.75E-03		
	WFEAOV14	3.08E+03	7.18E+05	4.29E-03		
	WFEAOV16	3.42E+03	8.84E+05	3.87E-03		
	WFEAOV15	2.00E+03	5.65E+05	3.55E-03		

Table B5 Relative expression levels of *PmAtNS* in different groups of domesticated *P. monodon* based on quantitative real-time PCR analysis

Sample group		Mean conc.		Ratio (target/*EF-1α*	Average	STDEV
		AtNS	*EF*-1α			
5-month-old	BU5OV4	9.96E+02	8.95E+04	1.11E-02	0.0304	0.01411
	BU5OV13	7.61E+03	2.07E+05	3.68E-02		
	BU5OV14	4.66E+03	2.04E+05	2.29E-02		
	BU5OV15	2.21E+03	4.57E+04	4.83E-02		
	BU5OV17	3.68E+03	1.12E+05	3.29E-02		
9-month-old	BU9OV2	4.34E+02	4.34E+04	1.00E-02	0.0209	0.01059
	BU9OV4	1.45E+03	1.04E+05	1.39E-02		
	BU9OV8	2.96E+03	2.11E+05	1.40E-02		
	BU9OV11	3.96E+03	9.47E+04	4.18E-02		
	BU9OV14	1.34E+03	6.26E+04	2.13E-02		
	BU9OV18	5.63E+03	2.86E+05	1.97E-02		
	BU9OV20	7.67E+03	3.03E+05	2.53E-02		
10-month-old	BU14OV5	3.30E+02	9.00E+04	3.67E-03	0.0118	0.00858
	BU14OV6	2.80E+02	1.18E+05	2.37E-03		
	BU14OV19	1.59E+03	1.13E+05	1.40E-02		
	BU14OV25	1.35E+03	8.46E+04	1.60E-02		
	BU14OV27	9.29E+03	3.41E+05	2.72E-02		
	BU14OV33	1.95E+03	2.91E+05	6.70E-03		
	BU14OV34	1.93E+03	3.16E+05	6.13E-03		
	BU14OV62	4.94E+03	2.70E+05	1.83E-02		
19-month-old	BU19OV1	1.41E+03	8.68E+04	1.63E-02	0.0274	0.01098
	BU19OV4	3.84E+03	1.66E+05	2.31E-02		
	BU19OV9	1.86E+03	9.44E+04	1.97E-02		
	BU19OV12	9.69E+03	2.67E+05	3.63E-02		
	BU19OV16	6.64E+03	1.60E+05	4.16E-02		

Table B6 Relative expression levels of *Pm-mago nashi* in different groups of domesticated *P. monodon* based on quantitative real-time PCR analysis

Sample group		Mean conc.		Ratio (target/*EF1α*)	Average	STDEV
		Mago nashi	*EF*-1α			
5-month-old	BU5OV4	2.01E+04	8.95E+04	2.25E-01	0.3374	0.20818
	BU5OV13	3.89E+04	2.07E+05	1.88E-01		
	BU5OV14	5.95E+04	2.04E+05	2.92E-01		
	BU5OV15	3.21E+04	4.57E+04	7.02E-01		
	BU5OV17	3.14E+04	1.12E+05	2.80E-01		
9-month-old	BU9OV2	2.17E+04	4.34E+04	5.00E-01	0.3963	0.08737
	BU9OV4	4.06E+04	1.04E+05	3.90E-01		
	BU9OV8	6.58E+04	2.11E+05	3.12E-01		
	BU9OV11	4.13E+04	9.47E+04	4.36E-01		
	BU9OV14	2.89E+04	6.26E+04	4.62E-01		
	BU9OV18	7.94E+04	2.86E+05	2.78E-01		
10-month-old	BU14OV5	6.63E+04	9.00E+04	7.37E-01	0.275	0.19976
	BU14OV6	2.34E+04	1.18E+05	1.98E-01		
	BU14OV19	2.43E+04	1.13E+05	2.15E-01		
	BU14OV25	2.19E+04	8.46E+04	2.59E-01		
	BU14OV27	4.54E+04	3.41E+05	1.33E-01		
	BU14OV33	7.02E+04	2.91E+05	2.41E-01		
	BU14OV34	3.00E+04	3.16E+05	9.49E-02		
	BU14OV62	8.73E+04	2.70E+05	3.23E-01		
19-month-old	BU19OV1	3.94E+04	8.68E+04	4.54E-01	0.2998	0.12066
	BU19OV4	5.14E+04	1.66E+05	3.10E-01		
	BU19OV9	3.56E+04	9.44E+04	3.77E-01		
	BU19OV12	4.73E+04	2.67E+05	1.77E-01		
	BU19OV16	2.92E+04	1.60E+05	1.83E-01		

BIOGRAPHY

Miss. Jintana Innuphat was born on February 7, 1984 in Krabi. She graduated with the degree of Bachelor of Science from the Department of Science (Biotechnology), Ramkhumhang University in 2007. She has enrolled a Master degree program at the Program in Biotechnology, Chulalongkorn University since 2011.

Publication related with this thesis

Innuphat, J., Sittikhankaew, K., Klinbunga, S., Menasveta, P., (2011). Molecular cloning and expression analysis of the *asparaginyl tRNA synthetase* gene in the giant tiger shrimp *Penaeus monodon*. The 23rd Annual Meeting and International conference of the Thai Society for Biotechnology "*Systems Biotechnology: Quality & Success*", February 1–2, Bangkok, Thailand (Oral presentation).